Traveling-wave surface haptics to guide bare finger movement over touch surfaces

Cai, Z.

DOI
10.4233/uuid:0bcd01b0-be96-4b3d-b43d-9ea761b5ce0a

Publication date
2025

Document Version
Final published version

Citation (APA)
Cai, Z. (2025). *Traveling-wave surface haptics to guide bare finger movement over touch surfaces*. [Dissertation (TU Delft), Delft University of Technology]. https://doi.org/10.4233/uuid:0bcd01b0-be96-4b3d-b43d-9ea761b5ce0a

Important note
To cite this publication, please use the final published version (if applicable).
Please check the document version above.

Traveling-wave surface haptics
to guide bare finger movement over touch surfaces

Dissertation
for the degree of Doctor

Zhaochong Cai

Delft, The Netherlands
September 2025

Propositions

accompanying the dissertation

TRAVELING-WAVE SURFACE HAPTICS TO GUIDE BARE FINGER MOVEMENT OVER TOUCHSCREENS

by

Zhaochong CAI

1. The key to producing a salient mechanical sensation while maintaining low power consumption is to use resonance. (this thesis)
2. Designing a structure with a specific geometry is the only way to ensure the existence of resonant traveling waves. (this thesis)
3. Designing haptic feedback based solely on perception is insufficient; users' adaptive movements must be considered. (this thesis)
4. The best haptic interfaces are those with which users rely less on their vision and more on their reflexes. (this thesis)
5. The ideal haptic interface should be designed not just for immediate usability but for long-term motor learning.
6. Passion for science is not innate; it is a drive you have to foster.
7. First-year PhD students candidly questioning experts is the silent engine with which science advances.
8. The most efficient time to complete a task is in the first hour after motivation strikes; the second is the last hour before the deadline.
9. "Reviewer #2" is not a person; it is a force of nature sent to humble confident Ph.D. students.
10. The three stages of a PhD: Excitement about the journey, questioning your life choice that led you here, and finally, acceptance. The sooner you reach stage three, the more productive you will be.

These propositions are regarded as opposable and defendable, and have been approved as such by the promotors Dr. M. Wiertlewski and prof. dr. ir. D. A. Abbink.

TRAVELING-WAVE SURFACE HAPTICS TO GUIDE BARE FINGER MOVEMENT OVER TOUCH SURFACES

TRAVELING-WAVE SURFACE HAPTICS TO GUIDE BARE FINGER MOVEMENT OVER TOUCH SURFACES

Dissertation

for the purpose of obtaining the degree of doctor
at Delft University of Technology
by the authority of the Rector Magnificus, prof. dr. ir. T.H.J.J. van der Hagen,
chair of the Board for Doctorates
to be defended publicly on
Tuesday 30 September 2025 at 12:30 o'clock

by

Zhaochong CAI

Master of Optical Engineering,
Zhejiang University, China,
born in Jiangxi, China

This dissertation has been approved by the promotors.

Composition of the doctoral committee:

Rector Magnificus	chairperson
Prof. dr. ir. D.A. Abbink	Delft University of Technology, *promotor*
Dr. M. Wiertlewski	Delft University of Technology, *promotor*
Independent members:	
Prof. dr. P.G. Steeneken	Delft University of Technology
Prof. dr. J.B.F. van Erp	University of Twente / TNO
Prof. dr. D.E. Colgate	Northwestern University, USA
Prof. dr. A.M.L. Kappers	Eindhoven University of Technology
Prof. dr. S.C. Pont	Delft University of Technology, reserve member

Keywords: Surface haptics, touchscreens, lateral force feedback, active force, resonant traveling waves, ultrasonic traveling waves, haptic guidance, potential field, targeting tasks

Printed by: Proefschriftmaken

ISBN 978-94-6518-120-2

An electronic copy of this dissertation is available at
https://repository.tudelft.nl/.

To my family.

CONTENTS

SUMMARY

Touch is fundamental to our perception of the world and to interaction with our physical surroundings. With touch we can intuitively and effortlessly move and shape objects and control complex machines. In most modern machines, the part that interfaces with user often integrate touchscreens or touchpads, owing to their ease of use. However, these interfaces often deliver very poor tactile feedback, which limits the usability in contexts such as driving, low-light environments, and for users with visual impairments. Existing solutions like vibrotactile feedback, are poor substitute to the richness of natural touch and offer only transient sensations. Surface haptic devices offer more complexity, but since they rely on friction modulation, they require continuous movement and cannot nudge the user to arbitrary directions. These limitations highlight the need for active lateral force devices that can guide users in an arbitrary direction.

This thesis introduces the Ultraloop, an active surface haptic device that generates net lateral forces using resonant traveling waves. Built around an oblong ring-shaped structure, the Ultraloop provides a large and flat interaction area with uniform force generation. Unlike existing active haptic devices, it operates at resonance, achieving a high vibration amplitude-to-input ratio, resulting in a more salient force feedback. Additionally, this thesis introduces a planar adaptation of the Ultraloop, the flatLoop, which is more compact with a height of just 5 mm, facilitating integration into consumer electronics.

These devices can guide users via their sense of touch and render complex forces fields by modulating the wave amplitude and phase control as a function of the position and velocity of the user. To evaluate their effectiveness, this thesis investigates two types of rendered haptic environments: position-based elastic potential fields and velocity-based viscous damping. Experimental user studies show that participants could perceive virtual 3D shapes (e.g., bumps and holes) and stepwise force fields that enhance their target-search performance. Moreover, directional cues provided by the force feedback enabled users to navigate toward a target without visual feedback, while viscous damping environments, where lateral force is a function of finger speed, reduced oscillations during selection, and improved overall targeting performance.

This doctoral work systematically explores the benefits of active force feedback in touch interactions by introducing resonant traveling wave-based haptic displays and performing user studies. By advancing surface-haptic technology, this research paves the way for next-generation touch interfaces that support eye-free interaction and effortless control of complex machines.

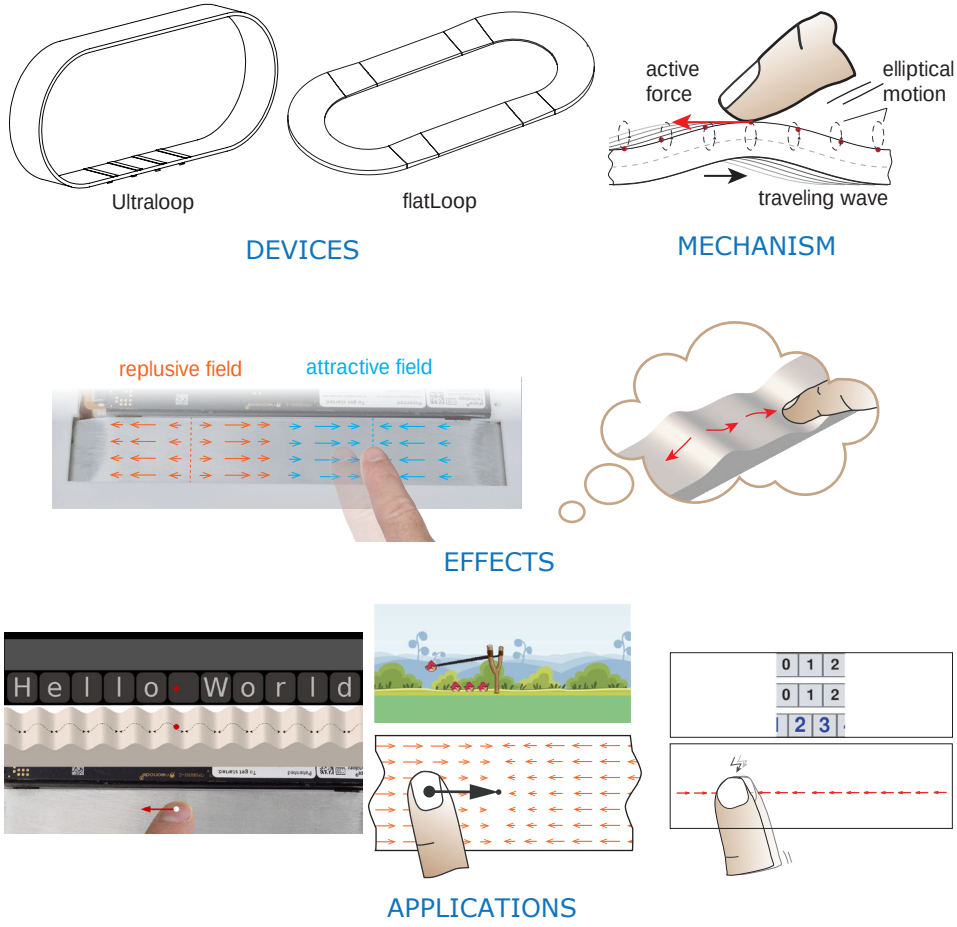

Figure 1: Visual illustration of the devices and interaction paradigms explored in this thesis.

SAMENVATTING

Aanraking is fundamenteel voor onze perceptie van de wereld en voor interactie met onze fysieke omgeving. Met aanraking kunnen we intuïtief en moeiteloos objected verplaatsen en vormgeven, evenals complexe machines bedienen. In de meeste moderne machines bevat het deel dat met de gebruiker integreert touchscreens of touchpads vanwege hun gebruiksgemak. Echter, deze interfaces bieden vaak beperkte tactiele feedback, wat de bruikbaarheid limiteert voor toepassingen zoals autorijden, omgevingen met weinig licht, en voor gebruikers met een visuele beperking. Bestaande oplossingen, zoals vibrotactiele feedback, zijn een gebrekkige vervanging voor de rijkheid van natuurlijke aanraking en bieden slechts vluchtige sensaties. Haptische oppervlaktetechnologieën bieden meer complexiteit, maar omdat ze afhankelijk zijn van wrijvingsmodulatie, vereisen ze continue beweging en kunnen ze de gebruiker niet in willekeurige richtingen sturen. Deze beperkingen benadrukken de noodzaak van actieve laterale krachtapparaten die gebruikers in een willekeurige richting kunnen begeleiden.

Deze thesis introduceert de Ultraloop, een actief haptisch oppervlak dat netto lateral krachten genereert met behulp van resonante lopende golven. De Ultraloop is gebouwd rondom been langwerpige ringvormige structuur en biedt een groot, vlak interactiegebied met uniforme krachtgeneratie. In tegenstelling tot bestaande actieve haptische apparaten werkt de Ultraloop op resonantie. Hierdoor wordt een hoge verhouding tussen vibratie-amplitude en invoer bereikt, wat resulteert in een duidelijker waarneembare krachtfeedback. Daarnaast introduceert deze thesis een vlakke aanpassing van de Ultraloop: de flatLoop. Omdat de flatLoop compacter is, met een hoogte van slechts 5 mm, is deze gemakkelijker te integreren in consumentenelektronica.

Deze apparaten kunnen gebruikers begeleiden via hun tastzintuig en complexe krachtvelden weergeven door de golfamplitude en fasecontrole te moduleren als functie van de positie en snelheid van de gebruiker. Om hun effectiviteit te evalueren, onderzoekt deze thesis twee soorten haptische omgevingen: op positie gebaseerde elastische potentiaalvelden en op snelheid gebaseerde viskeuze demping. Experimentele gebruikersstudies toonden aan dat deelnemers virtuele 3D-vormen, zoals hobbels en gaten, en stapsgewijze krachtvelden konden waarnemen die hun zoekprestaties verbeterde. Bovendien stelden de directionele aanwijzingen die door de krachtfeedback werden geboden gebruikers in staat om zonder visuele feedback naar een doel te navigeren. In omgevingen met viskeuze demping, waarbij de lateral kracht afhankelijk is van de vingerbeweging, verminderde dit oscillaties tijdens de selectie en verbeterde het de algehele doelgerichtheid van gebruikers.

Dit doctoraatswerk onderzoekt systematisch de voordelen van active krachtfeedback bij aanrakingsinteracties door resonante lopende golf-gebaseerde haptische weergaven te introduceren en gebruikersstudies uit te voeren. Door de ontwikkeling van oppervlaktetechnologieën op het gebied van haptiek vooruit te helpen, maakt dit onderzoek de weg vrij voor de volgende generatie aanraakinterfaces die niet-visuele interactie en

moeiteloze controle van complexe machines ondersteunt.

1

INTRODUCTION

1

Touch is fundamental to our perception of our environment and interaction with the physical world around us. Upon touching the various objects of our lives, tactile information reveals whether a fabric is soft, textured, and of high quality; or whether a dial is heavy, knurled, and precise in its operation. The forces caused by interactions between our hands and the environment create intricate deformations of our skin, which our brains interpret as a flurry of complex sensations. These sensations help us to make sense of the world, confirming or refining the mental models constructed from visual and auditory input before physical contact.

Tactile perception is the building block upon which our ability to explore, grasp, handle, and manipulate objects is built. Humans rely on touch to perform everyday tasks effortlessly and deftly. Simple actions, such as lifting a glass of water or locating keys in a pocket, are executed without vision and with minimal attention. In particular, when interacting with machines, bumps and dents can guide us to the center of the buttons and important features; clicks and detents inform us that an action has been executed as we press down; and a rapid succession of transients tells us how much a dial has been rotated. During these tasks, touch provides essential feedback to the brain regarding the movement of the limb and the properties of the surface of the object, which is critical for motor planning and adjustment. This continuous feedback loop, known as the sensorimotor loop [1], [2], endows humans with the unique ability to perform dexterous tasks, to control complex machines such as planes or cars and to operate computer peripherals such as keyboards, all without the need to look at the controls.

Over the last 50 years, haptic interfaces have been developed to provide programmable tactile and kinesthetic feedback to users. These interfaces function as small robotic systems whose end effectors can be manipulated by users. When encountering virtual objects, the robot applies forces that push back against their motion, creating the illusion of touching a virtual environment. In a typical impedance control scheme, the position of the handle is read and the controller generates the corresponding forces accordingly. By modulating the output forces with the user's movements, these devices can simulate properties such as viscosity, elasticity, or inertia, allowing users to feel the weight, resistance, or impact of objects. The ability to perceive these dynamic properties is essential for achieving deft movements. Such haptic devices have a wide range of applications, from virtual-reality-assisted assembly [3], [4] to teleoperated surgical instruments [5].

In recent years, touchscreens have become the dominant human-machine interface (HMI), replacing physical buttons and dials on devices such as smartphones, tablets, and vending machines. Their popularity stems from their intuitive and direct interaction, achieved through the colocalization of visual content and finger input. However, despite the increase in flexibility and programmability, touchscreens largely lack haptic feedback, offering only visual and auditory cues. This absence of tactile input can create challenges, particularly in scenarios such as driving, low-light conditions, or for users with visual impairments.

To bring back a sense of tangibility, newer touchscreens incorporate vibrotactile technology that produces vibrations upon user interaction. Vibrotactile feedback uses mechanical vibration, typically in the range of 50 to 500 Hz, to signal events such as clicks or notifications [6]. Its widespread adoption is attributed to its robustness, ease of implementation, low cost, and minimal energy requirements. However, vibrotactile feedback

is primarily limited to producing transient signals, which are perceived as clicks [7], rumbles or textures [8], [9].

An emerging alternative, known as surface haptics, provides continuous quasi-static feedback to the user's fingertip by modulating friction between the finger and the touch surface. This modulation is achieved through ultrasonic levitation, which reduces friction [10] or electroadhesion, which increases it [11]. For instance, in the ultrasonic levitation method, the friction of a glass plate can be reduced by 95% when subjected to transverse ultrasonic vibrations of 3 μm [12]. By varying friction as a function of the position of the user, surface haptics can create the feeling of touching silky textures [13] or 3D-like shapes [14], [15]. This position-based frictional feedback can also be used for haptic guidance. By making friction high on a virtual target and low everywhere else, users can reach targets 10% faster than without tactile feedback [16]–[18]. More complex patterns, such as gradually changed sinewaves, have shown to be useful in assisting users in setting a value for temperature control [19]. Additionally, by adjusting friction in response to applied pressure, it can mimic the sensation of pressing physical buttons [20], [21].

However, surface haptics is only effective when the finger is sliding. Although literature reported that a stationary finger can also perceive a sudden change in friction [22], the feedback is feint and it fails to provide directional cues. Furthermore, since the friction force is collinear in the direction of finger movement, it cannot generate forces in a direction different than the one where the finger is going. As a result, guiding fingers to specific locations on a 2D touch surface remains challenging by solely varying friction, as illustrated in Fig. 1.1. Many touchscreen interactions, such as target reaching and trajectory following, require continuous active lateral forces on the touch surface.

Active forces have been successfully implemented in classical force-feedback schemes to guide users or render virtual environments. By actively exerting forces on the user's hand, these systems can both push and pull, effectively guiding users along a desired path or toward specific targets while helping them avoid obstacles. A common approach involves the use of artificial potential fields, which dynamically generate force fields to direct movement [23]. Studies have demonstrated that such techniques improve precision and reduce efforts in various applications, including assistive surgical tasks [24], [25] and automotive training [26].

Building on these principles, it is possible to adapt active force-feedback techniques for fingertip guidance on touch surfaces. By generating controlled lateral forces directly on fingertips, users could be guided toward specific locations or along predefined trajectories, overcoming the limitations of friction-based surface haptics. Therefore, this thesis aims to develop surface haptic devices capable of providing active lateral force to the fingers and to investigate its impact on user behavior.

1.1. PROBLEM STATEMENTS

THE first challenge lies in developing a surface haptic device that can produce variable active force to push fingers. Such haptic displays must integrate seamlessly into touchscreens or touchpads, meaning they should contain no moving mechanical parts. Therefore, the mechanism for generating net force should rely on periodic movements, which enables the surface move back the the original position in one cycle.

A well-established approach to generating active forces on a touch surface leverages asymmetric friction, where in-plane oscillations are synchronized with friction modulation. This friction modulation is achieved through ultrasonic vibrations [27] or electroadhesion [28]. In this method, friction alternates between high and low as the plate moves forward or back within each oscillation cycle, resulting in a net lateral force. The lateral oscillation can be produced using a voice coil [27], oscillating at 854 Hz, reaching a lateral force of up to 450 mN [28]. One critical issue for such devices is the audible noise resulting from low-frequency oscillation. The noise was further eliminated by vibrating the place in the ultrasonic regime in the UltraShiver [29]. However, all of these devices operate in resonant mode, leading to nodal lines where the force is null. A more recent device, the SwitchPad mitigates this issue by dynamically switching between the first and second in-plane oscillation modes based on finger position, achieving a peak force of 250 mN [30]. While effective, asymmetric friction-based devices require complex hardware and control systems due to the need for synchronization between oscillation and friction modulation.

Alternatively, if the touch surface itself vibrates both laterally and longitudinally, i.e. moves elliptically, net lateral forces can be created due to non-linear interaction with the finger skin in contact. This approach does not require the synchronization between oscillation and friction modulation, simplifying control since only a single plate is involved. To achieve elliptical motion, one can excite both the longitudinal and bending modes simultaneously with a certain phase shift. This technique has been used in devices such as the LateralPad, which can generate active forces of up to ±50 mN [31], and 2MoTac, which simulates button clicks [32], [33]. However, this approach requires a precise matching of the resonant frequency of the dual modes, where careful mechanical design and stable mechanical properties are needed.

A more elegant way to achieve elliptical motion without requiring multiple modes is by employing flexural traveling waves. When the beam is excited by flexural waves, the surface of the beam follows an elliptical trajectory. However, generating traveling waves in a finite structure presents challenges due to wave reflections at boundaries. Kuribayashi et al. proposed a method in which one transducer excites the waves while another absorbs them, originally developed for ultrasonic motors [34]. Ghenna et al. explored the modal superposition of two adjacent bending modes, but since the operating frequency did not align with any resonant modes, the resulting force was weak and energy consumption was high [35]. Both methods suffer from low amplitude-to-input power ratios. Both ways achieve a small amplitude-to-input power ratio, though using powerful actuators.

Instead, resonance can be leveraged to produce traveling waves. To achieve resonance, we remember that any traveling wave can be decomposed into two standing waves with a quarter-wavelength phase shift. If these standing waves resonate at the same frequency, they form degenerate modes, generating a traveling wave with a significantly larger amplitude. This principle has been applied in circular ring structures used in traveling-wave ultrasonic motors [36], producing strong active forces on human fingertips [37] and delivering haptic effects such as button clicks [38]. However, the hollow and non-flat shapes of these structures make them unsuitable for touch applications. Thus, there remains a need for a surface haptic display that can generate resonant trav-

eling waves on a flat, continuous, and large touch surface.

The second challenge is the lack of design principles for virtual environments in haptic guidance on surfaces. In classical force-feedback systems, improving manipulation tasks in virtual environments is typically achieved by rendering "virtual fixtures" or "artificial potential fields" [39]–[41]. These scalar fields use artificial "hills" to represent obstacles and "valleys" to represent attractors, which are combined to guide or constrain users to move along the desired path. However, such principles have not yet been implemented or validated in the contexts of surface haptics, which, until recently, lacked the capability to generate active forces necessary to create potential fields. With the development of active force displays, it is now possible to apply these guidance principles to touch-based interactions, potentially enhancing a wide range of applications.

To address these challenges, this thesis investigates two fundamental research questions:

- **How can resonant traveling waves be used in surface haptic devices to generate active force and provide tactile feedback?** Resonant traveling waves offer advantages such as ease of control and a high Q-factor. Previous research has demonstrated strong force generation on the fingertip using traveling-wave-based ultrasonic motor [38], [43]. This thesis will explore the use of loop structures with degenerate modes to create traveling waves and investigate methods to control the direction and magnitude of the active force. This problem is visually summarized in Fig. 1.1.

- **How can virtual environments be designed using active force, and what guidance principles can enhance touch-based interactions?** Previous studies have shown that elastic or viscous force fields can improve user interaction with force-feedback devices [41], [44]. Applying these principles to surface haptics requires fine control over force production. This thesis will leverage the proposed device to examine the effects of different artificial potential fields and viscous fields, conducting both quantitative and qualitative evaluations through human subject testing.

In summary, this thesis will tackle these two challenges and, for the first time, provide a principle-based approach for controlling machines of all sizes and forms with the tip of the finger. By enabling bidirectional communication through haptic feedback, this work seeks to enhance sensorimotor integration, allowing users to maintain precise control over task dynamics.

1.2. THESIS OVERVIEW

THIS thesis is structured into seven chapters, including the Introduction, and is organized as follows, and the main work is visually represented in Fig. 1.2. **Chapter 2** is a review of the literature of related work. It begins by examining the principles and implementation of haptic guidance in classical force-feedback devices. This chapter then explores the neurophysiological bases of the human sensorimotor loop, focusing on how haptic feedback assists in human manipulation. Lastly, it discusses state-of-the-art sur-

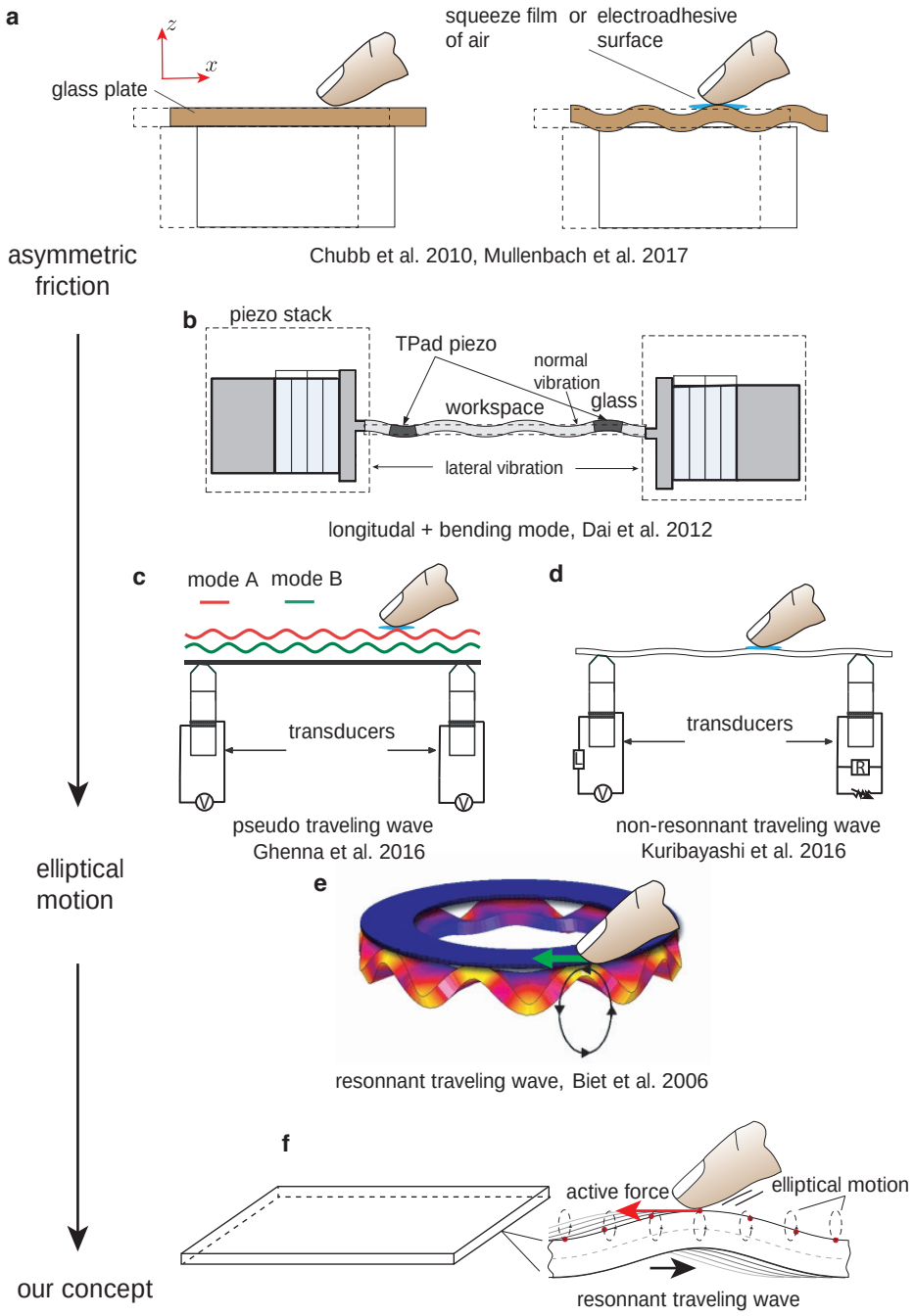

Figure 1.1: A visual representation of the state-of-the-art approaches leading to Problem 1: designing an active surface haptic device using resonant traveling waves. (a) Asymmetric friction principle for generating active forces [27]–[30]. (b) Active force generation through the combination of longitudinal and bending waves [31], [32]. (c) Modal superposition of two adjacent modes to produce active forces [35]. (d) Non-resonant traveling wave generation using one actuator for excitation and another for absorption [42]. (e) Ultrasonic motors using resonant traveling waves. They can generate strong lateral forces [37]. (f) Our concept: create such effects on flat surfaces with resonant traveling waves.

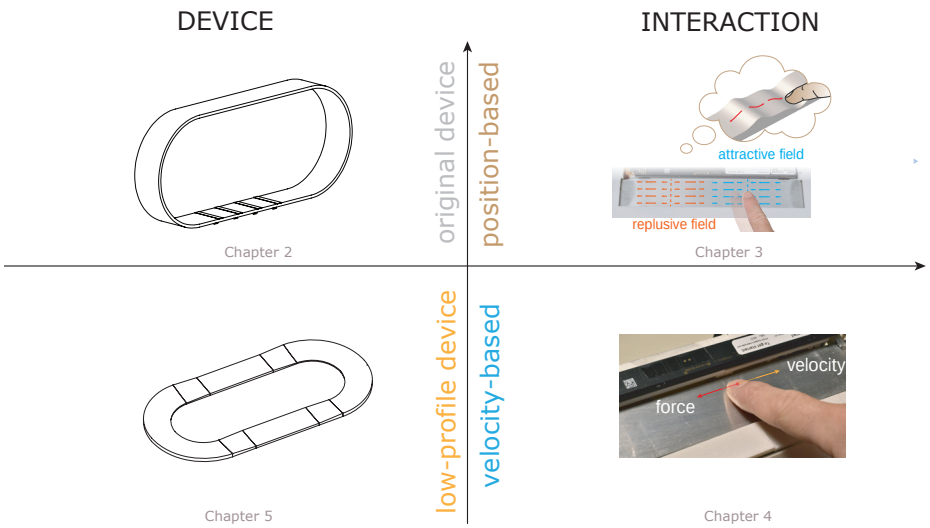

Figure 1.2: An overview of the structure of the main work in the thesis.

face haptic technologies, covering both friction modulation and active force feedback devices.

Chapter 3 presents the design and characterizations of force generation of a surface haptics device, called the Ultraloop, which is capable of producing active force. This chapter describes the analytical model of its acoustic design and reports the force measurement results obtained under various driving voltages and phase shifts. Finally, it demonstrates an application that simulates button clicks.

Chapter 4 explores the principles of haptic guidance on surfaces through potential field rendering. In this chapter, the Ultraloop is integrated with optical position tracking to generate force feedback based on the user's position. Three elastic potential fields are proposed and evaluated through human-subject experiments, including Fitts' pointing task, a shape perception task, and a direction perception task. A user study involving three applications is then presented to assess user experience. Both quantitative and qualitative results highlight the effectiveness of potential field rendering with the Ultraloop.

Chapter 5 examines the implementation of a viscous damping force field rendered by the Ultraloop. This chapter compares the effects of three types of viscous environments: positive damping, negative damping, and variable damping. In the variable damping condition, viscosity is high during slow movements and low during fast movements. These environments are evaluated through a Fitts' pointing task with human participants.

Chapter 6 introduces a compact, updated version of the Ultraloop, the flatLoop, maintaining the same length and radius as the original device, but with a reduced height of just 5 mm, making it more suitable for consumer electronics. This chapter begins with

the device's acoustic design, followed by its force characterization. It concludes with a human factor study, applying the device to a haptic keyboard, which integrates the button-click simulation from Chapter 3 and the potential field design from Chapter 4.

Chapter 7 concludes the thesis by summarizing the main contributions and limitations, as well as identifying future research directions.

REFERENCES

[1] D. A. Nowak and J. Hermsdörfer, *Sensorimotor control of grasping: physiology and pathophysiology*. Cambridge University Press, 2009.

[2] D. M. Wolpert, Z. Ghahramani, and M. I. Jordan, "An internal model for sensorimotor integration", *Science*, vol. 269, no. 5232, pp. 1880–1882, 1995.

[3] M. H. Abidi, A. Ahmad, S. Darmoul, and A. M. Al-Ahmari, "Haptics assisted virtual assembly", *IFAC-PapersOnLine*, vol. 48, no. 3, pp. 100–105, 2015.

[4] A. Seth, J. M. Vance, and J. H. Oliver, "Virtual reality for assembly methods prototyping: A review", *Virtual reality*, vol. 15, pp. 5–20, 2011.

[5] I. El Rassi and J.-M. El Rassi, "A review of haptic feedback in tele-operated robotic surgery", *Journal of medical engineering & technology*, vol. 44, no. 5, pp. 247–254, 2020.

[6] S. Choi and K. J. Kuchenbecker, "Vibrotactile display: Perception, technology, and applications", *Proceedings of the IEEE*, vol. 101, no. 9, pp. 2093–2104, 2012.

[7] E. Hoggan, S. A. Brewster, and J. Johnston, "Investigating the effectiveness of tactile feedback for mobile touchscreens", in *Proceedings of the SIGCHI conference on Human factors in computing systems*, 2008, pp. 1573–1582.

[8] M. Wiertlewski, J. Lozada, and V. Hayward, "The spatial spectrum of tangential skin displacement can encode tactual texture", *IEEE Transactions on Robotics*, vol. 27, no. 3, pp. 461–472, 2011.

[9] P. Strohmeier and K. Hornbæk, "Generating haptic textures with a vibrotactile actuator", in *Proceedings of the 2017 CHI Conference on Human Factors in Computing Systems*, 2017, pp. 4994–5005.

[10] L. Winfield, J. Glassmire, J. E. Colgate, and M. Peshkin, "T-pad: Tactile pattern display through variable friction reduction", in *Second Joint EuroHaptics Conference and Symposium on Haptic Interfaces for Virtual Environment and Teleoperator Systems (WHC'07)*, IEEE, 2007, pp. 421–426.

[11] O. Bau, I. Poupyrev, A. Israr, and C. Harrison, "Teslatouch: Electrovibration for touch surfaces", in *Proceedings of the 23nd annual ACM symposium on User interface software and technology*, 2010, pp. 283–292.

[12] M. Wiertlewski, R. Fenton Friesen, and J. E. Colgate, "Partial squeeze film levitation modulates fingertip friction", *Proceedings of the national academy of sciences*, vol. 113, no. 33, pp. 9210–9215, 2016.

[13] M. Wiertlewski, D. Leonardis, D. J. Meyer, M. A. Peshkin, and J. E. Colgate, "A high-fidelity surface-haptic device for texture rendering on bare finger", in *International Conference on Human Haptic Sensing and Touch Enabled Computer Applications*, Springer, 2014, pp. 241–248.

[14] S.-C. Kim, A. Israr, and I. Poupyrev, "Tactile rendering of 3d features on touch surfaces", in *Proceedings of the 26th annual ACM symposium on User interface software and technology*, 2013, pp. 531–538.

[15] C. Choi, Y. Ma, X. Li, *et al.*, "Surface haptic rendering of virtual shapes through change in surface temperature", *Science Robotics*, vol. 7, no. 63, eabl4543, 2022.

[16] V. Levesque, L. Oram, K. MacLean, *et al.*, "Enhancing physicality in touch interaction with programmable friction", in *Proceedings of the SIGCHI Conference on Human Factors in Computing Systems*, ser. CHI '11, May 2011, pp. 2481–2490, ISBN: 978-1-4503-0228-9. DOI: 10.1145/1978942.1979306.

[17] G. Casiez, N. Roussel, R. Vanbelleghem, and F. Giraud, "Surfpad: Riding towards targets on a squeeze film effect", in *Proceedings of the SIGCHI Conference on Human Factors in Computing Systems*, 2011, pp. 2491–2500.

[18] Y. Zhang and C. Harrison, "Quantifying the Targeting Performance Benefit of Electrostatic Haptic Feedback on Touchscreens", in *Proceedings of the 2015 International Conference on Interactive Tabletops & Surfaces*, ser. ITS '15, New York, NY, USA, 2015, pp. 43–46, ISBN: 978-1-4503-3899-8.

[19] C. Bernard, J. Monnoyer, S. Ystad, and M. Wiertlewski, "Eyes-off your fingers: Gradual surface haptic feedback improves eyes-free touchscreen interaction", in *Proceedings of the 2022 CHI Conference on Human Factors in Computing Systems*, 2022, pp. 1–10.

[20] J. Monnoyer, E. Diaz, C. Bourdin, and M. Wiertlewski, "Perception of ultrasonic switches involves large discontinuity of the mechanical impedance", *IEEE transactions on haptics*, vol. 11, no. 4, pp. 579–589, 2018.

[21] J. Monnoyer, L. Willemet, and M. Wiertlewski, "Rapid change of friction causes the illusion of touching a receding surface", *Journal of the Royal Society Interface*, vol. 20, no. 199, p. 20 220 718, 2023.

[22] J. Monnoyer, E. Diaz, C. Bourdin, and M. Wiertlewski, "Ultrasonic friction modulation while pressing induces a tactile feedback", in *Haptics: Perception, Devices, Control, and Applications: 10th International Conference, EuroHaptics 2016, London, UK, July 4-7, 2016, Proceedings, Part I 10*, Springer, 2016, pp. 171–179.

[23] K. Salisbury, D. Brock, T. Massie, N. Swarup, and C. Zilles, "Haptic rendering: Programming touch interaction with virtual objects", in *Proceedings of the 1995 symposium on Interactive 3D graphics*, ser. I3D '95, New York, NY, USA: Association for Computing Machinery, Apr. 1995, pp. 123–130, ISBN: 978-0-89791-736-0. DOI: 10.1145/199404.199426.

[24] J. Ren, K. A. McIsaac, R. V. Patel, and T. M. Peters, "A Potential Field Model Using Generalized Sigmoid Functions", *IEEE Transactions on Systems, Man, and Cybernetics, Part B (Cybernetics)*, vol. 37, no. 2, pp. 477–484, Apr. 2007, Conference Name: IEEE Transactions on Systems, Man, and Cybernetics, Part B (Cybernetics), ISSN: 1941-0492. DOI: 10.1109/TSMCB.2006.883866.

[25] J. Ren, R. V. Patel, K. A. McIsaac, G. Guiraudon, and T. M. Peters, "Dynamic 3-D Virtual Fixtures for Minimally Invasive Beating Heart Procedures", *IEEE Transactions on Medical Imaging*, vol. 27, no. 8, pp. 1061–1070, Aug. 2008, Conference Name: IEEE Transactions on Medical Imaging, ISSN: 1558-254X. DOI: 10.1109/TMI.2008.917246.

[26] E. Garcia–Canseco, A. Ayemlong–Fokem, A. Serrarens, and M. Steinbuch, "Haptic simulation of a gear selector lever using artificial potential fields", *IFAC Proceedings Volumes*, vol. 43, no. 13, pp. 426–429, 2010.

[27] E. C. Chubb, J. E. Colgate, and M. A. Peshkin, "Shiverpad: A glass haptic surface that produces shear force on a bare finger", *IEEE Transactions on Haptics*, vol. 3, no. 3, pp. 189–198, 2010.

[28] J. Mullenbach, M. Peshkin, and J. E. Colgate, "Eshiver: Lateral force feedback on fingertips through oscillatory motion of an electroadhesive surface", *IEEE transactions on haptics*, vol. 10, no. 3, pp. 358–370, 2016.

[29] H. Xu, M. A. Peshkin, and J. E. Colgate, "Ultrashiver: Lateral force feedback on a bare fingertip via ultrasonic oscillation and electroadhesion", *IEEE transactions on haptics*, vol. 12, no. 4, pp. 497–507, 2019.

[30] H. Xu, M. A. Peshkin, and J. E. Colgate, "Switchpad: Active lateral force feedback over a large area based on switching resonant modes", in *Haptics: Science, Technology, Applications: 12th International Conference, EuroHaptics 2020, Leiden, The Netherlands, September 6–9, 2020, Proceedings 12*, Springer, 2020, pp. 217–225.

[31] X. Dai, J. E. Colgate, and M. A. Peshkin, "Lateralpad: A surface-haptic device that produces lateral forces on a bare finger", in *2012 IEEE Haptics Symposium (HAPTICS)*, IEEE, 2012, pp. 7–14.

[32] P. Garcia, F. Giraud, B. Lemaire-Semail, M. Rupin, and M. Amberg, "2motac: Simulation of button click by superposition of two ultrasonic plate waves", in *Haptics: Science, Technology, Applications: 12th International Conference, EuroHaptics 2020, Leiden, The Netherlands, September 6–9, 2020, Proceedings 12*, Springer, 2020, pp. 343–352.

[33] P. Garcia, F. Giraud, B. Lemaire-Semail, M. Rupin, and A. Kaci, "Control of an ultrasonic haptic interface for button simulation", en, *Sens. Actuator A Phys.*, vol. 342, p. 113 624, Aug. 2022, ISSN: 0924-4247. DOI: 10.1016/j.sna.2022.113624.

[34] M. Kuribayashi, S. Ueha, and E. Mori, "Excitation conditions of flexural traveling waves for a reversible ultrasonic linear motor", *The Journal of the Acoustical Society of America*, vol. 77, no. 4, pp. 1431–1435, 1985.

[35] S. Ghenna, E. Vezzoli, C. Giraud-Audine, F. Giraud, M. Amberg, and B. Lemaire-Semail, "Enhancing variable friction tactile display using an ultrasonic travelling wave", *IEEE transactions on haptics*, vol. 10, no. 2, pp. 296–301, 2016.

[36] C. Zhao, *Ultrasonic motors: technologies and applications*. Springer Science & Business Media, 2011.

[37] M. Biet, F. Giraud, F. Martinot, and B. Semail, "A Piezoelectric Tactile Display Using Travelling Lamb Wave", in *EuroHaptics Conference*, Jul. 2006, pp. 567, 570.

[38] D. Gueorguiev, A. Kaci, M. Amberg, F. Giraud, and B. Lemaire-Semail, "Travelling ultrasonic wave enhances keyclick sensation", in *Haptics: Science, Technology, and Applications: 11th International Conference, EuroHaptics 2018, Pisa, Italy, June 13-16, 2018, Proceedings, Part II 11*, Springer, 2018, pp. 302–312.

[39] L. B. Rosenberg, "Virtual fixtures: Perceptual tools for telerobotic manipulation", in *Proceedings of IEEE virtual reality annual international symposium*, Ieee, 1993, pp. 76–82.

[40] K. Salisbury, D. Brock, T. Massie, N. Swarup, and C. Zilles, "Haptic rendering: Programming touch interaction with virtual objects", in *Proceedings of the 1995 symposium on Interactive 3D graphics*, 1995, pp. 123–130.

[41] J. Ren, K. A. McIsaac, R. V. Patel, and T. M. Peters, "A potential field model using generalized sigmoid functions", *IEEE Transactions on Systems, Man, and Cybernetics, Part B (Cybernetics)*, vol. 37, no. 2, pp. 477–484, 2007.

[42] M. Kuribayashi, S. Ueha, and E. Mori, "Excitation conditions of flexural traveling waves for a reversible ultrasonic linear motor", *J. Acoust. Soc. Am.*, vol. 77, no. 4, pp. 1431–1435, Apr. 1985, ISSN: 0001-4966. DOI: 10.1121/1.392037.

[43] M. Biet, F. Giraud, F. Martinot, and B. Semail, "A piezoelectric tactile display using travelling lamb wave", 2006.

[44] A. Q. Keemink, R. I. Fierkens, J. Lobo-Prat, *et al.*, "Using position dependent damping forces around reaching targets for transporting heavy objects: A fitts' law approach", in *2016 6th IEEE International Conference on Biomedical Robotics and Biomechatronics (BioRob)*, IEEE, 2016, pp. 1323–1329.

2

LITERATURE REVIEW

Thanks to an exceptional sensorimotor integration, humans excel at manipulation tasks such as grasping, reaching, and throwing, . Given the critical role of haptic perception in manipulation, researchers have long sought to provide relevant haptic feedback to facilitate the control of devices in remote or virtual environments without restricting the operator's movements. Recently, surface haptics has emerged as a promising approach to restore tangibility into touch-based interfaces, such as touchscreens and touchpads. A solid understanding of how force feedback affects human behavior, as well as the range of tactile feedback that state-of-the-art surface haptics can provide, is essential for designing effective surface haptic interfaces and guidance principles that enhance user performance. With this aim, this chapter reviews three key areas:

1. **Sensorimotor integration in human manipulation**: This section explores the human sense of touch and kinesthesia, the role of forward modeling in sensorimotor integration, and the influence of motor learning on movement control.

2. **Haptic guidance principles in force feedback**: This section examines the principles and implementations of haptic guidance, including virtual fixtures in both static and dynamic environments.

3. **Haptic feedback mechanisms in surface haptics**: This section introduces surface haptics as an emerging technology in human-machine interaction. It covers the underlying mechanisms, applications, and prior studies aimed at enhancing user performance through fingertip feedback.

2.1. HUMAN SENSORIMOTOR LOOP

HUMANS exhibit remarkable dexterity, such as effortlessly manipulating objects and exploring their surroundings haptically through the hands and fingers. Central to this ability is a complex interplay between mechanoreceptors and motor systems. This system integrates haptic feedback and motor actions, allowing for precise and adaptive control of movements. In this section, I will outline the biological foundations of human touch sensation, focusing on their roles in the sensorimotor loop that enables dexterous manipulation, and then gain insight into how the integration of sensory feedback with motor control allows for refined actions, such as grasping and manipulating objects, with learning models.

2.1.1. HUMAN SENSE OF TOUCH

The sense of touch can be categorized into two types. The first, known as the **cutaneous sense**, is associated with skin deformation and detects stimuli such as pressure and vibration. The second, **proprioception**, receives sensory inputs from muscles, tendons, and joints, providing information about body position and movement. Unlike other human senses, which are located to specific organs, touch sensation is distributed throughout the body and cannot be consciously deactivated. This distributed nature plays a crucial role in enabling humans to interact with the environment and coordinate motor actions.

The cutaneous sense is essential for finger-surface interactions, which are integral to everyday tasks such as dexterous use of tools and texture exploration. The precise

and rapid perception of tactile information is made possible by the complex structure of the fingertip and the cutaneous mechanoreceptors embedded within the skin. These specialized receptors convert mechanical vibrations into electrical signals, enabling the nervous system to interpret and respond to tactile stimuli effectively.

Mechanoreceptors in the glabrous skin are classified into two types based on their structures: free nerve endings and encapsulated nerve endings. Free nerve endings are responsible for detecting sensations such as touch, pressure, stretch, as well as tickling and itching. [1]. The encapsulated mechanoreceptors, on the other hand, include four types: Merkel corpuscles (Merkel discs), Ruffini corpuscles (bulbous corpuscles), Meissner corpuscles (tactile corpuscles) and Pacinian corpuscles or Vater-Pacinian corpuscles (Lamellar corpuscles). These mechanoreceptors differ in their rate of adaptation and the size of their receptive fields, which correspond to their specific roles in detecting mechanical stimuli.

When a mechanoreceptor detects a stimulus, it responds by firing impulses at an increased frequency. However, this heightened activity diminishes over time as the receptor adapts and returns to its baseline firing rate. The rate of adaptation differentiates mechanoreceptors into two categories: slow-adapting and fast-adapting receptors. Slow-adapting mechanoreceptors are Merkel discs and Ruffini corpuscles. They maintain their response to sustained stimuli over longer periods. Fast-adapting mechanoreceptors include Meissner corpuscles [2] and Pacinian corpuscles [3]. They respond rapidly to changes in stimuli but quickly return to their baseline state.

The receptive field refers to the region on the skin where mechanical stimuli can evoke a sensory response. The size of the receptive field determines the spatial resolution of tactile perception. Mechanoreceptors are further categorized into Type I and Type II based on their receptive field sizes. Type I mechanoreceptors, including Merkel corpuscles [4] and Meissner corpuscles [5], have small receptive fields and are densely distributed in areas requiring high tactile acuity, such as fingertips and lips. Type II mechanoreceptors, including Ruffini corpuscles and Pacinian corpuscles, have larger receptive fields and are primarily found in regions with lower tactile acuity.

The properties of mechanoreceptors are closely linked to their functional roles in tactile perception. For example, Pacinian corpuscles are responsive for detecting events acting on handheld objects, due to their properties of fast-adapting and relatively large receptive field (RA-II type). Perceptual functions of each mechanoreceptors type, along with their associated properties, are listed in Tab. 2.1.

Proprioception, one of the most important human senses, detects body position and movements. This sense is mediated by proprioceptors, located primarily in muscles, tendons, and joints [6]. Proprioception enables automatic or subconscious movements, such as walking or reaching to scratch an itch on our body. Additionally, proprioception is also essential to *learned movement patterns*, such as playing musical instruments or playing sports. These skills require deliberate practice to fine-tune these skills and build "muscle memory". For example, a pianist relies on proprioceptive input to perfect finger placement during repetitive practice, This repeated use of proprioceptive feedback strengthens neural circuits, leading to smoother, automatic actions.

mechanoreceptors	afferent type	response properties	perception function
Merkel	SA-I	sensitive to low-frequency dynamic skin deformations (< 5 Hz) and static force	texture perception, sus -tained pressure
Ruffini	SA-II	sensitive to static force, detect tension deep in the skin, respond to skin sketch.	static force, e.g. static grasping
Meissner	RA-I	sensitive to dynamic skin deformation of ~5-50 Hz, produce transient resp -onses to the onset ond offset of sti -mulation.	low frequency vibration, spatial discontinuities
Pacinian	RA-II	sensitive to high-frequency vibrations (~40-400Hz)	high frequency vibration, events acting on hand -held objects

Table 2.1: Summary of mechanoreceptors, their properties, and perceptual functions.

2.1.2. SENSORIMOTOR INTEGRATION

Reaching a target or grasping an object are fundamental motor tasks that humans perform rapidly and effortlessly in daily life. These tasks require the central nervous system (CNS) to plan actions by comparing the current motor state (such as hand position and velocity) with the targeted state (such as reaching a point or safely grasping an object). Given the prevalence of feedback control, one may ask if the CNS estimates the motor state purely through sensory information (visual, proprioceptive, and cutaneous cues).

Sensory feedback, however, is limited by physiological delays. For example, in a reaching task, it takes around 80–100 ms for visual or proprioceptive signals to influence ongoing movement, which is substantial compared to the typical movement duration of 300–700 ms [7]. Relying on sensory feedback alone to correct deviations would result in unstable and inaccurate movements. Therefore, motor control is thought to depend on a predictive internal model within the cerebellum, which estimates the motor state with minimal delay. This internal model integrates both sensory feedback (sensory inflow) and non-sensory feedback (motor outflow) to provide stable, rapid state estimation, supporting fast and well-coordinated movements. Below, I will illustrate these processes using two common motor tasks: target-directed reaching and object grasping.

Fast reaching movements. When reaching for a visible target, a motor plan is first developed through an inverse model. This inverse model has knowledge of the arm's dynamics and uses it to calculate the motor command based on the initial hand and target position. During movement, an internal forward model is generated. When a motor command is sent to the muscles, a "copy" of this command (known as an efference copy) is also sent to the model to produce a predicted motor state. This internal forward model allows the CNS to predict the endpoint location without waiting for the sensory input. This process allows for real-time adjustments of ongoing motor command through this non-sensory feedback loop.

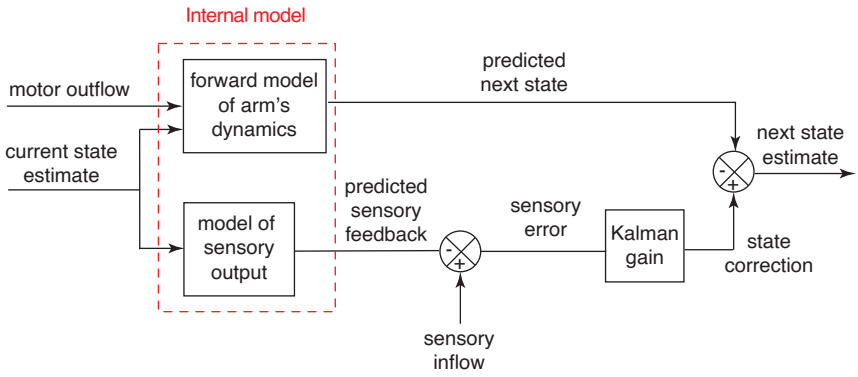

Figure 2.1: A schematic showing the internal model that uses the Kalman filter consists of two feedback processes: a non-sensory feedback process (upper part) and a sensory feedback process. The figure is modified from [8]

However, estimation based purely on motor outflow (known as "dead reckoning") lacks precision. Accurate motor state estimation also requires sensory feedback to correct estimation errors and refine the internal model. Therefore, another process in the model predicts sensory outputs (proprioceptive and visual feedback) based on the current state estimate. When sensory input is received, the difference between predicted and actual sensory feedback generates an error signal. This error signal corrects the state estimate, reducing drift in accuracy over time. The relative contributions of forward model predictions and sensory feedback are dynamically balanced by a Kalman gain, which dynamically adjusts based on the reliability of each source[8]. Accurate predictions of the motor state by the internal model provide reliable foundations for the CNS to generate corrective commands, which are based on the difference between the estimated state and the target location, as illustrated in Fig. 2.2. The influence of error signals in adjusting the command signal varies at different stages of reaching (e.g., initial and final stages). In the early phase, the motor command is based on an approximate target estimate, and an initial target foveation does not affect the accuracy in the final state. Instead, the motor plan is adjusted online during the course of the movement if the target remains visible. In a series of human behavior experiments, Prablanc et al. used a "target jump" paradigm, in which the target position shifted mid-movement [9]. They found that participants could smoothly adjust their hand trajectory toward the new target with minimal delay. This suggests that even at the initial stage of reaching, motor commands are not strictly preprogrammed (i.e., not purely ballistic) but are dynamically adjusted based on feedback.

In summary, sensorimotor integration during fast-reaching movements involves issuing an initial motor plan based on a rough distance estimate before movement onset, followed by dynamic adjustments during movement based on target discrepancy. Throughout the movement, to ensure an accurate yet rapid motor state estimate, an internal forward model integrates both motor outflow and sensory inflow.

Objects grasping. Reaching and grasping are fundamental components of object

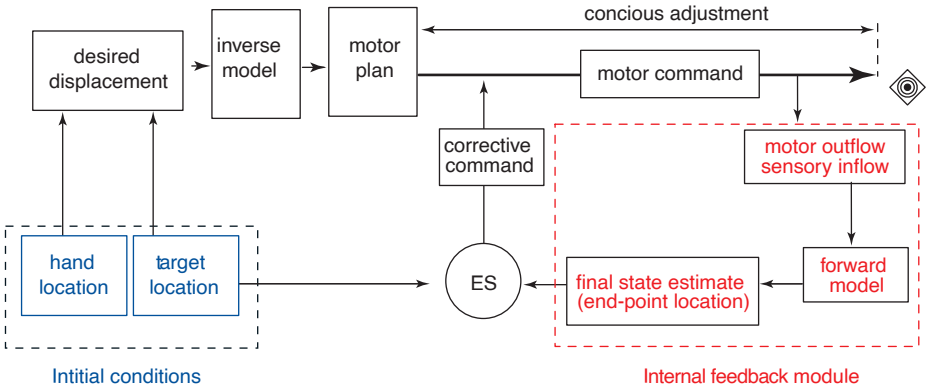

Figure 2.2: Hand movement control using an internal model of arm dynamics. The figure is modified from [10]

manipulation. Unlike reaching, which primarily relies on visual and proprioceptive cues, object grasping depends heavily on cutaneous feedback once the object has been reached. Grasping a stationary object on a surface can be divided into three phases: the pre-load phase, the loading phase, and the lifting phase.

During the pre-load phase, an initial grip force is applied based on prior experience with similar objects. This estimated force must be neither excessively large, which would be energy inefficient or risk damaging the object, nor too small, which could cause slippage or failure to hold the object.

Grip force regulation begins the moment the object is first touched, even before lateral forces are applied. Johansson and Westling studied the evolution of grip force when subjects grasped objects of varying masses and textures[11]. They observed that grip force increases more rapidly with slippery surfaces (e.g., silk) compared to rough surfaces (e.g., sandpaper). For objects with differing masses but identical surface textures, grip force increases at the same rate, though higher final forces are required for heavier objects. These findings indicate that the human brain can process tactile information upon initial contact to adjust grip force appropriately. In recent work, Willemet et al. demonstrated that the perception of slipperiness involves radial tensile strain of the skin [12]. This estimation of friction occurs during initial contact, based on skin deformation, before any noticeable slippage takes place.

In the loading phase, both grip force and load force (the upward force required to lift the object) increase simultaneously. During a precision grip, the grip force must be maintained within a range that prevents slippage (if too low) and avoids damaging the object (if too high). Notably, the grip force remains above a safety margin—typically 20% above the minimum grip force required to prevent slippage [13].

In the lifting phase, the object is fully detached from the surface, with the load force balancing the object's gravitational force. Throughout the lifting and holding process, the CNS monitors and adjusts the grip force by making corrections if discrepancies arise between the internal motor predictions and sensory feedback.

2.2. HAPTIC GUIDANCE

2.2.1. STATIC HAPTIC GUIDANCE

Haptic guidance involves applying additional force feedback to human operators interacting with remote or virtual environments to enhance task performance or reduce effort. A simple analogy is the use of a ruler to draw a straight line: the ruler constrains movement, thereby increasing speed, improving precision, and reducing cognitive load.

The first attempt at haptic guidance in physical interaction tasks was made by Rosenberg (1993) [14], who introduced the concept of "virtual fixtures" in teleoperation systems. These virtual fixtures are computer-generated forces that define forbidden regions that human operators cannot enter. When users approach the boundaries of these regions, the system generates a repulsive force that pushes them away. In several configurations of virtual fixtures, Rosenberg tested users' performance in a teleoperated peg-in-hole task. The results demonstrated that force feedback increased performance by up to 70%, marking the first immersive augmented reality system for teleoperation.

These virtual fixtures designed by Rosenberg are forbidden-region based (FRVFs) and operated in an on-off manner. Essentially, users feel a strong force when approaching restricted areas, while they are free to move outside the forbidden region. This straightforward design has since been adapted for various robotic-assisted applications.

For example, robotic surgery is a prominent area where haptic guidance has been in great use. In a knee replacement surgery [15], Davies et al. introduced "active constraints", a parallel concept to virtual fixtures in surgical applications. These constraints impose high stiffness on the robotic manipulator operated by the surgeon, preventing it from cutting into materials or tissues that must remain intact.

Robotic-assisted teleoperation is another area where FRVFs have found significant application. For example, in unmanned aerial vehicle (UAV) control, Zhang et al. proposed a method that provides haptic feedback through a control barrier functions (CBFs) [16]. When a user issues an unsafe control command, the system generates haptic feedback to guide the operator toward the nearest safe input command. This approach allows human operators to maintain full control of the UAV instead of losing the control authority. The study demonstrated that CBF-based haptic feedback improves the operator's ability to safely navigate UAVs and reduces perceived workload. Constraining operators' movements can also benefit motor training in surgery training by reducing cognitive and physical workload while enhancing both speed and accuracy [17], [18].

The other type of virtual fixture is guidance virtual fixtures (GVFs), which attract the manipulator into the desired path [19]. GVFs can be implemented through either **admittance control** or **impedance control** . Admittance control takes the user's applied force as input and generates velocity output, making it particularly useful in cooperative systems [20].

In contrast, impedance-based GVFs are enforced as elastic potential fields, where the output force is generated as a function of position. This type of GVF is often used in teleoperation systems. The potential field approach was initially developed in robotic systems for collision avoidance [21]. In this paradigm, each point in the workspace is assigned a potential value based on the distributions of targets and obstacles. A force field is generated by computing the negative gradient of the potential field, which ensures the force directs the mobile robots toward areas of lower potential.

Salisbury et al. introduced the concept of artificial potential fields to haptic rendering [22]. These fields are constructed in a similar way as in the robotics applications, that is, by combining attractive and repulsive fields to provide guidance. Later, more research addressed the design and evaluations of these fields. Ren et al. proposed a potential function based on a generalized sigmoid function [23]. This model allows intuitive adjustments to the affected area and the abruptness of the potential field near the boundaries of protected zones. In a catheter insertion task, a protective potential field was built with low values at the center of the vessel and high values near the vessel walls. Experimental results demonstrated that the potential fields effectively ensured obstacle avoidance while providing realistic and smooth feedback and guiding users toward targets without collisions. Additionally, the sigmoid function model has been applied to render simulated gear selector levers in automotive applications [24].

2.2.2. DYNAMIC HAPTIC GUIDANCE

Haptic guidance in the previous section assumes that the environment is stable enough for the use of static virtual fixtures. However, these approaches are not well-suited for dynamic systems that evolve over time and space, such as robot-assisted surgery, motor training in dynamic tasks, and vehicle driving. In such dynamic systems, constraint geometries and stiffness are considered to change during operation.

In robotic-assisted surgery, physiological motion (e.g. heartbeat or respiration) can be a disturbance to the safe manipulation of the tissues. In these scenarios, one has to consider moving fixtures instead of fixed ones. One prominent example is beating heart surgery, where the constant motion of the heart significantly alters the geometry of the workspace. To address this, dynamic 3D virtual fixtures have been developed, incorporating both GVFs and FRVFs that were designed with different potential field functions. [25]. These fixtures adapt in real-time to the beating heart, providing surgeons with haptic guidance that constrains hand movements while protecting sensitive tissues. This approach has been validated through several simulated surgical tasks, demonstrating a reduction in user error rates and reduced efforts. Similarly, a forbidden-region-based constraint that moves with the environment was implemented in a teleoperation setup [26]. Human subject experiments revealed that such moving virtual fixtures improve user precision and reduce the force applied during operations.

Dynamic haptic guidance has also been designed for motor training. In such scenarios, robots or machines physically assist the human operator by enforcing a desired pattern of kinematics during movement. This strategy is particularly useful for reducing performance errors in motor tasks where learning through actual practice may be dangerous or expensive, such as teleoperation, surgery, or haptic-assisted assembly. In some cases, haptic guidance is also applied in sports training, like guiding the correct motion path for a golf swing.

While haptic guidance has proven effective in motor training, several studies have shown that it does not always enhance motor learning and may even hinder it. For example, haptic guidance showed little benefit in tasks such as learning approximate posture during cricket bowling [27], manipulating a virtual stick with masses on both ends [28], and learning new movements with robotic assistance [29]. One possible explanation, based on Schmidt & Bjork's learning theory, is that users may become reliant

on the guidance. Since the dynamics of guided tasks differ from those of unguided tasks, the transfer of learning to real-world situations becomes less effective [30]. This creates a paradox: haptic guidance may improve performance during training but can impair learning for independent operation.

To address this challenge, Crespo and Reinkensmeyer proposed an adaptive guidance approach known as "guidance-as-needed" [31]. In this approach, the firmness of the guidance is adjusted based on the user's performance in a steering task. When the trainee performs well, the guidance decreases, encouraging adaptation to real-world, unguided conditions. The results indicated that training with "guidance-as-needed" led to slightly better outcomes than training with fixed guidance. Although the long-term effects of haptic guidance on learning were not evaluated, this method demonstrated the advantages of haptic guidance for short-term learning while limiting performance errors during training.

Another typical implementation requiring dynamic adjustments to haptic guidance based on environmental changes is vehicle driving support systems. Mulder et al. developed a haptic gas pedal that continuously provides feedback during car-following tasks [32]. This interface dynamically adjusts the feedback force or stiffness based on the distance to the lead vehicle. Human experiments conducted in a driving simulator demonstrated that this system enhances performance by improving car-following behavior while reducing control activity.

2.3. SURFACE HAPTICS: TECHNOLOGIES AND APPLICATIONS

WHILE haptic guidance and rendering have been widely implemented in virtual and remote applications using hand-held haptic devices, most daily interactions occur through finger-surface contact. Actions such as holding a glass of water or feeling the texture of a wooden table rely on sensory feedback from the fingertips, where thousands of mechanoreceptors convert mechanical stimuli into neural signals. Considering the importance of finger-surface interaction in manipulation and tactile perception, a new category of technology, known as surface haptics, has emerged. This approach enables control over surface properties and aims to create artificial tactile sensations or provide haptic guidance directly to the fingertip. Friction modulation has been the primary approach in surface haptics, as it is well-suited to the integration of common flat touch-based interfaces, such as touchscreens and touchpads.

This section first introduces several mechanisms that modulate surface friction, with a focus on the approach using ultrasonics, and then introduces recent advancements that modulate active lateral forces. This section concludes with an overview of implementations and applications.

2.3.1. FRICTION MODULATION

Friction modulation in surface haptics is primarily achieved through two mechanisms: ultrasonic lubrication, which reduces friction, and electroadhesion, which increases it. Both mechanisms have been relatively deeply explored.

Surface haptic devices using *ultrasonic lubrication* typically consist of a glass or an aluminum plate, where bending modes are excited to reduce friction between the finger

and the contact surface. This friction-reduction mechanism is notably robust and effective, achieving up to a 95% reduction in friction force experienced by a sliding finger with vibration amplitudes of ±3 μm, as illustrated in Fig. 2.3.

The ultrasonic lubrication effect can be explained by the partial squeeze film levitation theory, proposed by Wiertlewski et al. [33]. When the fingertip touches a vibrating surface, a thin layer of air is trapped between the asperities of the skin and the surface. This trapped air film, along with the plate, supports the pressure applied by the finger. This dynamic levitation increases the average separation between the fingertip asperities and the surface, thereby reducing real contact area and friction.

Piezoelectric actuators, particularly piezoceramic plates, are typically used to drive ultrasonic friction modulation. These actuators are compact, silent, and easily mountable on touchscreens; however, they require high voltage (up to 100 V) and consume a large amount of power by vibrating the entire screen, which limits their use in mobile devices. Additionally, the use of standing waves challenges the localization and uniformity of tactile sensation. Despite these limitations, ultrasonic friction modulation remains promising for grounded devices, such as vending machines, large graphical displays, vehicle dashboards, and home appliances.

To enable localized tactile sensations, one approach is to use phononic crystals, which constrain wave propagation within specific band gaps, thereby localizing friction modulation [34]. Such localization could enable multi-finger interactions or multi-user interactions in large displays while also reducing power consumption.

Electroadhesion, on the other hand, increases friction between the finger and the touch panel through electrostatic actuation. This mechanism applies alternating high voltages to the conductive layer of a capacitive touch panel, generating electrostatic attractive forces in the normal direction. Experimental data show that these electrostatic forces reduce the interfacial gap, allowing more microscopic contact between the finger asperities and the touchscreen surface. This increased contact area results in an enhanced friction force [35]. This principle has been effectively implemented in capacitive touchscreens, such as the TeslaTouch system, which pioneered several HCI applications for electroadhesion-based friction modulation [36]. This approach requires high-voltage circuitry (200–500 V), which increases the cost of the device. However, the key difficulty for the adoption of electroadhesion technology is in demonstrating a clear and compelling user benefit that justifies its implementation in touchscreens.

In recent years, other mechanisms to modulate surface friction have also been explored. Choi et al. proposed a novel approach for friction modulation by locally changing surface temperature [37]. This method leverages a phenomenon where the finger skin becomes softer at a higher temperature (e.g., from room temperature to 25 °C), thereby increasing the contact area between the finger and the surface, which subsequently increases friction. Experimental results show that this thermal modulation can increase finger friction by approximately 50 %, and rendered shapes such as bumps and zones, were clearly discernible. Although the current thermal setup is relatively bulky, it operates at much lower voltages compared to previous methods like ultrasonics or electroadhesion, typically requiring only a few volts.

While tactile sensation arises from the interaction between the fingertip and a surface, rendering tactile feedback is also possible by instrumenting user fingertips instead

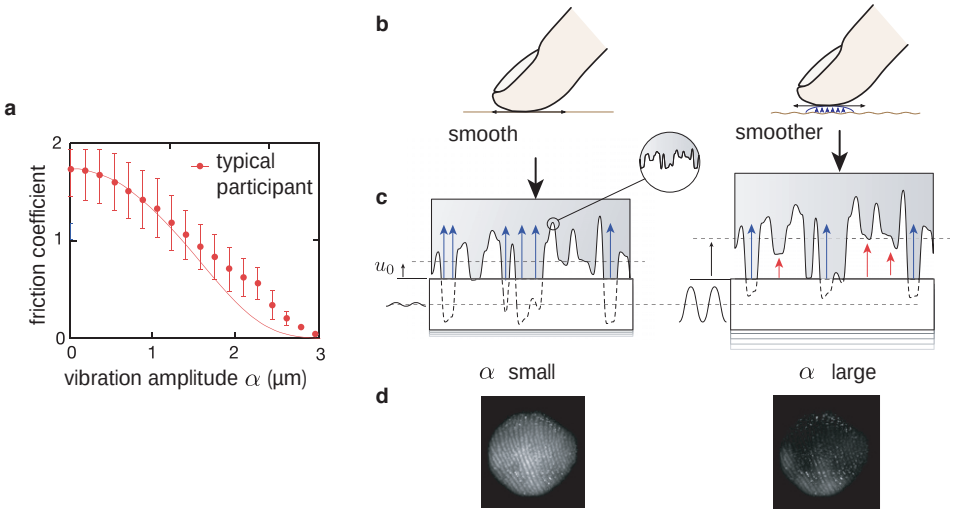

Figure 2.3: The mechanism of ultrasonic friction reduction. (a) The sliding friction coefficient decreases by up to 95% as the vibration amplitude increases to ±3 μm. (b) Illustration of the squeeze film effect: users perceive a smoother surface when it vibrates at ultrasonic frequencies. (c) View of the asperities. At a small vibration, the plate supports the pressing force. At a large vibration, both the plate and the air squeeze film support the pressing force, which also causes a larger interfacial separation. (Figure b is adapted from [40], and figures a, c, and d are adapted from [33].)

of the target surface. Bau and Poupyrev introduced an augmented reality tactile technology called "REVEL", which uses a user-worn device to modulate the tactile perception of real objects [38]. This technology uses a principle, called *reverse electrovibration*, wherein a weak electrical signal, applied anywhere on the user's body, generates an oscillating electrical field around the fingers. Mazursky et al. proposed a user-centered method called "Stick & Slip," which modulates finger-surface friction by applying liquid droplets directly onto the user's fingertip [39]. This finger-worn device coats the fingerpad with liquid droplets, adjusting friction as the finger interacts with different surfaces. Both "REVEL" and "Stick & Slip" enable versatile friction modulation across a wide range of everyday surfaces, making them well-suited for applications in mixed reality contexts.

2.3.2. ACTIVE LATERAL FORCE FEEDBACK

While surface haptics technology traditionally modulates passive lateral forces, i.e. friction, recent advancements have introduced the ability to modulate active lateral forces on the fingertips. Modulating active lateral forces can not only enable a wide range of tactile effects but also hold the potential for implementing guidance principles, as seen in classical haptics, such as the artificial potential field method, within fingertip interaction. This section reviews the state of the art in active surface haptics, as illustrated in Tab. 2.2. To actively push a finger on the surface without net displacements, periodic motions are desired, which send the device to its original position. There are two main approaches: elliptical motions of the surface and asymmetric friction modulation. In the *elliptical motion* approach, the surface points move in elliptical (or circular) trajec-

device	force production	working principle	human subject study	other experiments
LateralPad, 2012	±70 mN	excites both normal and lateral resonance at 22.3 kHz	none	force measurement; demonstrated a “bump”
aluminum beam (Ghenna, et al.), 2017	±100 mN	superimposes two successive flexural modes around 28.4 kHz	direction perception	none
2MoTac, 2020	not specified	excites both longitudal and bending resonances at 34 kHz	key click detection, perception threshold for different aspect ratio	none
ShiverPad, 2010	±100 mN	854 Hz lateral oscillation using voice coil + 39 kHz ultrasonic lubrication	edge tracing	demonstrated “toggle switch”
eShiver, 2017	±450 mN	1000 Hz oscillation using electromagnetic shaker + electroadhesion	none	force measurement
Ultrashiver, 2019	±400 mN	30 kHz lateral oscillation using piezoceremic plates + electroadhesion	none	force measurement, demonstrated Gaussian potenial well
SwitchPad, 2020	±250 mN	22.4 kHz 1st and 53.3 kHz 2nd longitudinal mode for lateral oscillation using piezoceremic discs + electroadhesion	button click detection	force measurement

Table 2.2: Examples of haptic surfaces based on active lateral force feedback and their user studies.

tories, typically with an amplitude of 1–2 micrometers. These relative motions produce frictional forces that propel objects in contact with the surface. One method to generate elliptical motion is by coupling two orthogonal standing wave modes—typically transverse and longitudinal modes—at the same frequency. For example, the Lateralpad device uses piezoelectric actuators to drive normal and lateral resonances on a glass plate at $\tilde{2}2.3$ kHz. By modulating the phase between the two resonances, the force exerted on the finger can be controlled. Similarly, the 2MoTac device produced lateral force by coupling bending and longitudinal resonance and used it to enhance button click sensations [41], [42]. However, generating high force in this approach requires precise matching of the resonant frequencies, which can be sensitive to external perturbations such as finger pressing.

Another approach to producing elliptical motion uses *flexural traveling waves*, which intrinsically cause elliptical motion of surface points, according to the Euler-Bernoulli beam theory. Ghenna et al. produced pseudo-traveling waves in a straight beam through the modal superposition of two adjacent bending modes. However, the working frequency is not in either of the two bending modes, resulting in a modest force production of 100 mN despite power actuators [43].

Generating resonant traveling waves in finite structures is challenging due to reflections at boundaries. One option involves the use of two degenerate modes, which are resonant modes that have different spatial patterns but share the same resonance frequency. When driven with two sinusoidal signals that are temporal out of phase, stable traveling waves are produced. Early attempts demonstrated that placing a finger on a commercial ultrasonic motor could feel a strong propelling sensation [44], which has since been applied to create button-click sensations [45]. While these motors are highly efficient due to resonance and can produce large forces, their circular surfaces and uneven teeth are unsuitable for touch interaction. Therefore, a flat traveling-wave-based haptic interface is desired.

The alternative to creating net lateral force is asymmetric friction modulation, which synchronizes in-plane oscillations with friction modulation (using ultrasonic lubrication or electro-adhesion). In essence, this approach creates different levels of friction as the plate oscillates in different directions within each cycle. For example, friction can be set high when the plate moves rightward and low when it moves leftward, producing a net rightward lateral force over one cycle. In this approach, lateral oscillations can be generated using a voice coil, as in ShiverPad [46], or an electromagnetic shaker, as in eShiver [47], both of which operate at around 1000 Hz. Although this approach can generate relatively large lateral forces (up to $\pm$450 mN), it suffers from audible noise due to low-frequency oscillations. UltraShiver mitigated this noise issue by vibrating the plate at an ultrasonic frequency ($\tilde{3}0$ kHz) [48]. However, Ultrashiver relied on a single longitudinal resonance to produce oscillations, and therefore force generation becomes null at the nodal lines of the resonant mode, resulting in an inconsistent force profile. SwitchPad addresses this by dynamically switching between the first and second longitudinal modes based on finger position. Specifically, when the force production by the first mode is weaker than that of the second mode, the device switches to the second mode. This switching strategy achieved a more consistent force profile with a maximum lateral force of 250 mN. This approach using asymmetric friction, however, requires a

complex system to modulate passive lateral force while actively oscillating the device.

2.3.3. SURFACE HAPTICS APPLICATIONS

Current touch-based devices, such as smartphones and tablets, rely solely on visual and auditory feedback, limiting realism and functionality when interacting with digital content. Surface haptics introduces tactile feedback to these flat interfaces, showing promising results in enhancing user performance and experience across metrics such as realism, enjoyment, confidence, and concentration. This section reviews implementations in texture and shape rendering, haptic guidance for targeting, haptic control design, and other applications.

Tactile rendering in surface haptics includes texture rendering and shape rendering. Texture rendering is used to simulate material properties, while shape rendering augments displayed graphical content and surface features.

Texture rendering. Since textures are perceived by humans through active exploration, friction modulation is well-suited for texture rendering due to its intrinsic passive property and its capability to render high frequency. By varying the friction as a function of finger position, spatial features of textures can be directly mapped onto the distribution of friction on a touch surface [38], [49], [50]. For fine textures, position-based rendering may be ineffective, as these artificially registered textures can be challenging to perceive. Instead, velocity-based rendering offers a more effective alternative [49] . Other methods for simulating textures include data-driven approaches and the use of local gradients. In the data-driven approach, the friction profile is modeled based on data collected from probes sliding over real textures [51]–[53]. Mapping the local gradients of an image to the frequency and amplitude of the driving signals are also effective in rendering high-realism textures [54].

Shape rendering. Macro shapes, such as bumps, holes, and other surface features, can be rendered based on the lateral force principle, which was established in the early work of Minsky et al. [55] and Robles-De-La-Torre and Hayward [56]. They demonstrated that rendering lateral forces as the gradient of 3D shapes (e.g., bumps and holes) provides users with a haptic illusion corresponding to the perceived geometry. This principle can be directly applied in active force surface displays capable of both pushing and pulling the finger to simulate going up and down over a "bump". For instance, LateralPad demonstrated the sensation of a "bump" by varying lateral force, though no user studies were conducted [57]. Similarly, UltraShiver simulated a "hole" through this method [48].

In friction modulation displays cannot directly map local gradients to lateral forces, as they only provide resistance. Kim et al. proposed an algorithm that maps the dot product of the local gradient and the unit vector of finger velocity onto the friction in an electroadhesion display [58]. The effectiveness of this algorithm was validated with user studies.

While bumps and holes are common 3D features, perceiving shapes with edges is more common in everyday interactions, such as searching for keys, finding the end of a tape, distinguishing coins, or touching the edges of leaves. Friction modulation has limited effectiveness in rendering edge sensations, as it changes friction across the entire touch surface without localized feedback. In a user study, Xu et al. noted that the

lack of edge-specific feeling might lead to low detection rates for geometric 2D shapes, such as squares and triangles that were rendered through abrupt friction changes in their approach [59]. In contrast, net lateral forces have proven effective for rendering virtual contours by generating forces orthogonal to finger movement [46].

Haptic guidance. Haptic guidance on surfaces involves directing users to a target quickly and precisely. Pointing interaction is a common task in various touch interfaces, including smartphones, laptops, and tablets. This task includes diverse actions, such as moving a cursor to an icon, scrolling to set an alarm, and performing drag-and-drop operations on mobile devices. Human performance in pointing tasks typically follows Fitts' law [60], and adding haptic feedback has been shown to enhance the user experience. However, despite extensive research on creating effective haptic feedback with handheld devices [61], the implementation of tactile feedback in touch interfaces remains limited, mainly due to challenges in providing feedback on flat surfaces and controlling cutaneous stimuli.

Friction modulation has been implemented to enhance pointing tasks by proving variable friction. A simple way is to provide a binary friction profile that is high on the target and low friction elsewhere, offering users a sudden change in resistance upon reaching the target. Studies show its effectiveness in ultrasonic devices [40], [62], [63] and eletroadhesion devices [64], resulting in a 7–9% reduction in task completion time, compared to solely based on visual feedback. However, friction-based feedback only informs users when they have reached a target but does not guide them throughout their movement. Active force feedback devices could potentially address these limitations by offering continuous directional guidance. To date, no studies have investigated the use of active lateral force feedback for target acquisition on touch displays.

Virtual controls. Virtual controls are widely used in electronic interfaces. They are favored by manufacturers for their design flexibility and the sleek, compact appearance they enable. However, the lack of haptic feedback their physical counterparts offer is known to reduce user performance and degrade user experience, as it disrupts muscle memory and increases visual load. Today, vibrotactile feedback—the most developed haptic technology—has improved the experience of virtual controls by introducing some degree of tactile sensation (see a review paper [65]). Due to actuator limitations, however, vibrotactile feedback is mainly seen in mobile devices such as smartphones and smartwatches, with limited use in larger displays. Additionally, vibrotactile provides a transient stimulus instead of continuous feedback, far from offering realistic sensation and functionality compared to physical controls. Surface haptics, which modulate friction or active lateral forces, could enhance the tangibility of virtual controls. The use of surface haptics to design haptic controls, such as buttons, sliders, and toggle switches, is discussed here.

Buttons offer the simplest form of interaction, "selection," and are ubiquitous in human-machine interfaces. Haptic feedback in these physical buttons plays a key role in building muscle memory that allows users to use them effortlessly and unconsciously, even in high-frequency tasks such as typing. The absence of haptic feedback in touchscreen interfaces disrupts this reflex and requires significant visual attention, which can overload visual processing or present usability challenges, particularly for visually impaired users.

Simulating button clicks through ultrasonic friction modulation is based on an observation where users perceive an illusion of a descending surface when friction is abruptly reduced [66]. Early implementation on an ultrasonic plate was achieved by Tashiro et al., who used rapid friction changes to simulate the buckling and restitution of a mechanical button [67]. Later, psychophysical experiments showed that the perception threshold of a friction change is much lower in the case of decreasing than increasing for a stationary finger [68]. Monnoyer et al. attributed the sensation of "ultrasonic switches" to an accumulation of stress and a sudden release in the fingerpad, causing a large discontinuity of the mechanical impedance, which is similar to the buckling of physical buttons [69].

However, creating a realistic button-click sensation through ultrasonic friction modulation requires several times higher vibration amplitudes than those required to perceive frictional changes with a sliding finger [70]. The reliability of detection can also be influenced by the natural impedance of the finger. For instance, users with fingers of extreme impedance may find it difficult to perceive. By contrast, net tangential forces can potentially induce a larger impedance change by both pushing and pulling the finger skin.

Gueorguiev et al. simulated button clicks by switching the traveling waves in an ultrasonic motor at two predefined thresholds of normal force, achieving a lower perception threshold for clicks than friction modulation alone [45]. Garcia et al. implemented this approach to simulate button clicks in a beam by superimposing a longitudinal and a bending wave [41], [42]. Yet, these button clicks are not localized, as ultrasonic devices naturally produce sensations uniformly across surfaces. Xu et al. proposed a localized button-click sensation by switching the lateral force direction using an active force feedback device UltraShiver [71]. Such localizable button clicks allow for multi-finger and multi-user interactions and, importantly, hold promise for applications such as touch-typing keyboards.

Despite these implementations of realistic button-click sensations discussed above, most studies focus on the mechanisms behind these sensations, perception thresholds, and subjective experiences. However, quantitative evaluations of the impacts of artificial button-click sensations on real interaction tasks, such as typing, are still limited.

Other virtual controls include sliding controls such as sliders, knobs, and toggle switches. These controls require users' relative motion and surface haptics can be designed to provide feedback when a certain distance has been traveled. Levesque et al. simulated the feeling of rotating the wheels of an alarm clock with programmable friction in an ultrasonic plate [62]. In subsequent work, they examined the design space for these scrolling interactions with quantitative evaluations [72]. Later, Giraud et al. designed a haptic knob using ultrasonic friction modulation and observed improvements in task accuracy [73]. Bernard et al. proposed a haptic slider that has gradual tactile feedback provided by an ultrasonic plate. After training with visual and auditory feedback, users could set a value without looking at the screen [74].

While friction modulation is effective for discrete tactile feedback in knobs, creating a realistic sensation of a toggle switch may require active forces to attract users to the two stable wells or resting positions. The ShivePad, for example, simulated the tactile feeling of flipping a toggle switch by generating two potential fields, comprised of line sources and sinks [46].

Applications design. Various applications that use surface haptics in human-computer interaction (HCI) have been demonstrated. They showcased many benefits of adding tangibility to touch surfaces and inspired further potential uses.

One major objective of these applications is to augment the realism of visual content. A variety of implementations illustrate this purpose, such as simulating different textures [36], replicating the sensation of rubbing on a canvas [36], simulating the impact of a ball hitting a surface in a game [62], and adding tactile elements to children's books (e.g., fur or fabric textures) [75]. The addition of tactile feeling to these visuals improves the enjoyment and engagement during interaction and, importantly, allows for a heightened sense of the existence of virtual elements, supporting a more immersive virtual reality experience.

Another significant aim of these applications is to improve user performance in low-level interaction tasks. By incorporating tactile feedback, these tasks can be performed with greater speed, precision, and often with reduced visual attention. Examples include file drag-and-drop manipulation [36], [62], text editing [62], slider adjustments [74], dial tuning [75], and image editing [36]. These tasks benefit from surface haptics with greater enjoyment, engagement, and a more realistic interaction experience. Surface haptics have also been developed to assist visually impaired individuals in interacting with and interpreting digital information, as well as in various assistive applications [76]. Lastly, surface haptic has also been explored in social touch applications, such as communicating literal texture, emotional information, or experiences to a partner [77].

REFERENCES

[1] G. J. Tortora and B. H. Derrickson, *Principles of anatomy and physiology*. John Wiley & Sons, 2018.

[2] R. S. Johansson, U. Landstro, R. Lundstro, *et al.*, "Responses of mechanoreceptive afferent units in the glabrous skin of the human hand to sinusoidal skin displacements", *Brain research*, vol. 244, no. 1, pp. 17–25, 1982.

[3] R. T. Verrillo, "Investigation of some parameters of the cutaneous threshold for vibration", *The Journal of the Acoustical Society of America*, vol. 34, no. 11, pp. 1768–1773, 1962.

[4] R. S. Johansson and J. R. Flanagan, "Coding and use of tactile signals from the fingertips in object manipulation tasks", *Nature Reviews Neuroscience*, vol. 10, no. 5, pp. 345–359, 2009.

[5] M. A. Srinivasan, J. Whitehouse, and R. H. LaMotte, "Tactile detection of slip: Surface microgeometry and peripheral neural codes", *Journal of neurophysiology*, vol. 63, no. 6, pp. 1323–1332, 1990.

[6] J. C. Tuthill and E. Azim, "Proprioception", *Current Biology*, vol. 28, no. 5, R194–R203, 2018.

[7] J. Paillard, "Fast and slow feedback loops for the visual correction of spatial errors in a pointing task: A reappraisal", *Canadian journal of physiology and pharmacology*, vol. 74, no. 4, pp. 401–417, 1996.

[8] D. M. Wolpert, Z. Ghahramani, and M. I. Jordan, "An internal model for sensorimotor integration", *Science*, vol. 269, no. 5232, pp. 1880–1882, 1995.

[9] C. Prablanc and O. Martin, "Automatic control during hand reaching at undetected two-dimensional target displacements", *Journal of neurophysiology*, vol. 67, no. 2, pp. 455–469, 1992.

[10] M. Desmurget and S. Grafton, "Forward modeling allows feedback control for fast reaching movements", *Trends in cognitive sciences*, vol. 4, no. 11, pp. 423–431, 2000.

[11] R. S. Johansson and G. Westling, "Roles of glabrous skin receptors and sensorimotor memory in automatic control of precision grip when lifting rougher or more slippery objects", *Experimental brain research*, vol. 56, pp. 550–564, 1984.

[12] L. Willemet, K. Kanzari, J. Monnoyer, I. Birznieks, and M. Wiertlewski, "Initial contact shapes the perception of friction", *Proceedings of the National Academy of Sciences*, vol. 118, no. 49, e2109109118, 2021.

[13] B. B. Edin, G. Westling, and R. S. Johansson, "Independent control of human fingertip forces at individual digits during precision lifting.", *The Journal of physiology*, vol. 450, no. 1, pp. 547–564, 1992.

[14] L. B. Rosenberg, "Virtual fixtures: Perceptual tools for telerobotic manipulation", in *Proceedings of IEEE virtual reality annual international symposium*, Ieee, 1993, pp. 76–82.

[15] B. Davies, M. Jakopec, S. J. Harris, *et al.*, "Active-constraint robotics for surgery", *Proceedings of the IEEE*, vol. 94, no. 9, pp. 1696–1704, 2006.

[16] D. Zhang, G. Yang, and R. P. Khurshid, "Haptic teleoperation of uavs through control barrier functions", *IEEE transactions on haptics*, vol. 13, no. 1, pp. 109–115, 2020.

[17] S. Payandeh and Z. Stanisic, "On application of virtual fixtures as an aid for telemanipulation and training", in *Proceedings 10th Symposium on Haptic Interfaces for Virtual Environment and Teleoperator Systems. HAPTICS 2002*, IEEE, 2002, pp. 18–23.

[18] M. Hong and J. W. Rozenblit, "A haptic guidance system for computer-assisted surgical training using virtual fixtures", in *2016 IEEE International conference on systems, man, and cybernetics (SMC)*, IEEE, 2016, pp. 002 230–002 235.

[19] J. J. Abbott, P. Marayong, and A. M. Okamura, "Haptic virtual fixtures for robot-assisted manipulation", in *Robotics Research: Results of the 12th International Symposium ISRR*, Springer, 2007, pp. 49–64.

[20] P. Marayong and A. M. Okamura, "Speed-accuracy characteristics of human-machine cooperative manipulation using virtual fixtures with variable admittance", *Human Factors*, vol. 46, no. 3, pp. 518–532, 2004.

[21] J.-O. Kim and P. Khosla, "Real-time obstacle avoidance using harmonic potential functions", 1992.

[22] K. Salisbury, D. Brock, T. Massie, N. Swarup, and C. Zilles, "Haptic rendering: Programming touch interaction with virtual objects", in *Proceedings of the 1995 symposium on Interactive 3D graphics*, 1995, pp. 123–130.

[23] J. Ren, K. A. McIsaac, R. V. Patel, and T. M. Peters, "A potential field model using generalized sigmoid functions", *IEEE Transactions on Systems, Man, and Cybernetics, Part B (Cybernetics)*, vol. 37, no. 2, pp. 477–484, 2007.

[24] E. Garcia–Canseco, A. Ayemlong–Fokem, A. Serrarens, and M. Steinbuch, "Haptic simulation of a gear selector lever using artificial potential fields", *IFAC Proceedings Volumes*, vol. 43, no. 13, pp. 426–429, 2010.

[25] J. Ren, R. V. Patel, K. A. McIsaac, G. Guiraudon, and T. M. Peters, "Dynamic 3-d virtual fixtures for minimally invasive beating heart procedures", *IEEE transactions on medical imaging*, vol. 27, no. 8, pp. 1061–1070, 2008.

[26] T. L. Gibo, L. N. Verner, D. D. Yuh, and A. M. Okamura, "Design considerations and human-machine performance of moving virtual fixtures", in *2009 IEEE International Conference on Robotics and Automation*, IEEE, 2009, pp. 671–676.

[27] R. Wallis, B. Elliott, and M. Koh, "The effect of a fast bowling harness in cricket: An intervention study", *Journal of sports sciences*, vol. 20, no. 6, pp. 495–506, 2002.

[28] M. K. O'Malley, A. Gupta, M. Gen, and Y. Li, "Shared control in haptic systems for performance enhancement and training", *Journal of Dynamic Systems, Measurement, and Control*, 2006.

[29] J. Liu, S. Cramer, and D. Reinkensmeyer, "Learning to perform a new movement with robotic assistance: Comparison of haptic guidance and visual demonstration", *Journal of neuroengineering and rehabilitation*, vol. 3, pp. 1–10, 2006.

[30] R. A. Schmidt and R. A. Bjork, "New conceptualizations of practice: Common principles in three paradigms suggest new concepts for training", *Psychological science*, vol. 3, no. 4, pp. 207–218, 1992.

[31] L. M. Crespo and D. J. Reinkensmeyer, "Haptic guidance can enhance motor learning of a steering task", *Journal of motor behavior*, vol. 40, no. 6, pp. 545–557, 2008.

[32] M. Mulder, M. Mulder, M. Van Paassen, and D. Abbink, "Haptic gas pedal feedback", *Ergonomics*, vol. 51, no. 11, pp. 1710–1720, 2008.

[33] M. Wiertlewski, R. Fenton Friesen, and J. E. Colgate, "Partial squeeze film levitation modulates fingertip friction", *Proceedings of the national academy of sciences*, vol. 113, no. 33, pp. 9210–9215, 2016.

[34] T. Daunizeau, D. Gueorguiev, S. Haliyo, and V. Hayward, "Phononic crystals applied to localised surface haptics", *IEEE Transactions on Haptics*, vol. 14, no. 3, pp. 668–674, 2021.

[35] M. Ayyildiz, M. Scaraggi, O. Sirin, C. Basdogan, and B. N. Persson, "Contact mechanics between the human finger and a touchscreen under electroadhesion", *Proceedings of the National Academy of Sciences*, vol. 115, no. 50, pp. 12 668–12 673, 2018.

[36] O. Bau, I. Poupyrev, A. Israr, and C. Harrison, "Teslatouch: Electrovibration for touch surfaces", in *Proceedings of the 23nd annual ACM symposium on User interface software and technology*, 2010, pp. 283–292.

[37] C. Choi, Y. Ma, X. Li, *et al.*, "Surface haptic rendering of virtual shapes through change in surface temperature", *Science Robotics*, vol. 7, no. 63, eabl4543, 2022.

[38] O. Bau and I. Poupyrev, "Revel: Tactile feedback technology for augmented reality", *ACM Transactions on Graphics (TOG)*, vol. 31, no. 4, pp. 1–11, 2012.

[39] A. Mazursky, J. Serfaty, and P. Lopes, "Stick&slip: Altering fingerpad friction via liquid coatings", in *Proceedings of the CHI Conference on Human Factors in Computing Systems*, 2024, pp. 1–14.

[40] G. Casiez, N. Roussel, R. Vanbelleghem, and F. Giraud, "Surfpad: Riding towards targets on a squeeze film effect", in *Proceedings of the SIGCHI Conference on Human Factors in Computing Systems*, 2011, pp. 2491–2500.

[41] P. Garcia, F. Giraud, B. Lemaire-Semail, M. Rupin, and M. Amberg, "2motac: Simulation of button click by superposition of two ultrasonic plate waves", in *Haptics: Science, Technology, Applications: 12th International Conference, EuroHaptics 2020, Leiden, The Netherlands, September 6–9, 2020, Proceedings 12*, Springer, 2020, pp. 343–352.

[42] P. Garcia, F. Giraud, B. Lemaire-Semail, M. Rupin, and A. Kaci, "Control of an ultrasonic haptic interface for button simulation", *Sensors and Actuators A: Physical*, vol. 342, p. 113 624, 2022.

[43] S. Ghenna, E. Vezzoli, C. Giraud-Audine, F. Giraud, M. Amberg, and B. Lemaire-Semail, "Enhancing variable friction tactile display using an ultrasonic travelling wave", *IEEE transactions on haptics*, vol. 10, no. 2, pp. 296–301, 2016.

[44] M. Biet, F. Giraud, F. Martinot, and B. Semail, "A piezoelectric tactile display using travelling lamb wave", 2006.

[45] D. Gueorguiev, A. Kaci, M. Amberg, F. Giraud, and B. Lemaire-Semail, "Travelling ultrasonic wave enhances keyclick sensation", in *Haptics: Science, Technology, and Applications: 11th International Conference, EuroHaptics 2018, Pisa, Italy, June 13-16, 2018, Proceedings, Part II 11*, Springer, 2018, pp. 302–312.

[46] E. C. Chubb, J. E. Colgate, and M. A. Peshkin, "Shiverpad: A glass haptic surface that produces shear force on a bare finger", *IEEE Transactions on Haptics*, vol. 3, no. 3, pp. 189–198, 2010.

[47] J. Mullenbach, M. Peshkin, and J. E. Colgate, "Eshiver: Lateral force feedback on fingertips through oscillatory motion of an electroadhesive surface", *IEEE transactions on haptics*, vol. 10, no. 3, pp. 358–370, 2016.

[48] H. Xu, M. A. Peshkin, and J. E. Colgate, "Ultrashiver: Lateral force feedback on a bare fingertip via ultrasonic oscillation and electroadhesion", *IEEE transactions on haptics*, vol. 12, no. 4, pp. 497–507, 2019.

[49] V. Levesque and J. M. Cruz-Hernandez, *Method and apparatus for simulating surface features on a user interface with haptic effects*, US Patent 9,196,134, Nov. 2015.

[50] M. Wiertlewski, D. Leonardis, D. J. Meyer, M. A. Peshkin, and J. E. Colgate, "A high-fidelity surface-haptic device for texture rendering on bare finger", in *International Conference on Human Haptic Sensing and Touch Enabled Computer Applications*, Springer, 2014, pp. 241–248.

[51] J. Jiao, Y. Zhang, D. Wang, *et al.*, "Data-driven rendering of fabric textures on electrostatic tactile displays", in *2018 IEEE Haptics Symposium (HAPTICS)*, IEEE, 2018, pp. 169–174.

[52] R. H. Osgouei, J. R. Kim, and S. Choi, "Data-driven texture modeling and rendering on electrovibration display", *IEEE Transactions on Haptics*, vol. 13, no. 2, pp. 298–311, 2019.

[53] G. Ilkhani, M. Aziziaghdam, and E. Samur, "Data-driven texture rendering on an electrostatic tactile display", *International Journal of Human–Computer Interaction*, vol. 33, no. 9, pp. 756–770, 2017.

[54] S. Wu, X. Sun, Q. Wang, and J. Chen, "Tactile modeling and rendering image-textures based on electrovibration", *The Visual Computer*, vol. 33, pp. 637–646, 2017.

[55] M. Minsky, O.-y. Ming, O. Steele, F. P. Brooks Jr, and M. Behensky, "Feeling and seeing: Issues in force display", in *Proceedings of the 1990 symposium on Interactive 3D graphics*, 1990, pp. 235–241.

[56] G. Robles-De-La-Torre and V. Hayward, "Force can overcome object geometry in the perception of shape through active touch", *Nature*, vol. 412, no. 6845, pp. 445–448, 2001.

[57] X. Dai, J. E. Colgate, and M. A. Peshkin, "Lateralpad: A surface-haptic device that produces lateral forces on a bare finger", in *2012 IEEE Haptics Symposium (HAPTICS)*, IEEE, 2012, pp. 7–14.

[58] S.-C. Kim, A. Israr, and I. Poupyrev, "Tactile rendering of 3d features on touch surfaces", in *Proceedings of the 26th annual ACM symposium on User interface software and technology*, 2013, pp. 531–538.

[59] C. Xu, A. Israr, I. Poupyrev, O. Bau, and C. Harrison, "Tactile display for the visually impaired using teslatouch", in *CHI'11 Extended Abstracts on Human Factors in Computing Systems*, 2011, pp. 317–322.

[60] P. M. Fitts, "The information capacity of the human motor system in controlling the amplitude of movement.", *Journal of experimental psychology*, vol. 47, no. 6, p. 381, 1954.

[61] C. Forlines and R. Balakrishnan, "Evaluating tactile feedback and direct vs. indirect stylus input in pointing and crossing selection tasks", in *Proceedings of the SIGCHI Conference on Human Factors in Computing Systems*, 2008, pp. 1563–1572.

[62] V. Levesque, L. Oram, K. MacLean, *et al.*, "Enhancing physicality in touch interaction with programmable friction", in *Proceedings of the SIGCHI conference on human factors in computing systems*, 2011, pp. 2481–2490.

[63] F. Kalantari, E. Lank, Y. Rekik, L. Grisoni, and F. Giraud, "Determining the haptic feedback position for optimizing the targeting performance on ultrasonic tactile displays", in *2018 IEEE haptics symposium (HAPTICS)*, IEEE, 2018, pp. 204–209.

[64] Y. Zhang and C. Harrison, "Quantifying the targeting performance benefit of electrostatic haptic feedback on touchscreens", in *Proceedings of the 2015 International Conference on Interactive Tabletops & Surfaces*, 2015, pp. 43–46.

[65] S. Choi and K. J. Kuchenbecker, "Vibrotactile display: Perception, technology, and applications", *Proceedings of the IEEE*, vol. 101, no. 9, pp. 2093–2104, 2012.

[66] J. Monnoyer, L. Willemet, and M. Wiertlewski, "Rapid change of friction causes the illusion of touching a receding surface", *Journal of the Royal Society Interface*, vol. 20, no. 199, p. 20 220 718, 2023.

[67] K. Tashiro, Y. Shiokawa, T. Aono, and T. Maeno, "Realization of button click feeling by use of ultrasonic vibration and force feedback", in *World Haptics 2009-Third Joint EuroHaptics conference and Symposium on Haptic Interfaces for Virtual Environment and Teleoperator Systems*, IEEE, 2009, pp. 1–6.

[68] J. Monnoyer, E. Diaz, C. Bourdin, and M. Wiertlewski, "Ultrasonic friction modulation while pressing induces a tactile feedback", in *Haptics: Perception, Devices, Control, and Applications: 10th International Conference, EuroHaptics 2016, London, UK, July 4-7, 2016, Proceedings, Part I 10*, Springer, 2016, pp. 171–179.

[69] J. Monnoyer, E. Diaz, C. Bourdin, and M. Wiertlewski, "Perception of ultrasonic switches involves large discontinuity of the mechanical impedance", *IEEE transactions on haptics*, vol. 11, no. 4, pp. 579–589, 2018.

[70] D. Gueorguiev, E. Vezzoli, A. Mouraux, B. Lemaire-Semail, and J.-L. Thonnard, "The tactile perception of transient changes in friction", *Journal of The Royal Society Interface*, vol. 14, no. 137, p. 20 170 641, 2017.

[71] H. Xu, R. L. Klatzky, M. A. Peshkin, and J. E. Colgate, "Localizable button click rendering via active lateral force feedback", *IEEE Transactions on Haptics*, vol. 13, no. 3, pp. 552–561, 2020.

[72] V. Lévesque, L. Oram, and K. MacLean, "Exploring the design space of programmable friction for scrolling interactions", in *2012 IEEE Haptics Symposium (HAPTICS)*, IEEE, 2012, pp. 23–30.

[73] F. Giraud, M. Amberg, and B. Lemaire-Semail, "Design and control of a haptic knob", *Sensors and Actuators A: Physical*, vol. 196, pp. 78–85, 2013.

[74] C. Bernard, J. Monnoyer, S. Ystad, and M. Wiertlewski, "Eyes-off your fingers: Gradual surface haptic feedback improves eyes-free touchscreen interaction", in *Proceedings of the 2022 CHI Conference on Human Factors in Computing Systems*, 2022, pp. 1–10.

[75] V. Levesque, J. M. Cruz-Hernandez, A. Weddle, and D. M. Birnbaum, *System and method for simulated physical interactions with haptic effects*, US Patent 9,330,544, May 2016.

[76] J. Lim, Y. Yoo, H. Cho, and S. Choi, "Touchphoto: Enabling independent picture taking and understanding for visually-impaired users", in *2019 International Conference on Multimodal Interaction*, 2019, pp. 124–134.

[77] J. Mullenbach, C. Shultz, J. E. Colgate, and A. M. Piper, "Exploring affective communication through variable-friction surface haptics", in *Proceedings of the SIGCHI Conference on Human Factors in Computing Systems*, 2014, pp. 3963–3972.

3

ULTRALOOP: RESONANT TRAVELING WAVES-BASED DEVICE

PREFACE

There is currently a lack of surface haptic devices capable of generating strong lateral forces while maintaining moderate power consumption and a large, flat interaction area. This chapter introduces the development of Ultraloop, a traveling wave-based active surface haptic device designed to overcome these limitations.

The Ultraloop leverages resonant traveling waves to generate uniform active lateral forces across its surface. Unlike traditional friction modulation techniques, which can only resist a user's motion, this device actively pushes the user's fingertip, creating a more dynamic and versatile tactile experience.

This chapter reports the analytical model to the Ultraloop's design and the force characterizations as a function of vibration amplitude and phase shift. I also present a proof-of-concept application demonstrating its ability to simulate a button click sensation. A six-axis force sensor measures the lateral and normal forces applied when users interact with the Ultraloop.

This chapter is based on:

Zhaochong Cai, and Michaël Wiertlewski, Ultraloop: Active lateral force feedback using resonant traveling waves, IEEE Transactions on Haptics, **16**(4), 2023.

ABSTRACT

The sensation of touching virtual texture and shape can be provided to a touchscreen user by varying the friction force. Despite the saliency of the sensation, this modulated frictional force is purely passive and strictly opposes finger movement. Therefore, it is only possible to create forces along the direction of movement, and this technology cannot stimulate a static fingertip or provide forces that are orthogonal to the direction of movement. The lack of orthogonal force limits the guidance to a target in an arbitrary direction, highlighting the need for active lateral forces to give directional cues to the fingertip. This chapter presents a surface haptic interface that uses ultrasonic traveling waves to create active lateral forces on bare fingertips. The device is built around a ring-shaped cavity where two degenerate resonant modes around 40 kHz are excited with a 90-degree phase shift. The interface is capable of providing active forces up to 0.3 N to a static bare finger uniformly over a 140×30 mm^2 surface. The model and design of the acoustic cavity, force measurements, and an application to create a key-click sensation are described. This work demonstrates a promising method for uniformly producing large lateral forces on a touch surface.

3.1. INTRODUCTION

TOUCHSCREENS and capacitive buttons offer designers the flexibility to program human-machine interfaces but deprive users of tactile feedback typically found in mechanical buttons. Without feedback, the interaction becomes cognitively demanding and requires constant visual attention. Surface haptic interfaces can restore tactile feedback by creating rich and tangible interfaces. Among these technologies, friction modulation is a popular method to stimulate users' sense of touch. It operates by changing the force applied to a sliding fingertip. Friction can be modulated either by ultrasonic lubrication, which uses acoustic levitation to reduce friction [1]–[3], or electroadhesion which relies on electrostatic attraction to increase friction [4]–[6]. Both methods are able to render a wide range of effects, from textures, shapes, to viscosity by modulating the magnitude of the friction force as a function of the user motion [4], [7], [8].

However, frictional forces are essentially passive forces that only resist finger motion instead of actively pushing fingers. Because of this, modulating frictional force is only effective on a sliding finger and the force is oriented opposite to the movement direction. Although literature reported that a stationary finger can also perceive a sudden change in friction [9], the feedback is feint and it fails to provide directional cues. Applications such as guiding the finger or navigating through a curved channel, require an active lateral force.

One strategy to generate active lateral forces on a touchpad is to use asymmetric friction. Asymmetric friction devices synchronize in-plane oscillation and friction modulation either via ultrasonic vibration[10] or electroadhesion[11]. During part of one oscillation cycle, friction is set to high, while during the rest of the oscillation cycle, the friction is set to low, causing a non-zero asymmetric force profile during one full cycle. The lateral oscillation can be created with a voice coil [10] excited at low frequency and can reach a maximum lateral force of up to 450 mN [11]. However, these devices suffer from the audible noise produced by lateral oscillation. UltraShiver eliminated the

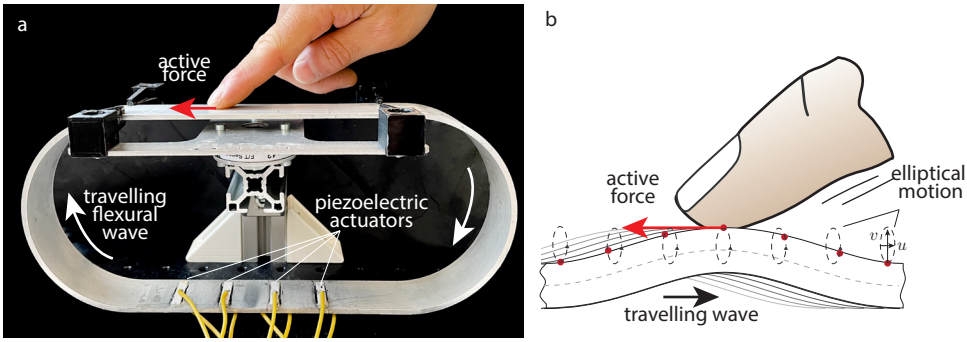

Figure 3.1: (a) Ultraloop is a traveling wave surface haptic interface. Piezoelectric actuators excite two degenerate modes of the structure that superimpose as a traveling wave. (b) The traveling wave creates an elliptical motion of the surface points which actively pushes the fingertip.

audible noise by vibrating the plate in an ultrasonic regime [12]. However, this device operates with resonant mode and therefore has several nodal lines where the sensation is null. To circumvent this problem, a new device SwitchPad switches between the first and the second in-plane oscillation mode according to the finger position [13], achieving a 250 mN peak force.

The other principle that generates active lateral forces induces an elliptical motion of the surface. Elliptical motion can be achieved by exciting both the longitudinal and bending modes of a plate at the same frequency. Using this strategy, the LateralPad can produce active shear forces of ±50 mN [14], and the 2MoTac can generate shear forces to simulate a button-click [15], [16]. However, matching the resonant frequency of the two modes requires a precise mechanical design and stable mechanical properties. Another approach to induce an elliptical motion at the surface is to leverage flexural traveling waves. This method is the driving mechanism behind commercial ultrasonic motors [17]. Biet et al. first reported that placing the finger on an ultrasonic motor creates a strong propelling sensation [18]. Such motors can be used to create button clicks [19]. Despite its compelling force feedback, ultrasonic motors are not specifically designed for haptic application and their circular shape makes them ill-suited as tactile interfaces which are typically rectangular. Ghenna et al. proposed a device that can generate traveling waves in a straight beam actuated by two Langevin transducers [20]. However, the design does not use resonance and achieves modest active forces of 100 mN despite powerful actuators.

This chapter reports a novel haptic device, the Ultraloop (Fig. 3.1a), that can generate active lateral forces up to 300 mN using resonant traveling waves. The active forces are uniformly produced on a rectangular surface (140 × 30 mm) which is large enough for comfortable interaction. The ring-shaped structure has no acoustic boundary and therefore is ideal for efficiently propagating traveling waves and creating sufficiently strong active forces to create numerous applications. A keyclick simulation is demonstrated, as a proof of concept, to show its capability to manipulate lateral forces temporally and spatially for various effects.

3.2. DESIGN OF A TRAVELING WAVE STRUCTURE

3.2.1. TRAVELING WAVE EXCITATION AND LATERAL FORCE GENERATION

Because of the wave reflection in the boundary, generating traveling waves in a finite beam comes with compromises. One strategy pioneered by Kuribayashi et al. [21], is to use two actuators: one to excite a traveling wave and the other to absorb it before it reflects on the boundary created by end of the beam. One key limitation of this approach is that because the wave is absorbed, the vibration can only achieve a modest displacement.

Producing larger displacement is possible by leveraging resonance. Our method uses the fact that two orthogonal resonant standing waves superimpose in a traveling wave if they are excited with a ±90° phase shift such that:

$$\sin(\omega t)\sin(kx) + \cos(\omega t)\cos(kx) = \cos(kx - \omega t) \tag{3.1}$$

where t is the time, x is the position, ω is the angular frequency and k is the wave number.

The superposition is achieved by exciting two successive flexural modes of the beam at the average frequency of each mode [20], [22]. However, because the frequency is in between two modes, the efficiency of the actuation is limited. A more efficient method to generate traveling waves is to superimpose two degenerate modes of a closed-loop structure. These two degenerate modes have an identical resonant frequency, achieving higher efficiency. Examples include circular shape structures such as ultrasonic motors [17], ring-type resonator which already has been used in linear ultrasonic motors [23], and linear transportation system [24]. To generate traveling waves, our design relies on an oblong ring which provides a rectangular area that is convenient to interact with.

When traveling waves are propagating in the beam, the neutral line follows a transverse sinusoidal trajectory while the particles on the surface move along an elliptical locus due to an additional longitudinal movement. When an object, such as a finger, contacts the surface points, a relative displacement at the contact point leads to frictional force, pushing the object in the opposite direction than the wave propagation (Fig. 3.1b).

3.2.2. ORTHOGONAL DEGENERATE MODES

The Ultraloop has a ring-type structure, comprising two straight beams of length L and two semicircular segments of radius R (Fig. 3.2a). For specific geometry, this type of structure has two orthogonal frequency-degenerate modes necessary to generate traveling waves. Here, we will briefly derive the solutions for the two degenerate modes. A comprehensive model of this resonator can be found in [25], [26].

DIFFERENTIAL EQUATIONS AND BOUNDARY CONDITIONS

The Ultraloop has a uniform width w and thickness h, with Young's modulus E and density ρ. By applying the Euler-Bernoulli beam theory and employing Hamilton's principle, we yield governing partial differential equations.

For the straight part,

$$-\rho A\frac{\partial^2 v_s}{\partial t^2} + \rho I\frac{\partial^2}{\partial t^2}\frac{\partial^2 v_s}{\partial x^2} - EI\frac{\partial^4 v_s}{\partial x^4} = 0 \tag{3.2}$$

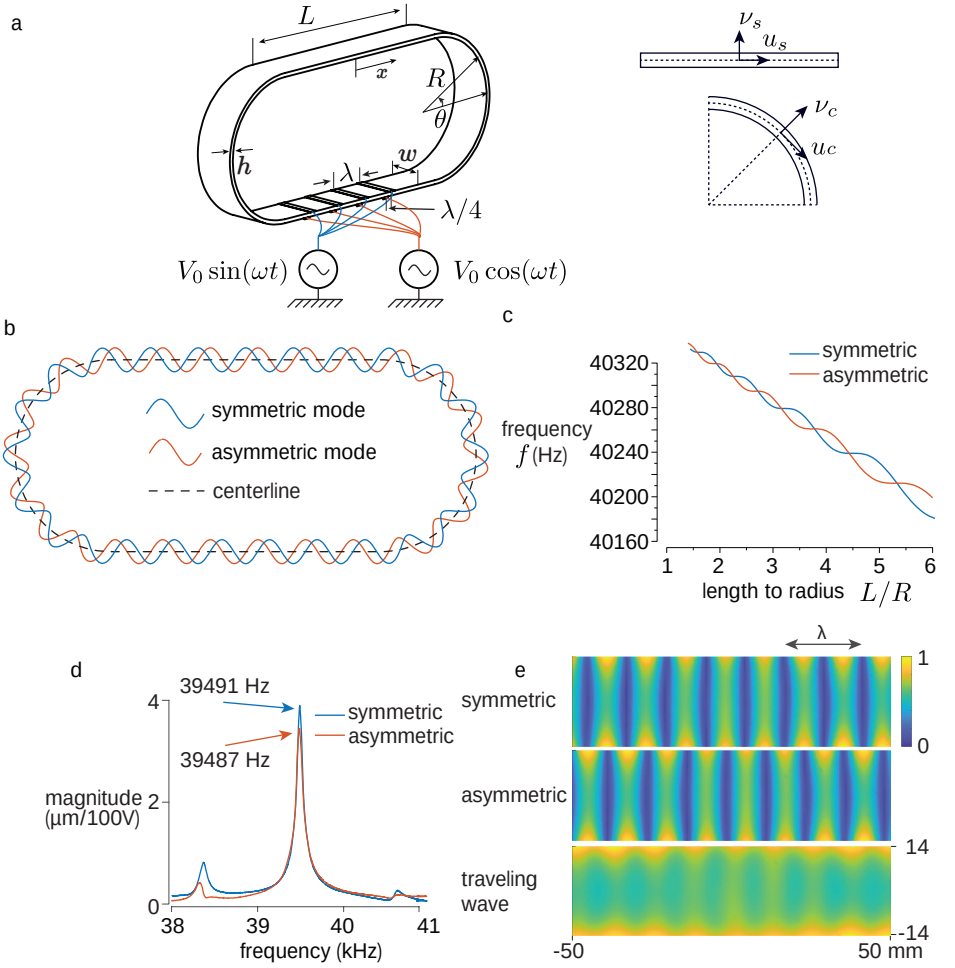

Figure 3.2: (a) Schematic view of the Ultraloop. (b) Symmetric and asymmetric mode of the 24th order. (c) Natural frequency of the 24th modes for various length-to-radius ratios. (d) Experimental Bode plot of the two frequency-degenerate modes. (e) Mode shapes of symmetric mode, asymmetric mode and the resulting traveling wave are shown as normalized colormaps. The color at each grid corresponds to the vibration amplitude measured by a laser Doppler vibrometer. Note that the symmetric mode and asymmetric mode are orthogonal to each other.

where $A = wh$ is the area of the cross-section, $I = wh^3/12$ is the second moment of area, and $v_s(x,t)$ is the transverse displacement.

For the curved part,

$$\rho AR\left(\frac{\partial^4 u_c}{\partial\theta^2\partial t^2} - \frac{\partial^2 u_c}{\partial t^2}\right) + \frac{EI}{R^3}\left(\frac{\partial^6 u_c}{\partial\theta^6} + 2\frac{\partial^4 u_c}{\partial\theta^4} + \frac{\partial^2 u_c}{\partial\theta^2}\right) - \frac{\rho I}{R}\left(\frac{\partial^6 u_c}{\partial\theta^4\partial t^2} + 2\frac{\partial^4 u_c}{\partial\theta^2\partial t^2} + \frac{\partial^2 u_c}{\partial t^2}\right) = 0 \tag{3.3}$$

where $u_c(x,t)$ is the longitudinal displacement respectively.

We then consider the boundary conditions. Because of the continuity of the structure, the boundary where the straight and curved parts connect must have the same displacements and rotations. Now we only consider modes in the top and the right segments of the ring-type structure, and the modes in the bottom and the left segments can be filled according to boundary conditions. Therefore, the boundary conditions on the top right connection can be described as:

$$v_s\left(\frac{L}{2},t\right) = v_c\left(-\frac{\pi}{2},t\right) \tag{3.4}$$

$$\frac{\partial v_s}{\partial x}\left(\frac{L}{2},t\right) = \frac{\partial v_c}{\partial s}\left(-\frac{\pi}{2},t\right) \tag{3.5}$$

SOLUTIONS

We use the method of separation of variables to decompose the solutions to a spatial part (i.e. the mode shape) with the variable x or θ, multiplied by a harmonic part along time with an angular frequency ω, i.e. $v_s(x,t) = V_s(x)\sin(\omega t)$ and $u_c(\theta,t) = U_c(\theta)\sin(\omega t)$. Note that here we only use u_c to represent the motion of the curved part due to an additional constraint between its transverse movement and its longitudinal movement, i.e. $v_c = -\partial u_c/\partial\theta$ if applying inextensionality condition.

Next, we will only consider the particular solutions of interest with the form of $\pm\sin$ and $\pm\cos$, which are flexural modes along the length of the Ultraloop. In this case, there are two solutions considering all the combinations:

- Solution 1: $\{V_s, U_c\} = \{A_s\cos k_s x, A_c\sin k_c\theta\}$, and the orthogonal mode $\{V_s, U_c\} = \{A_s\sin k_s x, A_c\cos k_c\theta\}$.
- Solution 2: $\{V_s, U_c\} = \{A_s\sin k_s x, A_c\sin k_c\theta\}$, and the orthogonal mode $\{V_s, U_c\} = \{A_s\cos k_s x, A_c\cos k_c\theta\}$.

where k_s and k_c are the wave number in the straight part and the curved part respectively, A_s and A_c are the transverse vibration amplitude in the straight part and the longitudinal vibration amplitude of the curved part respectively. Considering the relationship between v_c and u_c and assuming $v_c(x,t) = V_c(x)\sin(\omega t)$, we have $V_c = -dV_c/d\theta$. These solutions in the form of transversal displacement can be expressed as:

- Solution 1: $\{V_s, V_c\} = \{A_s\cos k_s x, -A_c k_c\cos k_c\theta\}$, and the orthogonal mode $\{V_s, V_c\} = \{A_s\sin k_s x, A_c k_c\sin k_c\theta\}$.

- Solution 2: $\{V_s, V_c\} = \{A_s \sin k_s x, -A_c k_c \cos k_c \theta\}$, and the orthogonal mode $\{V_s, V_c\} = \{A_s \cos k_s x, A_c k_c \sin k_c \theta\}$.

Based on the form of V_s and V_c, the former mode in Solution 1 has symmetry in both x and y axis, and is therefore referred to as the symmetric mode. Its orthogonal mode, which has an origin symmetry, is referred to as asymmetric mode. Notably, Solution 1 exists only when n is an even number. In contrast, the former mode in Solution 2 has symmetry in y axis, while its orthogonal mode has a x symmetry. Solution 2 exists only when n is an odd number. We chose the 24^{th} degenerate mode since its corresponding wavelength is of similar size to what is used in friction modulation ultrasonic devices and large enough to easily place piezoelectric actuators. The mode shape is shown in Fig. 3.2b.

Substituting any of the above four modes into Eq. 3.2 and Eq. 3.3, the following two equations relating k_s and k_c are obtained:

$$k_s^4 - \alpha_s k_s^2 \omega^2 - \gamma_s \omega^2 = 0 \tag{3.6}$$

where $\alpha_s = \rho / E$ and $\gamma_s = \rho A / EI$, and

$$\omega^2(\gamma_c k_c^4 - 2\gamma_c k_c^2 + \alpha_c k_c^2 + \alpha_c + \gamma_c) - k_c^6 + 2k_c^4 - k_c^2 = 0 \tag{3.7}$$

where $\alpha_c = \rho A R^4 / EI$ and $\gamma_c = \rho R^2 / E$.

Now we use the symmetric mode of Solution 1 as an example of how to derive the mode shapes. By substituting the solution into the boundary conditions Eq. 3.4 and Eq. 3.5, while remembering that $ds = Rd\theta$, we obtain

$$A_s \cos\left(k_s \frac{L}{2}\right) = -A_c k_c \cos\left(-k_c \frac{\pi}{2}\right) \tag{3.8}$$

$$-A_s k_s \sin\left(k_s \frac{L}{2}\right) = \frac{A_c k_c^2}{R} \sin\left(-k_c \frac{\pi}{2}\right) \tag{3.9}$$

We have now four equations Eq. 6.1, 6.2, 3.8 and 3.9 with four unknowns including k_s, k_c, ω, and a ratio $\Gamma = \frac{A_s}{A_c k_c}$. The values of the unknowns are, therefore, fully defined. However, the equations are transcendental, so we numerically solve this system of equations to find the solutions.

First, we express the ratio Γ in two ways derived from Eq. 3.8 and 3.9

$$\Gamma_1 = \frac{-\cos(-k_c \frac{\pi}{2})}{\cos(k_s \frac{L}{2})} \quad \text{and} \quad \Gamma_2 = \frac{-k_c \sin(-k_c \frac{\pi}{2})}{R k_s \sin(k_s \frac{L}{2})} \tag{3.10}$$

then define a cost function:

$$g = (\Gamma_1 - \Gamma_2)^2 \tag{3.11}$$

The cost function g has a single argument, k_c, since k_s can be expressed by k_c using Eq. 6.1 and Eq. 6.2. Note that g equals 0 only when $\Gamma_1 = \Gamma_2$, which are equivalent to the constraints given by Eq. 3.8 and Eq. 3.9. Therefore, solving these equations becomes a problem of finding k_c for which $g(k_c) = 0$.

We can compute g as a function of k_c, and each local minimum of g would corresponds to a symmetric mode of a given order. Similarly, for the other three types of mode shapes, i.e. asymmetric mode of Solution 1 and the two degenerate modes of Solution 2, solutions of k_c can be found by computing the local minimum of their corresponding cost function g. Notably, all the flexural modes with an even order are given by Solution 1, while all those with an odd order are given by Solution 2.

Another important feature of the two degenerate modes is that their natural frequencies are identical for specific length-to-radius L/R ratios. Fig. 3.2c shows the resonant frequency dependence on the length-to-radius ratio of the 24^{th} symmetric and asymmetric modes. The two frequency curves coincide at discrete values, which are preferred for traveling wave generation.

In summary, resonant frequencies of any mode can be calculated numerically given a certain size of the Ultraloop. An iterative process can be used to achieve desired dimensions and resonances. Optimization of design parameters can be further investigated based on the model. Here we choose the following geometrical parameters for the Ultraloop: $L = 140$ mm, $R = 50$ mm, $h = 2.75$ mm and $w = 30$ mm. The device is made from aluminum 5052, with $E = 69$ GPa and $\rho = 2680$ kg/m^3. With these numbers, we calculated the natural frequencies of 24^{th} degenerate modes to be 40287 Hz and 40294 Hz. In practice, the resonant frequencies coincided but their values are lower than the analytical model predicts probably due to the error from Euler-Bernoulli beam assumption, see Fig. 3.2d. The actual mode shapes of 24^{th} degenerate modes as well as their superposition under a 90° phase shift were measured with a laser Doppler vibrometer, see Fig. 3.2e.

3.3. IMPLEMENTATION

3.3.1. ULTRALOOP FABRICATION AND PIEZOELECTRIC ACTUATORS

We fabricated the Ultraloop by electrical discharge machining and polished its top surface to make it smooth to the touch. Eight piezoelectric actuators were glued on the bottom plate of the structure, with four on the upper surface to excite the symmetric mode and the other four on the lower surface to excite the asymmetric mode. The piezoelectric actuators on the lower surface are shifted by a quarter wavelength. These piezoelectric actuators are 25 mm long, 5 mm wide and 0.3 mm thick piezo ceramic plates (SMPL25W5T30311, Steiner & Martins Inc) glued with epoxy adhesive (DP490, 3M). The piezoelectric patches are ≈5 times smaller than the wavelength. Each set of ceramics is placed on the antinode of each mode.

The two driving signals for the piezoelectric actuators are generated by a functional generator (AFG 1062, Tektronix) and amplified by two 20× amplifiers (PD200, PiezoDrive). The maximum amplitude was ±80 V. The amplitude and phase shift was controlled through Matlab.

Although the analytical model predicts resonant frequencies of the two degenerate modes, their actual values can shift. During experiments, we first identified the resonant frequencies with a vibrometer. The working frequency was set as the middle of two resonant frequencies.

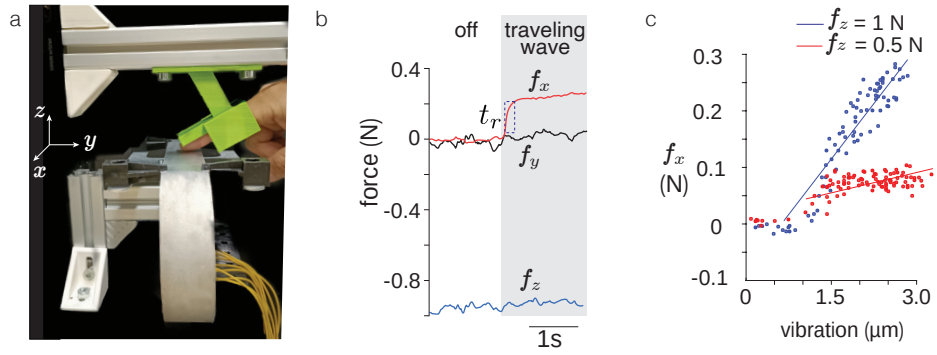

Figure 3.3: Lateral force generation on a fixed finger. (a) Force measurement setup. The index finger is fixed by a supporting frame. (b) A typical trial where traveling waves produce a noticeable lateral force after a rise time of t_r = 0.19 s. (c) Influence of the vibration amplitude on the lateral force.

3.3.2. VIBRATION AND FORCE MEASUREMENTS

The ultrasonic vibration of the Ultraloop was measured by a Laser Doppler Vibrometer (OFV-503 and OFV-5000, Polytec). A laser beam was focused on the top surface and normal to this plane. Therefore the normal velocity of the oscillation of surface points on the Ultraloop was recorded. Displacement can be recovered by integrating the velocity. A force measurement setup was used to measure the lateral forces applied to the participant's finger, as shown in Fig. 3.3a. The Ultraloop is supported by four 3d-print PLA fixtures at each corner of the upper straight part. These fixtures are mounted on a supporting plate, which stands on the top of the six-axis force sensor (Nano 43, ATI). The force data is acquired by a data acquisition card (USB 6351, National Instruments) at a sampling rate of 1 kHz.

The index finger of the participant was fixed by a supporting frame, with the finger pad facing the top surface of the Ultraloop. The supporting frame is attached to a manual linear stage on the z-axis. During each force measurement, the supporting frame, along with the finger was lowered down until the normal force reached ≈1 N.

3.4. RESULTS

3.4.1. LATERAL FORCE GENERATION

Fig. 3.3b shows a typical trial of active lateral force generation on a fixed finger. When there was no vibration, forces on the lateral plane f_x and f_y remained almost zero. When traveling waves were generated on the Ultraloop by turning on both channels (39.5 kHz, 90° phase shift). Lateral force f_x experienced a rapid increase from 0 to roughly 0.22 N. Additionally, a static object placed on the Ultraloop surface can be moved smoothly (see supplementary video). The results show a significant lateral force generation on even a stationary object once traveling waves are present.

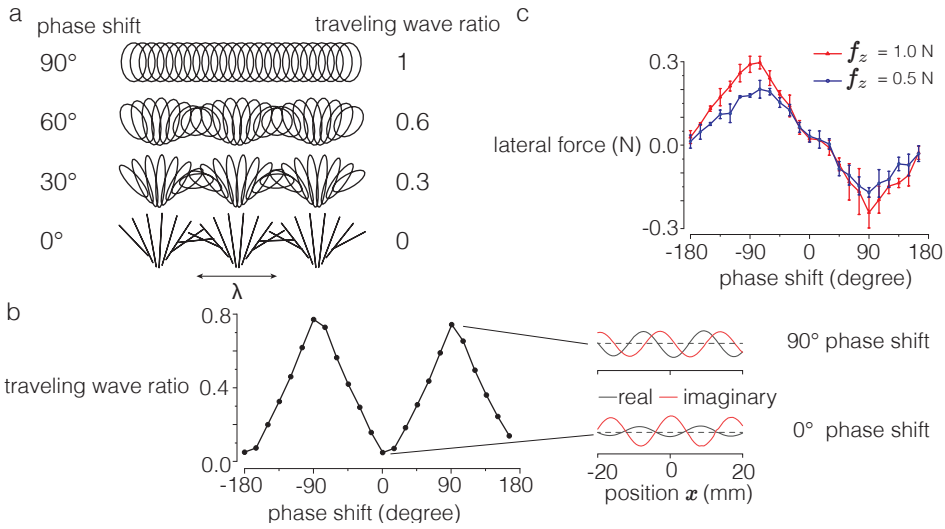

Figure 3.4: Effect of the phase shift. (a) Theoretical result of surface point trajectories under different phase shifts between the two degenerate modes. The traveling wave ratio is defined as the ratio between the minimum amplitude to the maximum amplitude across the surface. (b) Measured traveling wave ratio for different phase shifts. The insets show the spatial distribution of the real and imaginary parts of the wave given by the Fourier transform. (c) The lateral force was measured under two normal forces: 1 N and 0.5 N. Force at each phase shift was measured 3 times on the same finger and averaged. The error bar shows the standard deviation.

3.4.2. LATERAL FORCE VS VIBRATION AMPLITUDE

For large vibration amplitude, we would expect that the ellipsoidal movement of the surface be scaled and therefore the force would increase. We measured lateral forces f_x under various amplitudes when normal force f_z = 0.5 N and 1.0 N and Fig. 3.3c shows a linear dependence of the lateral force on the vibration amplitude. The linear regression for f_z = 1.0 N leads to coefficient b = 0.13 N/μm. Our setup does not exceed ±3 μm, but with more powerful piezoelectric actuators it might be possible to reach even larger lateral forces. In addition, under small vibration amplitude (less than ±1.3 μm), the force appears weaker than the linear fit line. For vibration amplitude smaller than ±1.0 μm, lateral force becomes insignificant compared to the measurement noise of our setup, suggesting that there is a minimum amplitude that needs to be reached to produce meaningful lateral forces.

The maximum vibration amplitude is ±3 μm. Increasing amplitude might increase the force, but at the same time increase the potential for levitation, which might indicate that a plateau could be reached for higher vibration amplitude.

3.4.3. EFFECT OF ARBITRARY PHASE SHIFTS

The quality of the traveling wave is strongly influenced by the correct superposition of the symmetric and asymmetric modes. To investigate this effect, we studied how the phase shift between the two modes influences the traveling wave generation. The superposition leads to a pure traveling wave only if the modes are shifted by ±90°. If the

phase shift is 0° or ±180°, the waves superpose in a standing wave leading to squeeze film levitation. The pure traveling wave generates a uniform elliptical motion of the surface, however, nodal lines will appear if the phase shift is not perfectly ±90°. The effect of the phase shift on the surface motion is shown in Fig. 3.4a. The ellipses tilt and shrink to straight lines as the phase shift changes from 90° to 0°. For a 90° phase shift, the ellipses are identical along the surface and have the largest aspect ratio. For 0° phase shift, the trajectories are lines, which cannot cause any net lateral force during.

Fig. 3.4b shows the traveling wave ratio, measured with the vibrometer, which quantifies the uniformity of the wave magnitude across the length of the interface. A large traveling wave ratio corresponds to a high-purity traveling wave, where the real and imaginary parts of the wave are shifted by a quarter wavelength. The real and imaginary parts are found using the Fourier transform on the time domain displacement trace. Standing waves are found when the traveling wave ratio is close to zero and the real and imaginary are shifted by half a wavelength.

The lateral forces measured at these phase shifts follow a similar trend as the traveling wave ratio. Fig. 3.4c shows the force peaks at −90° and 90° and attenuates to almost zero at 0 phase shift under both normal force cases (1 N and 0.5 N). Notably, the force reverses its direction when the phase shift is negative. Additionally, a lateral force under $f_z = 1$ N is higher than the force under $f_z = 0.5$ N.

3.4.4. APPLICATION: KEY-CLICK SIMULATION

To demonstrate the potential application of this device, we implemented a button click, similar to [19]. The button click signal is a square wave where the traveling wave is turned on to the right (−90° phase shift) when the normal force exceeds 0.5 N, and then to the left (+90° phase shift) when the normal force exceeds 0.8 N, as shown in Fig. 3.5a. With this control scheme, the finger experiences a sudden change in the shear force direction when the finger presses down.

We simulated several click events on the Ultraloop and recorded both the normal force and lateral force, which are presented in Fig. 3.5b. Consistent with previous results, the lateral force first rises as the finger applies increasing pressure, then drops suddenly to a negative value when the phase shift reverses. The fast change in force direction produces a distinct confirmation of a successful click.

3.5. CONCLUSION

In this chapter, we report the development of a surface haptic device using resonant traveling waves, to generate a large active lateral force of up to 300 mN on static fingertips. The device has a simple loop structure that circulates acoustic energy, making it energy-efficient. The device does not have moving parts making it suitable to be integrated into multimodal human-machine interfaces. The chapter describes the theory that allows computing the optimal geometry and material suitable for any design. The force can be operated by tuning the phase shift and the amplitude of the traveling wave which opens the door for a host of haptic effects. By controlling the force as a function of the user's motion, we anticipate being able to render a virtual environment, such as potential wells or viscous environment, effectively creating a force-feedback device for fingertips.

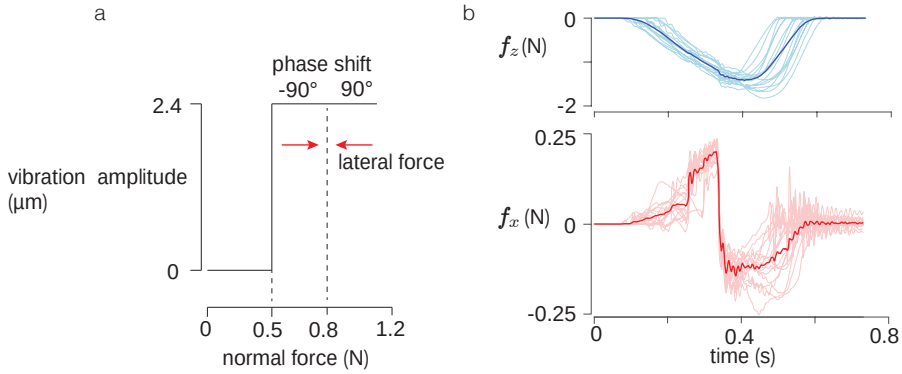

Figure 3.5: (a) Control scheme to render a key-click illusion. Vibration is turned on when the normal force reaches 0.5 N. Phase shift switches from −90° to 90° when the normal force rises to 0.8 N. The red arrows indicate the lateral force direction under different phase shifts. (b) Force measurement during pressing on the top surface of the Ultraloop with the index finger 16 times. The curves are aligned with the moment when the lateral force crosses the x-axis. Bold curves are the average of the 16 trials. The sudden reverse of the lateral force direction confirms a clear key-click event. Because of latency, the lateral force lags behind the normal force.

Our future work will focus on reproducing virtual shapes by incorporating a finger position tracking. Psychophysical experiments will be implemented to evaluate the benefit of this interface when interacting with complex environments. In addition, we will miniaturize the design of Ultraloop and allow it to work in two-dimensional plane.

REFERENCES

[1] T. Watanabe and S. Fukui, "A method for controlling tactile sensation of surface roughness using ultrasonic vibration", in *Proceedings of 1995 IEEE International Conference on Robotics and Automation*, vol. 1, May 1995, pp. 1134–1139. DOI: 10.1109/ROBOT.1995.525433.

[2] L. Winfield, J. Glassmire, J. E. Colgate, and M. Peshkin, "T-pad: Tactile pattern display through variable friction reduction", in *2007 2nd Joint EuroHaptics Conference and Symposium on Haptic Interfaces for Virtual Environments and Teleoperator Systems*, 2007, pp. 421–426.

[3] M. Wiertlewski, F. R. Fenton, and J. E. Colgate, "Partial squeeze film levitation modulates fingertip friction", *Proc. Nat. Acad. Sci.*, vol. 113, no. 33, pp. 9210–9215, Aug. 2016. DOI: 10.1073/pnas.1603908113.

[4] O. Bau, I. Poupyrev, A. Israr, and C. Harrison, "TeslaTouch: Electrovibration for touch surfaces", in *Proceedings of the 23nd annual ACM symposium on User interface software and technology*, ser. UIST '10, New York, NY, USA, Oct. 2010, pp. 283–292, ISBN: 978-1-4503-0271-5. DOI: 10.1145/1866029.1866074.

[5] C. D. Shultz, M. A. Peshkin, and J. E. Colgate, "Surface haptics via electroadhesion: Expanding electrovibration with Johnsen and Rahbek", in *2015 IEEE World Haptics Conference (WHC)*, Jun. 2015, pp. 57–62. DOI: 10.1109/WHC.2015.7177691.

[6] M. Ayyildiz, M. Scaraggi, O. Sirin, C. Basdogan, and B. N. J. Persson, "Contact mechanics between the human finger and a touchscreen under electroadhesion", *Proc. Nat. Acad. Sci.*, vol. 115, no. 50, pp. 12 668–12 673, Dec. 2018. DOI: 10.1073/pnas.1811750115.

[7] M. Wiertlewski, D. Leonardis, D. J. Meyer, M. A. Peshkin, and J. E. Colgate, "A High-Fidelity Surface-Haptic Device for Texture Rendering on Bare Finger", en, in *Haptics: Neuroscience, Devices, Modeling, and Applications*, M. Auvray and C. Duriez, Eds., ser. Lecture Notes in Computer Science, Berlin, Heidelberg: Springer, 2014, pp. 241–248, ISBN: 978-3-662-44196-1. DOI: 10.1007/978-3-662-44196-1_30.

[8] V. Levesque, L. Oram, K. MacLean, *et al.*, "Enhancing physicality in touch interaction with programmable friction", in *Proceedings of the SIGCHI Conference on Human Factors in Computing Systems*, ser. CHI '11, May 2011, pp. 2481–2490, ISBN: 978-1-4503-0228-9. DOI: 10.1145/1978942.1979306.

[9] J. Monnoyer, E. Diaz, C. Bourdin, and M. Wiertlewski, "Ultrasonic Friction Modulation While Pressing Induces a Tactile Feedback", in *Haptics: Perception, Devices, Control, and Applications*, F. Bello, H. Kajimoto, and Y. Visell, Eds., 2016, pp. 171–179, ISBN: 978-3-319-42321-0. DOI: 10.1007/978-3-319-42321-0_16.

[10] E. C. Chubb, J. E. Colgate, and M. A. Peshkin, "ShiverPaD: A Glass Haptic Surface That Produces Shear Force on a Bare Finger", *IEEE Trans. Haptics*, vol. 3, no. 3, pp. 189–198, Jul. 2010, ISSN: 2329-4051. DOI: 10.1109/TOH.2010.7.

[11] J. Mullenbach, M. Peshkin, and J. E. Colgate, "eShiver: Lateral Force Feedback on Fingertips through Oscillatory Motion of an Electroadhesive Surface", *IEEE Trans. Haptics*, vol. 10, no. 3, pp. 358–370, Jul. 2017, ISSN: 2329-4051. DOI: 10.1109/TOH.2016.2630057.

[12] H. Xu, M. A. Peshkin, and J. E. Colgate, "UltraShiver: Lateral Force Feedback on a Bare Fingertip via Ultrasonic Oscillation and Electroadhesion", *IEEE Trans. Haptics*, vol. 12, no. 4, pp. 497–507, Oct. 2019, ISSN: 2329-4051. DOI: 10.1109/TOH.2019.2934853.

[13] H. Xu, M. A. Peshkin, and J. E. Colgate, "SwitchPaD: Active Lateral Force Feedback over a Large Area Based on Switching Resonant Modes", en, in *Haptics: Science, Technology, Applications*, 2020, pp. 217–225, ISBN: 978-3-030-58147-3. DOI: 10.1007/978-3-030-58147-3_24.

[14] X. Dai, J. E. Colgate, and M. A. Peshkin, "LateralPaD: A surface-haptic device that produces lateral forces on a bare finger", in *2012 IEEE Haptics Symposium (HAPTICS)*, Mar. 2012, pp. 7–14. DOI: 10.1109/HAPTIC.2012.6183753.

[15] P. Garcia, F. Giraud, B. Lemaire-Semail, M. Rupin, and M. Amberg, "2MoTac: Simulation of Button Click by Superposition of Two Ultrasonic Plate Waves", en, in *Haptics: Science, Technology, Applications*, 2020, pp. 343–352, ISBN: 978-3-030-58147-3. DOI: 10.1007/978-3-030-58147-3_38.

[16] P. Garcia, F. Giraud, B. Lemaire-Semail, M. Rupin, and A. Kaci, "Control of an ultrasonic haptic interface for button simulation", en, *Sens. Actuator A Phys.*, vol. 342, p. 113 624, Aug. 2022, ISSN: 0924-4247. DOI: 10.1016/j.sna.2022.113624.

[17] C. Z. Rosen, B. V. Hiremath, and R. Newnham, "Ultrasonic wave motor: The first actuator incorporating ceramic technology", in *Piezoelectricity*, IV. New York, NY, USA: America Institute of Physics, 1991, pp. 381–383, ISBN: 0-88318-647-0.

[18] M. Biet, F. Giraud, F. Martinot, and B. Semail, "A Piezoelectric Tactile Display Using Travelling Lamb Wave", in *EuroHaptics Conference*, Jul. 2006, pp. 567, 570.

[19] D. Gueorguiev, A. Kaci, M. Amberg, F. Giraud, and B. Lemaire-Semail, "Travelling Ultrasonic Wave Enhances Keyclick Sensation", en, in *Haptics: Science, Technology, and Applications*, D. Prattichizzo, H. Shinoda, H. Z. Tan, E. Ruffaldi, and A. Frisoli, Eds., 2018, pp. 302–312, ISBN: 978-3-319-93399-3. DOI: 10.1007/978-3-319-93399-3_27.

[20] S. Ghenna, E. Vezzoli, C. Giraud-Audine, F. Giraud, M. Amberg, and B. Lemaire-Semail, "Enhancing Variable Friction Tactile Display Using an Ultrasonic Travelling Wave", *IEEE Trans. Haptics*, vol. 10, no. 2, pp. 296–301, Apr. 2017, ISSN: 2329-4051. DOI: 10.1109/TOH.2016.2607200.

[21] M. Kuribayashi, S. Ueha, and E. Mori, "Excitation conditions of flexural traveling waves for a reversible ultrasonic linear motor", *J. Acoust. Soc. Am.*, vol. 77, no. 4, pp. 1431–1435, Apr. 1985, ISSN: 0001-4966. DOI: 10.1121/1.392037.

[22] B.-G. Loh and P. Ro, "An object transport system using flexural ultrasonic progressive waves generated by two-mode excitation", *IEEE Trans. Ultrason., Ferroelect., Freq. Control*, vol. 47, no. 4, pp. 994–999, Jul. 2000, ISSN: 1525-8955. DOI: 10.1109/58.852083.

[23] W. Seemann, "A linear ultrasonic traveling wave motor of the ring type", en, vol. 5, no. 3, pp. 361–368, Jun. 1996, ISSN: 0964-1726. DOI: 10.1088/0964-1726/5/3/015.

[24] G. P. L. Thomas, M. A. B. Andrade, J. C. Adamowski, and E. C. N. Silva, "Development of an Acoustic Levitation Linear Transportation System Based on a Ring-Type Structure", *IEEE Trans. Ultrason., Ferroelect., Freq. Control*, vol. 64, no. 5, pp. 839–846, May 2017, ISSN: 1525-8955. DOI: 10.1109/TUFFC.2017.2673244.

[25] X. Liu, D. Shi, Y. Civet, and Y. Perriard, "Modelling and optimal design of a ring-type structure for the generation of a traveling wave", in *2013 International Conference on Electrical Machines and Systems (ICEMS)*, Oct. 2013, pp. 1286–1291. DOI: 10.1109/ICEMS.2013.6713262.

[26] G. P. L. Thomas, C. Y. Kiyono, A. Gay Neto, and E. C. N. Silva, "Conceptual Design of Oblong Ring Vibrators", *J. Vib. Acoust.*, vol. 142, no. 2, Dec. 2019, ISSN: 1048-9002. DOI: 10.1115/1.4045380.

4

POTENTIAL FIELD RENDERING

PREFACE

The development of the Ultraloop, a traveling wave-based surface haptic device introduced in Chapter 3, has the potential for investigating the impact of active force feedback on user interactions. This chapter advances the Ultraloop by transforming it into a force feedback-enabled surface haptic device that responds dynamically to a user's finger position. This functionality is achieved through the integration of position sensing and a real-time control system. Using this enhanced device, we conducted human experiments to study three types of elastic potential fields, each designed with distinct objectives, including Shape perception, target selection and directional navigation. Additionally, this chapter introduces three applications based on these potential fields, showcasing their potential in practical user interfaces.

This chapter is based on:

Zhaochong Cai, David Abbink, and Michaël Wiertlewski, Attracting Fingers with Waves: Potential Fields Using Active Lateral Forces Enhance Touch Interactions, in CHI Conference on Human Factors in Computing Systems (CHI '25), April 26–May 01, 2025, Yokohama, Japan. ACM, New York, NY, USA.

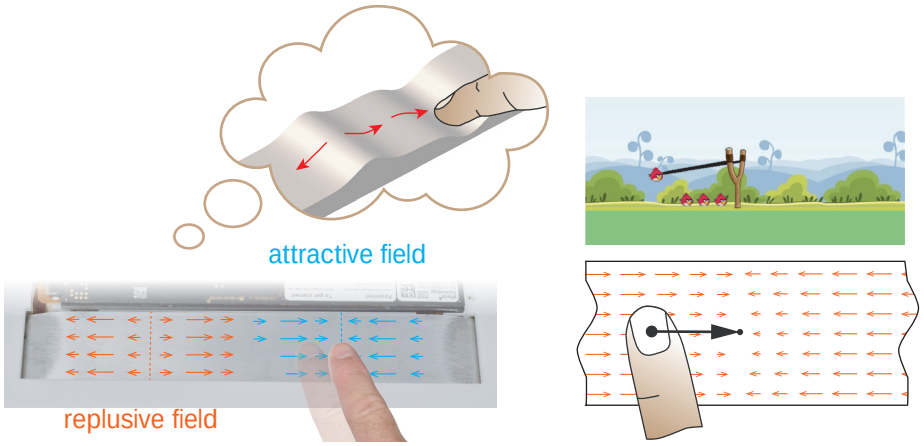

Figure 4.1: We implemented potential field rendering on a touchpad by tuning the traveling wave ratio to vary active forces. These forces are modulated based on the user's movements. By building attractive and repulsive fields (left), the surface is not perceived as a flat but a wavy surface with bumps and holes (middle). These bumps and holes can be used to create numerous haptic effects, such as a slingshot (right), basins of attraction, icons, keyboards, toggle switches, and paths for haptic guidance. In user studies, we found positive impacts of rendered potential fields during touch interactions in both users' performance and experience.

ABSTRACT

Touchscreens and touchpads offer intuitive interfaces but provide limited tactile feedback, usually just mechanical vibrations. These devices lack continuous feedback to guide users' fingers toward specific directions. Recent innovations in surface haptic devices, however, leverage ultrasonic traveling waves to create active lateral forces on a bare fingertip. This chapter investigates the effects and design possibilities of active forces feedback in touch interactions by rendering artificial potential fields on a touchpad. Three user studies revealed that: (1) users perceived attractive and repulsive fields as bumps and holes with similar detection thresholds; (2) step-wise force fields improved targeting by 22.9% compared to friction-only methods; and (3) active force fields effectively communicated directional cues to the users. Several applications were tested, with user feedback favoring this approach for its enhanced tactile experience, added enjoyment, realism, and ease of use.

4.1. INTRODUCTION

Touchscreens and touchpads are increasingly replacing traditional mechanical buttons, dials, and sliders in human-machine interfaces. Their programmability offers a wide range of intuitive interactions with visual elements, such as tapping to select, pinching to zoom, and swiping to scroll. However, their operations can be arduous because they lack the haptic feedback of their mechanical counterparts. Without mechanical feedback, users cannot engage their reflexive sensorimotor loops for automatic manipulation that tactile and proprioceptive inputs offer. As a consequence, these interactions rely heavily on visual attention, which is impractical for visually impaired individuals and can be

dangerous in situations that require continuous situational awareness, such as driving or flying.

Haptic feedback on touch panels can effectively reduce visual demand and enhance interactions. The common way to implement haptic feedback in consumer devices is to use vibrotactile actuators. The distinct vibration patterns they create inform users of a message or confirm users' operation, such as tapping or reaching a target [1]. However, the transient stimuli has limited expressiveness. A new class of devices broadly called surface haptics can provide continuous quasi-static feedback by modulating the friction between a surface and a fingertip through ultrasonic levitation [2] or electroadhesion[3]. By making the friction high on virtual targets and low everywhere else, studies have shown that users can reach targets 10% faster [2], [4], [5]. More complex patterns, such as sine waves, have shown to be useful. For example, by gradually changing the spatial wavelength of friction-modulated texture, these devices can assist users in setting a value for temperature control [6]. A similar method was used to render shapes, such as bumps or holes, on flat surfaces by mapping the local gradients of the 3D features to the friction level [7]. Despite these clear benefits, a major limitation still exists. Friction modulation only reacts against the movement of a finger due to its passivity. Thus it is only effective when the user is moving along the path of guidance. The technology fails to guide the finger in a direction other than the ongoing one. To guide users toward an arbitrary-located target, we must provide users' fingers with continuous directional forces.

Recent developments in surface haptics have demonstrated that active lateral forces could be directly applied to a user's fingertip [8]–[11]. Contrary to friction modulation, these techniques can modify the magnitude and direction of the force acting on a fingertip, so that they can both resist and push their movements. For now, the literature has been focused on characterizing the force generation with only a few studies validating its effectiveness on users, which are edge following [12] and event-based feedback, i.e. button clicks simulation [13]–[16] . Since the 90s, "virtual fixtures" and artificial potential fields have had successful implementations in enhancing users' operation and yielded some haptic guidance principles [17], [18]. These principles could potentially be adapted to fingertip guidance using active surface haptics. While several works showcased the potential field rendering with active forces feedback, they are limited to simple demonstrations of force-position functions [9], [11], [12]. To date, these guidance principles on touch surfaces remain untested in users, and their design possibilities are unexplored.

Here, to investigate the effects of artificial potential fields on users, we implement an impedance control scheme on a traveling wave-based active force feedback touchpad, the Ultraloop [8]. We create elastic potential fields that can attract and repulse the fingertip by actively modulating these lateral forces based on finger position. These lateral forces are controlled by tuning the phase shift and amplitude of the traveling waves. We compute the potential fields as the local negative gradients of the topography that should be felt. We ran three human-factor experiments implementing seperate potential fields to evaluate the effectiveness of the method. First, we investigated whether participants could perceive the magnitude and type of macroscale shapes like bumps and holes, rendered by Gaussian-shaped potential fields. Results showed that partici-

pants can detect bumps and holes with a sensory threshold of 30 mN. Second, we evaluated user's performance in a Fitts' pointing task. When the target was presented with a step-change attraction force field around a high friction zone, users improved their speed by 22.9% to varying friction alone. In addition, we demonstrated that potential fields could convey a sense of direction to a static user. Lastly, we designed three applications exploiting the results of the aforementioned quantitative studies to evaluate user subjective experience. These applications include (1) a haptic keyboard, which is the combination of potential wells and bumps, (2) an Angry Birds game in which users can feel the intensity and direction of the pulling sensation from a slingshot, and (3) a three-digit lock game where users can quickly locate the password under the guidance of active force field. Users' responses to a subjective questionnaire show that all these applications provide a high level of enjoyment, reduced visual engagement, and increased realism.

In summary, we implemented programmable elastic potential field rendering for fingertip guidance by controlling ultrasonic traveling waves. We validated that the rendering has positive impacts on users in three-fold:

1. Differentiable shape rendering, including bumps and holes, which can be applied to virtual keyboards.

2. Improved performance in pointing tasks, which are fundamental for navigating icons.

3. Simulation of physical interactions, such as the pulling sensation of an elastic slingshot.

For the first time, our results demonstrate the various benefits of active force feedback, making it a promising approach to revolutionize touch interactions toward effortless control of complex machines using fingertips and support eyes-free interaction.

4.2. RELATED WORK

4.2.1. HAPTIC GUIDANCE IN CLASSICAL FORCE FEEDBACK

Salisbury et al. introduced the idea of *artificial potential pields* in haptic rendering [18]. In this approach, a scalar field is constructed with artificial "hills" representing obstacles and "valleys" representing attractors. These potential fields are used to guide or constrain users to move along desired paths or avoid obstacles. These early studies suggested that imposing force as the negative gradients of potential fields could provide passive contact surfaces for three-dimensional virtual bodies. However, the design of these fields, in general, was left as an open question.

Ren et al. later proposed a potential function based on a generalized sigmoid function, which offers an intuitive way to adjust the affected area and abruptness of the potential field near the edges of protected zones [19]. In a catheter insertion task, for example, this model created a protective potential field with lower values at the vessel center and higher values near the vessel walls. Experimental results showed that the generated potential fields were sufficient to ensure obstacle avoidance while maintaining the responsiveness necessary for realistic feedback in haptic rendering. Additionally, the

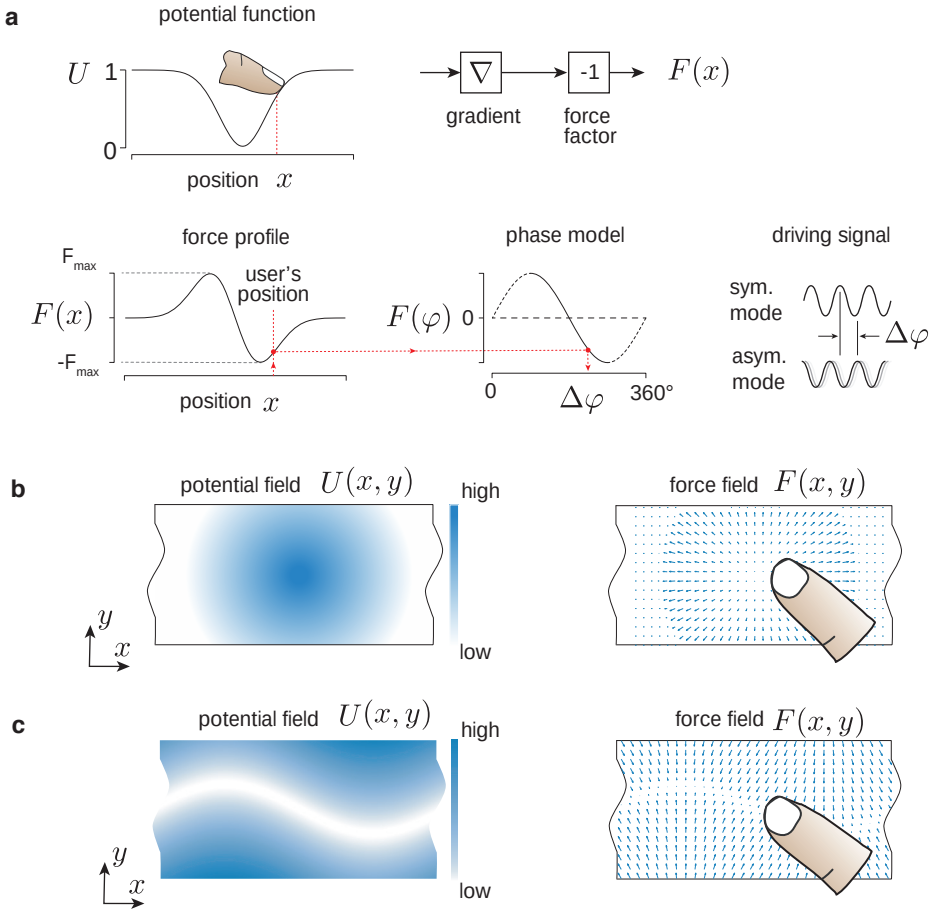

Figure 4.2: Visualization of potential field rendering for a bare finger in a one- (a) and two-dimensional case (b, c).

sigmoid function model was applied to render a simulated gear selector lever for automotive applications [20].

4.2.2. SURFACE HAPTICS RENDERING

When touchscreens and touchpads have taken over the market, the haptic landscape has evolved, moving beyond traditional force feedback devices to new rendering methods, such as vibrotactile and surface haptics. The latter, surface haptics devices, can provide continuous force feedback on a user's finger by modulating friction, either via ultrasonic lubrication, which reduces friction [16], [21], [22], or via electroadhesion, which increases friction [3], [23], [24].

Both technologies are effective in changing lateral force on a bare finger in motion across the screen. By rendering high friction on a target and low friction elsewhere, these

techniques can enhance targeting performance by 7–9% compared to visual feedback alone [2], [4], [5]. Additionally, surface haptics can simulate the perception of macro shapes, such as bumps or dips, by mapping frictional forces to the gradient of height maps [7], [25]–[28].

Despite their effectiveness, they are passive and cannot act on a static finger or push in a direction misaligned with the user's motion. Active force feedback is therefore essential to produce forces in arbitrary directions or to act on a resting finger.

4.2.3. ACTIVE LATERAL FORCE ON SURFACES

A new family of surface haptic devices that can generate net shear forces has recently emerged. One approach uses a moving overlay on top of a touchscreen to drag the finger to move [29]. The finger actually contacts the film and moves with it as a whole, thereby being used for conveying gesture messages to users through proprioception rather than for tactile rendering. Instead of moving the entire touch surface, net tangential forces can be generated directly on a static touch surface via oscillation, enabling users to interact with bare fingertips. Two principles have been explored.

The first principle relies on creating an asymmetry of friction by synchronizing a high or low frictional state with periodic in-plane oscillations. The frictional can be modulated through ultrasonic standing waves [9], [10], [12], [30] or electroadhesion [31], [32]. In-plane oscillations are preferably produced using ultrasonic compressive modes [9] to avoid audible noise; however, this results in nodal lines where tactile sensation is absent. The SwitchPad overcomes this limitation by dynamically switching resonant modes based on user position, achieving a uniform force profile of up to 250 mN [10], though with more complex control.

The second principle produces net lateral forces through periodic surface elliptical motions. Devices such as the LateralPad [11] and 2MoTac [14] create elliptical movements by exciting standing waves in both longitudinal and transverse directions. Alternatively, flexural traveling waves can also produce elliptical surface motions [33], as seen in rotary traveling motors, which generate strong pushing sensations on the fingertip [34]. However, the shape of motors is not suitable for a rectangular touchpad format. In a straight beam, traveling waves can be generated by superimposing two adjacent bending modes, resulting in modest forces of 100 mN on a finger [35]. The Ultraloop, used in this chapter, superimposes two degenerate bending modes with identical resonant frequencies, achieving uniform forces of 300 mN with $\pm$ 3 μm vibrations on a touchpad format [8].

4.3. BUILDING POTENTIAL FIELDS

We first briefly review the principle for rendering potential fields in one- and two-dimensional (1D and 2D) cases. We then propose the implementation of this principle by controlling the traveling wave ratio on a ultrasonic active force interface.

4.3.1. POTENTIAL FIELD RENDERING PRINCIPLE

The rendering principle is based on creating force fields within surfaces as negative gradients of potential fields. This principle has been widely used in force feedback de-

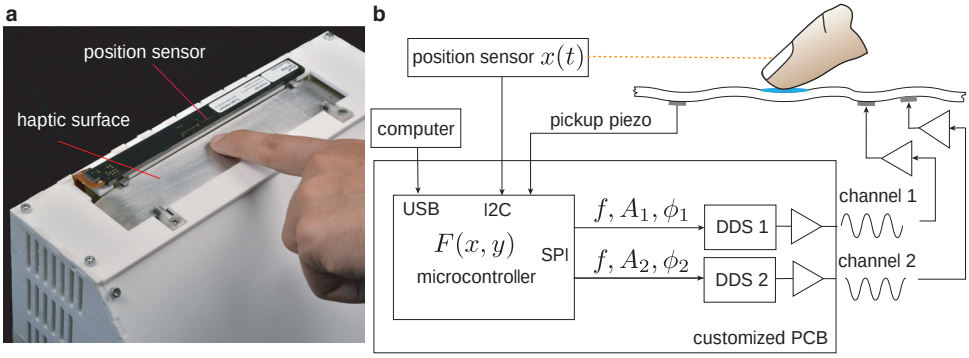

Figure 4.3: Control traveling waves to render programmable potential fields. (a) An ultrasonic traveling waves-based haptic touchpad, the Ultraloop, used in this study. Users interact with the surface to experience haptic guidance or rendered objects. (b) System architecture for real-time programmable impedance rendering. Dual output channels to the haptic touchpad are updated based on finger position in real time, allowing for application-specific rendering of features (such as bumps), position-dependent friction, and impedance profiles.

vices [19] and active surface haptic devices [9], [11], [12] to create haptic illusions or guide users. Figure 4.2a illustrates the principle for fingertip interaction in the 1D case. The input is the current finger position $x(t)$. The force is determined by first calculating the derivative of the potential function $g(x) = \nabla U(x)$, and then scaling it by a factor such that the range of the derivative linealy maps to the range of force production. Lastly, the desired force $F(t)$ is mapped to the force generation model to produce the driving signal. As the finger moves across the surface, the driving signal is continuously updated, typically above a rate of 1000 Hz.

For 2D rendering, the force $F(x, y)$ is obtained by taking the gradient $G(x, y) = \nabla U(x, y)$ and scaling it, which is then translated into control signals. This method allows for creating diverse vector fields to support a wide range of interactive experiences, such as rendering bumps(Fig. 4.2b, holes, basins of attractions, path sinks (Fig. 4.2c), or saddle points.

4.3.2. TRAVELING WAVE-BASED DEVICE: ULTRALOOP

One necessity for the implementation of the potential field rendering is reliable and large active force generation on a relatively large flat surface. In this chapter, we use our lab-built resonant traveling wave-based device, the Ultraloop [8] , and developed it for this study. The disclosed Ultraloop has a ring-shaped aluminum cavity, with a $140 \times 30\ mm^2$ flat upper surface for touch interaction. The length-to-radius ratio of the ring is designed as 2.8 to satisfy the requirement for degenerate modes. These two degenerate standing wave modes, corresponding to the 24^{th} order, have orthogonal spatial forms, being $cos(kx)$ and $sin(kx)$, but share the same resonance. Their superposition with a $\pm 90°$ temporal phase shift forms a traveling wave, described mathematically as $cos(kx)cos(\omega t) \pm sin(kx)sin(\omega t) = cos(kx \mp \omega t)$. The high-amplitude traveling waves induce surface elliptical motions to push fingers, with rightward force at 90° and leftward force at $-90°$. As reported in [8], when the phase is not at $\pm 90°$, partial traveling

waves are generated, and the lateral force varies sinusoidally with the phase shift or traveling wave ratio, fitted by data points measured by manually tuning a function generator. This capability of uniform and large force production, combined with the feature of force varying with phase, makes the Ultraloop a strong candidate for the implementation of potential field rendering.

We replicated the aluminum cavity of the Ultraloop for force generation, using the same acoustic design as [8], and used a $100 \times 30\text{mm}^2$ area for touch interaction. The ring-shaped touchpad and its control circuit are housed in a 3D-printed case, as shown in Fig. 4.3a.

4.3.3. IMPLEMENTATION OF CONTROL

To control active forces in response to user movements, we employ two Direct Digital Synthesis (DDS) components (AD9834, Analog Devices, Inc.) to generate two channels of ultrasonic sine waves. DDS is a technique for generating precise and frequency-agile analog waveforms (in this case, sine waves) from a digital, fixed-frequency reference oscillator. We selected this method because it provides fast, high-resolution digital control over both the frequency and, critically, the phase of the two output channels. These channels are synchronized with a tunable phase shift using a Teensy 3.6 microcontroller. Users movements are tracked by a position sensor (NNAMC1580PC01, Neonode) with a resolution of 10 pixels/mm, mounted above the touch surface. The sensor communicates finger positions in x and y to the microcontroller via I2C protocol at 2000 Hz. The microcontroller, programmed using Arduino, runs an internal loop that reads the user's position, looks up the stored force profile, and generates the phase and amplitude commands for the DDS chips using the sinusoidal force-phase model. The force profiles, which are task-specific, are precomputed from the desired potential field based on the rendering principle. A graphical user interface (GUI), programmed in Python, displays the visuals of the interaction task or applications and communicates the computed force profile to the microcontroller via USB. This process allows for dynamic updates of the displayed potential fields when switching to different interaction tasks.

To identify the resonant frequency, we monitor the vibration amplitude using a piezoelectric sensor attached to the lower plate, which has been calibrated with a Laser Doppler vibrometer. An initial frequency sweep is conducted around 39425 Hz to fine-tune the resonant frequency by identifying the peak output from the piezoelectric sensor. The frequency tracking ensures a consistent vibration intensity over time. The frequency, amplitude, and phase shift data are encoded and sent to the DDSs via the SPI bus to generate corresponding sine waves. The signals (max. ± 3.3 V) are amplified 20-fold (PD400, PiezoDrive) to actuate piezoelectric elements bonded to the aluminum plate. The tailored touchpad produces $\pm$ 2.1 μm vibration with ± 3.3 V $\times$ 20 input voltages at a resonance of 39425 Hz. A diagram of this implementation is shown in Fig. 4.3b.

4.4. STUDY 1: SHAPE DETECTION THRESHOLDS

In this experiment, we examine whether users could discriminate the type and amplitude of virtual bumps and holes created by repulsive and attractive potential fields.

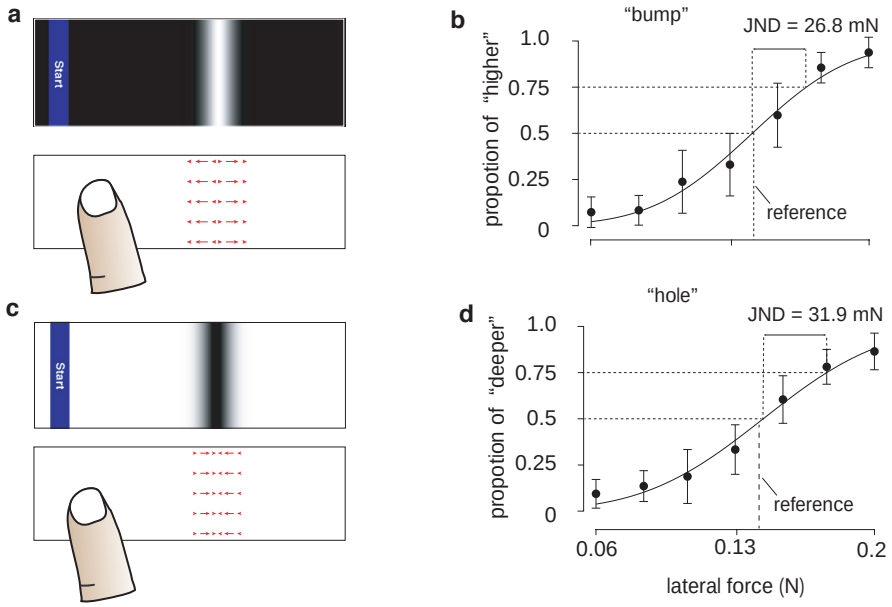

Figure 4.4: (a, c) Top: graphical user interface; Bottom: force field. (b, d) Response proportion for detecting "bump" (b) or "hole" (d) as a function of active lateral force, with error bars showing standard deviations. The 75% just-noticeable difference thresholds are indicated.

4.4.1. STUDY DESIGN

To simulate the sensations of bumps and holes, we implemented repulsive and attractive potential fields from Gaussian functions. These Gaussian potential functions had an identical width δ of 24 pixels and different amplitudes (A = 1, 0.88, 0.77, 0.65, 0.52, 0.42, and 0.30 for the experimental group; A=0.71 for thereference) as shown in Fig. 4.4 a and c. The gradients of these Gaussian functions were linearly translated into lateral forces, such that the Gaussian with $A = 1$ corresponded to the maximum force output (F_{max}) and the Gaussian with $A = 0.71$ corresponded to $0.71F_{max}$. These forces were then mapped to phase shifts using the data-driven force-phase model presented in Fig. 4.2a.

The experiment followed a two-alternative forced choice protocol. During each trial, participants were presented with two potential fields and asked to select the one perceived with higher amplitude. Each comparison consisted of the reference shape (A = 0.71) (the mean of the experimental fields $A = 0.77$ and 0.65) and one of the seven experimental fields. The order of the two stimuli was randomized, and participants were unaware of which was the reference. Stimuli were presented at the same location on the touchpad to ensure consistant force generation. Participants used the "Ctrl" key to switch between the two stimuli.

Each participant completed two experimental blocks: one containing repulsive potentials and the other containing attractive potentials. Each block included 56 comparison pairs (7 amplitudes × 8 repeats). The order of the blocks and the pairs within each block were shuffled.

Participants. Twelve participants (6 females and 6 males, aged 22-30, all right-handed) were recruited. All reported no sensory impairments or skin conditions. All the user studies in this chapter were approved by the Ethical Committee Board.

Experimental procedure. Participants were seated in a chair with the haptic interface in front of them. Their arms rested comfortably on an armrest and they interacted using the index finger of their dominant hand. Participants wore headphones playing pink noise to mask any device-related sounds. A GUI displayed the visuals of the potential fields and recorded participants' selections. Before starting the experiments, the touchpad was cleaned, and participants sanitized their fingers using alcohol wipes. These procedures were also applied to other studies in this chapter.

During each trial, participants used a keyboard to make their selections: pressing "A" to choose the first and "S" to choose the second stimulus in a trial, and "Ctrl" to toggle between the two stimuli. There were no restrictions on the number of toggles, but participants were encouraged to make selections promptly.

Before the amplitude discrimination task, we conducted a pilot study to examine participants' perception of the type of the shapes. In this study, participants were presented with seven randomly selected experimental stimuli and asked to classify each as a "bump" or a "hole." Results showed that all repulsive potentials were identified as "bumps" and all the attractive ones as "holes." The result is consistent with prior work that shows a high discrimination accuracy for detecting bump versus hole using friction modulation [36].

4.4.2. RESULTS

Figure 4.4b and d illustrate the response rate of participants for perceiving experimental stimuli as more intense than the reference (i.e. a higher bumps or a deeper hole). Both the detection for "bump" and "hole" follows a typical sigmoidal shape of a psychometric curve. Stimuli with amplitudes significantly different from the reference (A = 1.0, 0.88, 0.42, and 0.30) were detected with high accuracy (> 78.3%), while stimuli closer to the reference (A = 0.65 or 0.52) were detected with lower accuracy (60.3 %), which is close to a 50 % rate expected by chance. A fitted profit function in the psychometric model reveals points of equivalence at A = 0.704 for bump detection and A = 0.721 for hole detection. The 75% just-noticeable difference (JND) is 26.8 mN for bump and 31.9 mN for holes.

Participants also provided subjective feedback after completing the experiment. Most of them founded that the sensations of touching a "bump" or a "hole" were trivial to differentiate. Two described the perception of bump as "first climbing up a hill and then down a slope", with the reverse sensation for "holes". Another participant noted that he/she identified a "bump" by "feeling my finger decelerating before accelerating". Additionally, two participants mentioned that detecting "holes" was slightly more challenging, and required more time to make a decision, aligning with the higher JND observed for holes.

The well-fitted sigmoidal curves in the psychometric model, combined with subjective comments, confirm that the Gaussian potential fields rendered by active force can be effectively perceived as "bumps" and "holes" by users. This discrimination ability suggests this approach could be applied to the design of tangible interfaces, such as tac-

tile icons or keys of a keyboard.

4.5. STUDY 2: FITTS' POINTING TASK

Sliding on a touchpad to move the cursor to an icon, dragging and dropping or scrolling an alarm clock can be considered a pointing task to a desired location, which is elemental in human-computer interactions. Here, we investigate whether adding active force feedback during sliding can improve users performance in Fitts' pointing task.

4.5.1. STUDY DESIGN

A one-dimensional pointing task was designed, requiring participants to slide against the touchpad to locate a target using sensory cues. We used a repeated within-subjects design with three independent factors: feedback condition, target distance, and target width. A GUI displayed the task.

We evaluated user performance across four feedback modalities: active force, friction modulation, vision-only, and vision combined with active force, see Fig. 4.5. In the first two haptic-only conditions, targets were invisible, requiring participants to recognize them solely through touch. The last two conditions had visible targets, allowing us to assess whether adding active force feedback improves pointing performance.

For *friction modulation*, we employed a step-wise friction profile, with high friction in the target and low friction elsewhere, similar to prior studies [2], [4], [5]. Friction modulation was actuated with two standing-wave modes that are in phase. In *active force* and *vision + active force* conditions, a step-wise force profile was applied: outside the target, a uniform lateral force was used to direct the finger toward the target; while inside the target, the touchpad was deactivated to produce a high friction area as in *friction modulation*. In the *vision* condition, friction was uniformly low to eliminate any friction-induced feedback. The amplitude of driving voltages remained constant at ± 66 V across all conditions.

We tested three target distances (200, 400, and 600 pixels) and three target widths (16, 32, and 48 pixels). The control-to-display ratio was set to 10 pixels/mm, meaning the smallest and farthest target was 1.6 mm wide and 60 mm far on the touchpad. The ratio is comparable to standard laptop touchpads. The target sizes were chosen to reflect typical pointing tasks on touchpads. For example, 16-pixel targets represent small icons, such as a volume control in the corner of a laptop screen, while 48-pixel targets represent large icons, such as browser shortcuts on the taskbar. These combinations of distances and widths created nine movement conditions, yielding seven distinct indices of difficulty (ID) from 2.369 to 5.267, defined as $\log_2(\frac{D}{W}+1)$, where D is the target distance and W is the width.

Task. Participants received the task sounds indicating the start and selecting actions through headphones. During each trial, they slid their index finger across the surface to locate the target as quickly and accurately as possible. The trial includes the following steps, adapted from [2]:

1. *Initial state.* The blue start area appears on either the left or right side of the interface randomly to prevent potential orientation bias. In *vision* or *vision + active force* conditions, the red target is also displayed.

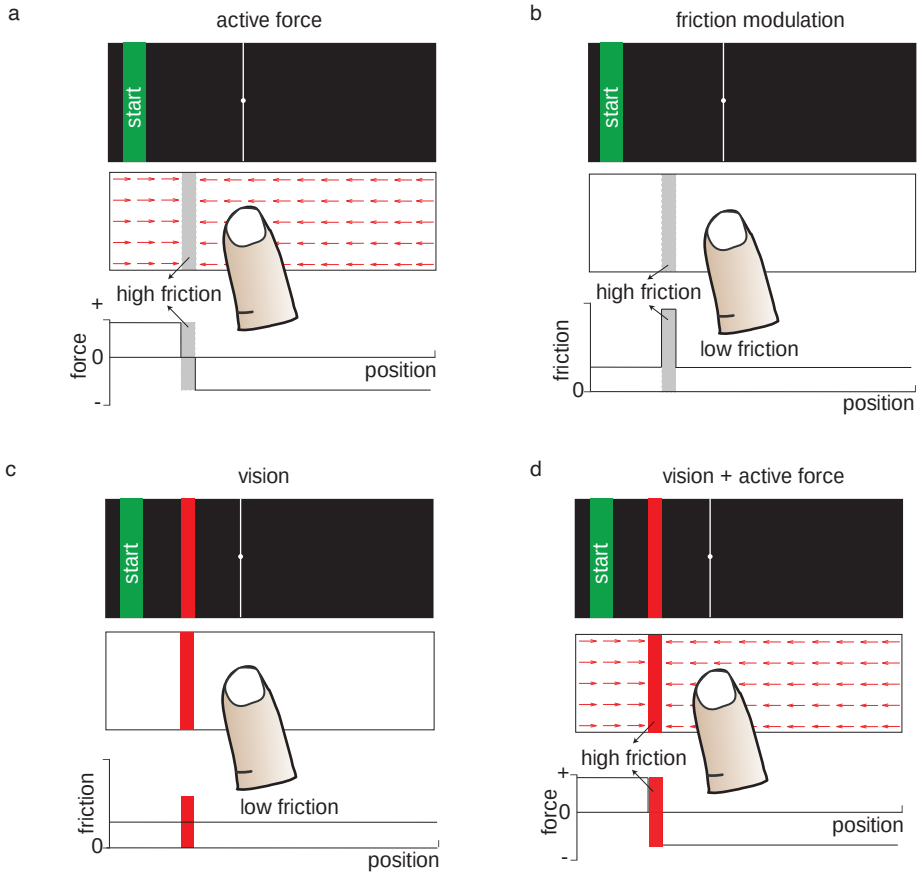

Figure 4.5: Implementation of designs for force and friction profiles, evaluated as four feedback conditions in a pointing task. (a) *active force* and (d) *vision + active force* conditions share an identical force profile, where forces consistently push the finger toward the target. In (b) *friction modulation* condition, friction is high inside and low outside the target area. In (c) *vision* condition, friction remains consistently low. Targets are visible only in conditions (c) and (d).

2. *Trigger start.* Participants move the white cursor that represents the finger position to the start area, and hold for 0.6 s. An audible sound is heard, and the start area turns green. The clock starts.

3. *Slide to find.* Participants slide their finger to locate the target using haptic or visual cues. They are allowed to move back and forth over the target to confirm the target location in all conditions.

4. *Lift-off to select.* Participants lift their finger at the perceived target location. A sound is played to confirm the action of selection.

Participants began with a training session with the same tasks as the experimental one to familiarize themselves with the sensation and task requirements. They were encouraged to adjust the normal force applied to optimize their perception of the feedback. Training continued until participants felt familiar with the haptic sensations and task procedures but was limited to a maximum of 15 minutes per participant. After training, participants completed two experimental sessions, totaling 216 trials, including 4 feedback conditions × 3 distances × 3 widths × 6 repeats. Each session included 108 trials, with a three-minute break provided between sessions. To minimize anticipation or adaptation effects, the order of feedback and movement conditions was randomized.

Participants. Twelve participants (5 females and 7 males, aged 23-29, all right-handed) were recruited for this study. All reported no sensory impairments or skin ailments. None participated in S1.

4.5.2. RESULTS

We conducted a repeated measures analysis of variance (RM-ANOVA) on four dependent variables: completion time, approach time, selection time, and entry count. The independent variables are feedback conditions, target distances, and target widths. Additionally, we examined Fitts' law parameters and collected subjective responses from participants.

Overall observations. We observed that the maximum deviation between the selected and desired target position across all participants and conditions was 35 pixels (≈ 3.5 mm on the touchpad). Given that this deviation is relatively small compared to the full selection range of 1000 pixels, it suggests thatparticipants relied on sensory cues to select rather than guessing. This observation implies that both *friction modulation* and *active force* feedback provided effective cues on the presence of the target. The other observation is that the majority of extra-long trials (duration > 3 s), which accounts for 3.5% of total (91 trials), occurs in *friction modulation* (82 trials), with far fewer in *active force* (8 trials) and *vision* (1 trial).

Completion time and Fitts' law. RM-ANOVA shows significant effects on completion time from target widths ($F_{2,22} = 138.57,\ p < 0.001$), target distances ($F_{2,22} = 47.545,\ p < 0.001$) and feedback modality ($F_{3,33} = 187.63,\ p < 0.001$). Figure 4.6a presents the average completion times across nine movement conditions and four feedback conditions. For haptic-only conditions, *active force* required shorter completion time than *friction modulation* for all the nine movement conditions. When averaging all these movement conditions, *active force* reduced the targeting duration by 22.9 % from 2.165 s to 1.669

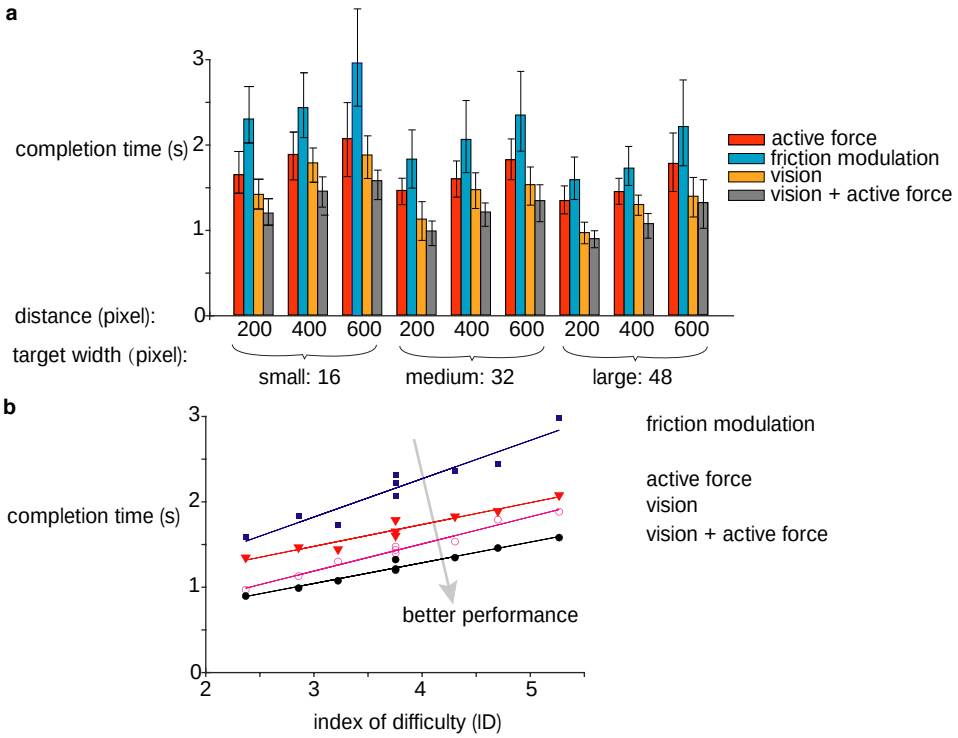

Figure 4.6: (a) Mean completion time in a pointing task across nine movement conditions. (b) Linear regression for mean completion time based on Fitts' indices of difficulty (ID).

s, compared to *friction modulation*, with Post-hoc Tukey-Kramer tests also confirming the significant differences between them with $p < 0.01$ across all widths and distances. These results highlight the clear advantage of active force feedback in eyes-free targeting tasks. Additionally, when combined with visual feedback, active force further reduced completion time by 15.5%, from 1.433 to 1.211 s, with post-hoc comparisons showing a significant difference between *vision* and *vision+active force* ($p < 0.05$) for all movement conditions. The Fitts' law analysis reveals a strong linear relationship between the averaged completion time and the index of difficulty across all feedback conditions (Fig. 4.6b; $r^2 > 0.91$). The reciprocal of the slope, which represents the index of performance, highlights the notable differences between feedback modalities. For haptic-only conditions, *active force* has a higher index than *friction modulation* (3.92 bits/s vs. 2.23 bits/s), while for visual-present conditions, vision+ active force outperforms vision (4.13 bits/s vs. 3.14 bits/s.), as summarized in (Tab. 4.1). These comparisons demonstrate the advantages of active force feedback in both vision-present and eyes-free modalities.

Source for faster pointing. We investigate the source of reduced completion times in active force-assisted conditions. Specifically, these improvements could be due to faster movements toward target under the attractive force field, or due to quicker selection enhanced by sensory feedback from the active force. We performed Post-hoc Tukey-

condition	a	b	r^2	index of performance
active force	0.7152	0.2551	0.939	3.92
friction modulation	0.4751	0.4489	0.915	2.23
vision	0.2337	0.3180	0.978	3.14
vision + active force	0.3188	0.2419	0.970	4.13

Table 4.1: Fitts' law parameters for four feedback conditions. In Fitts' law, movement time is modeled as $a + b \times$ ID. The index of performance is defined as the reciprocal of the slope, i.e., $1/b$.

Kramer tests to compare feedback conditions based on approach time (the duration from initial moving to the first entry into the target area), selection time (the remaining component of completion time) and entry count (the number of times the participant crosses the target boundaries).

Results show that all feedback conditions differ significantly in terms of overall completion time ($p < 0.001$). However, the most pronounced differences are observed in selection time, where all pairwise comparisons yield a high significant difference level $p < 0.001$, as illustrated in Fig. 4.7a. In contrast, the differences in approach time are less significant ($p < 0.05$) or not significant (e.g. *vision* vs *active force*) (except *vision* vs *vision + active force* where $p < 0.01$). The variation in selection time is partially supported by participants' sliding behavior. Figure 4.7b reveals significant differences between haptic conditions: *active force* (mean = 2.17, SD = 0.8069) and *friction modulation* (mean = 2.41, SD = 1.03); between vision-present conditions: *vision* (mean = 1.47, SD = 0.60) and *vision + active feedback* (mean = 1.54, SD = 0.69), and no significant difference between *vision* and *vision + active force*. On average, the *active force* condition requires 0.237 fewer entry counts than *friction modulation*. This observation suggests that active force rendered target enhances user confidence by providing more compelling cues for target location.

Subjective response. Ten out of twelve participants provided feedback on their preferences and perceptions of the sensations. All ten participants expressed a clear preference for *active force* feedback over *friction modulation* for efficiently locating a target. They also described targets rendered with active force as having a "clear edge", whereas those by friction modulation felt like a "sticky region". Additionally, six participants noted a learning effect during both the training and experimental sessions. They commented that they initially moved cautiously to detect and identify the presence of a target but were able to move faster and more confidently after several minutes. This observation suggests that users' performance may improve with extended training.

4.6. STUDY 3: DIRECTIONAL NAVIGATION

In this study, we investigate if suddenly activating a potential field under a stationary finger communicate a directional cue to users and help them navigate toward the target.

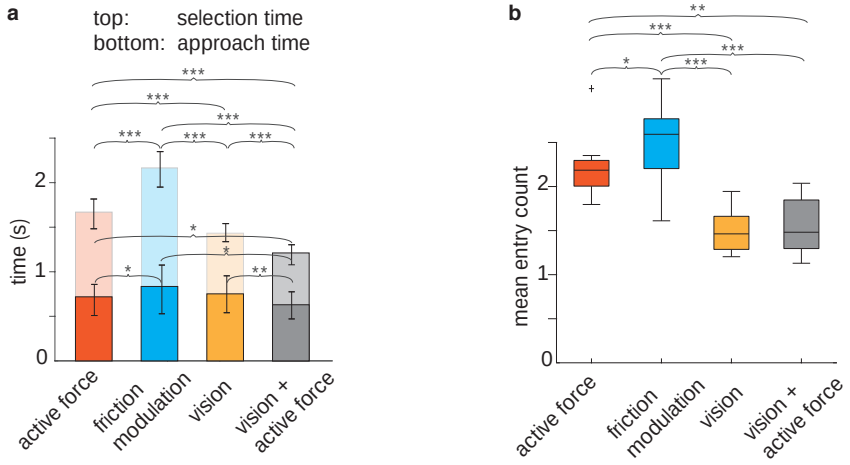

Figure 4.7: (a) The completion time of a pointing task comprises two components: approach time (dark-colored bar at the bottom) and selection time (light-colored bar at the top). (b) Box plot of entry count for each feedback condition. Stars indicate the significance level: * $p < 0.05$, ** $p < 0.01$ and *** $p < 0.001$

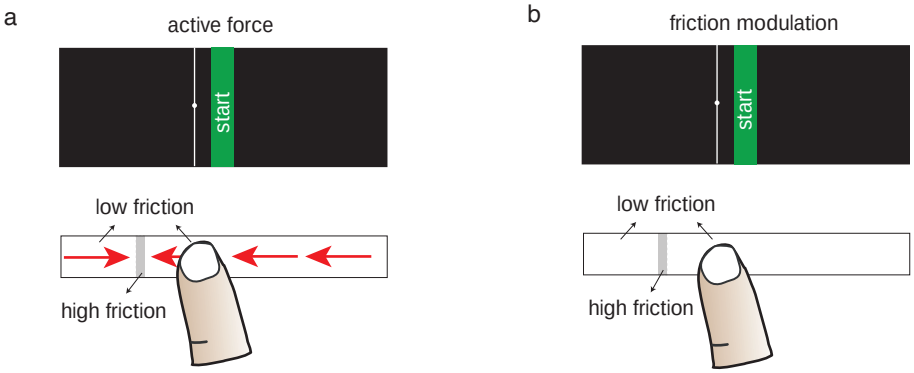

Figure 4.8: Top: GUI of a pointing task with directional navigation. The invisible target can locate to the right or left of the start area. Bottom: force or friction field in *active force* (a) or *friction modulation* (b) condition, respectively.

4.6.1. STUDY DESIGN

We deployed a pointing task using the GUI where the start area was located at the center, as shown in Fig. 4.8. We used a repeated within-subjects design with three independent variables: feedback conditions, target widths, and target distances. Feedback conditions were *active force* are *friction modulation*. The force and friction profiles are presented in Fig. 4.8. Target distance to the start area were ± 250 pixels and ± 350 pixels, and target widths were 16 pixels and 32 pixels.

During the experiments, participants first placed their index finger on the start area, where no tactile feedback was provided. Once the active force or friction modulation profile issued, they started the pointing task. They were encouraged to use the directional cues to facilitate target searching.

Participants. Ten participants (5 females and 5 males, aged 21–28, all right-handed) were recruited for this study. All reported no sensory impairments or skin ailments. None participated in S1-2.

4.6.2. RESULTS

RM-ANOVA on completion time reveals a statistically significant effect of feedback conditions ($F_{1,9} = 92,\ p = 5.1 \times 10^{-6}$), and target widths ($F_{1,9} = 9.4,\ p = 0.014$), but no significant effect of target distances ($F_{1,9} = 0.055,\ p = 0.82$). Post-hoc comparisons show a significant difference between *active force* and *friction modulation* in all the four movement conditions ($p < 0.001$), as shown in the box plots of completion times in Figure 4.9a. On average, *active force* leads to a considerably shorter completion time compared to *friction modulation* (1.82 s vs. 3.10 s), reflecting a 41.26% reduction. This improvement is even more significant than the 22.9% reduction observed in S2.

To identify the source of this reduction, we analyzed the error rates in participants' initial moving direction. The friction modulation condition exhibited a considerably higher error rate of 51%, close to random choice. By contrast, the error rate in *active force* condition was only 12%, demonstrating that active force feedback provides salient directional cues.

Movement trajectories further highlight the difference in participants' selection behavior in these two feedback conditions. For a condition where the target width is 16 pixels and the distance is 350 pixels, trajectories in active force show a clear bias towards the target side. Conversely, trajectories under friction modulation were more evenly distributed between both directions (Fig. 4.10). These biased trajectories and the lower error rate indicate that the directional force field effectively directed the users toward lower potential, resulting in shorter completion times.

4.7. USER EXPERIENCE WITH APPLICATIONS

Here, we showcase three applications to demonstrate the role of potential fields in enhancing touch interaction tasks. The designed potential fields in these applications correspond to those in S1-3. For each application, we outline the motivation behind its design, detail its implementation, and evaluate user experience based on subjective responses.

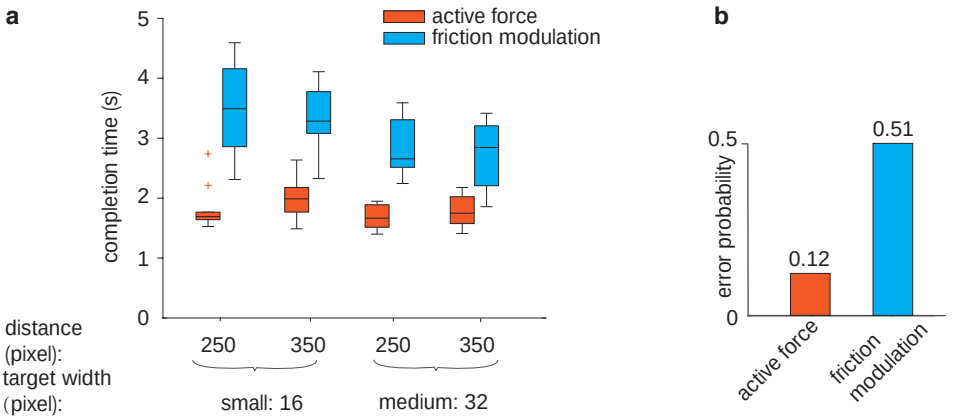

Figure 4.9: (a) Mean completion time in a pointing task with directional navigation. (b) The error rate in terms of correctly moving to the target side upon the onset of active force or friction modulation activation.

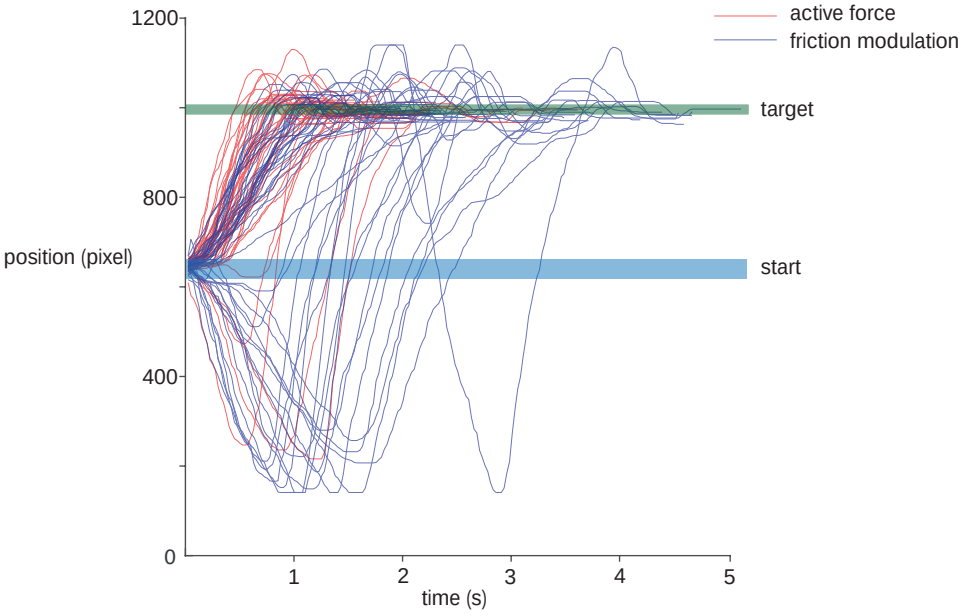

Figure 4.10: Trajectories in a pointing task with directional navigation where the target width is 16 pixels and the target distance is 350 pixels. Red: *active force* condition; blue: *friction modulation* condition.

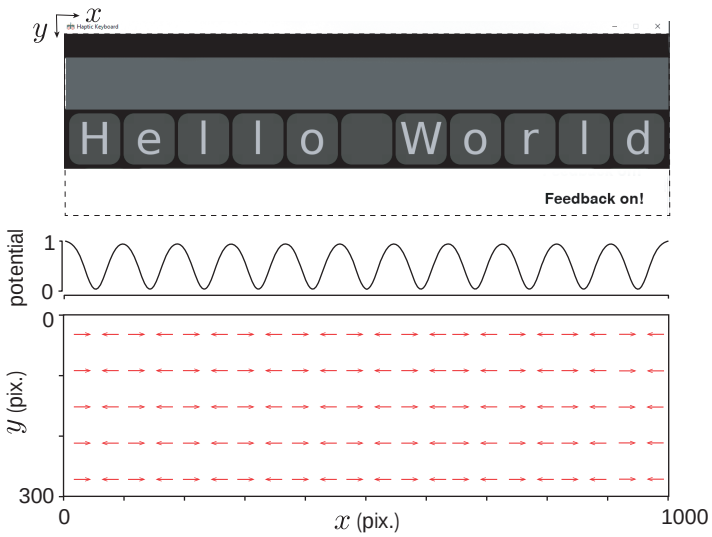

Figure 4.11: Design of a virtual keyboard rendered by Gaussian potential wells. From top to bottom is the graphical user interface, potential function regarding x and the force field.

4.7.1. APPLICATION DESIGN

Haptic Keyboard. Typing on a featureless touchpad or touchscreen requires users to visually search for keys and avoid clicking on incorrect locations (e.g. between keys). This process is significantly slower and more visually demanding compared to typing on a physical keyboard, where muscle memory enables effortless key localization. The potential field approach can be suitable to help users navigate to the desired keys on a virtual keyboard.

Here, we create attractive potential fields centered in the middle of each key, similar to those evaluated in the psycho-physical study in S1. The overall potential field on the surface is the sum of these individual potentials, as shown in Fig. 4.11. The exemplar displays the text "Hello World" to showcase how haptic feedback guide users in locating and sliding to keys. In practical applications, this approach can be customized to support various layouts, such as the standard "QWERTY" configuration. Additionally, it can be integrated with key-click sensation, as described in [8], to restore both the key localization and key press functions. We will examine whether these potential fields can improve users' ability to locate keys and avoid clicking on wrong keys.

Three-Digit Lock. The Three-Digit Lock game was created to assess whether users can locate a "password", using only tactile feedback, as illustrated in Fig. 4.12. In this game, users discover a randomly generated three-digit password by sliding on the touchpad to rotate the dials in each row. The design incorporates a directional step-wise force field, similar to that in S3. The "valley" of the attractive potential field corresponds to the location of the password on the dial. The step-change force around a sticky region is implemented to assist users in locating the correct digit effectively.

Angry Birds Game. An attractive potential field was designed to replicate the pulling

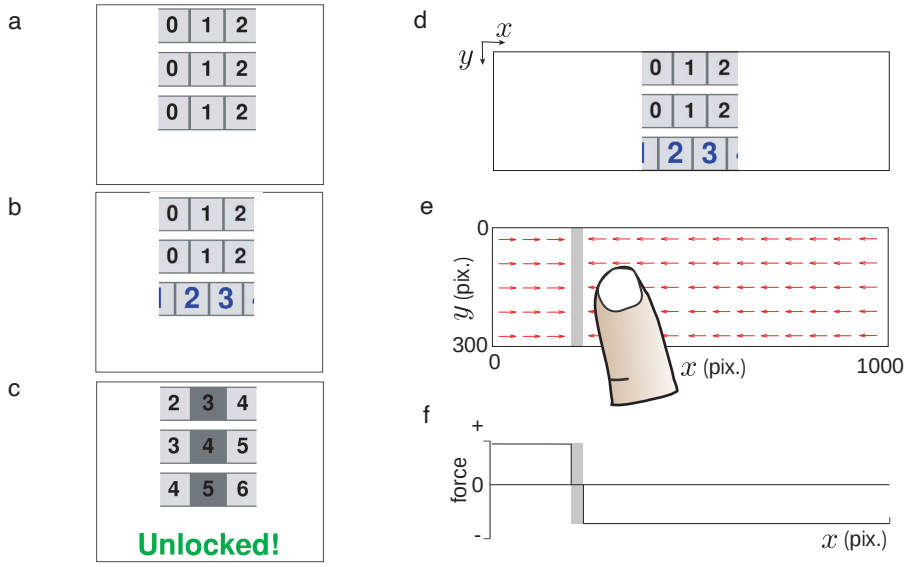

Figure 4.12: A three-digit lock game that facilitates password finding using step-wise attractive force fields.

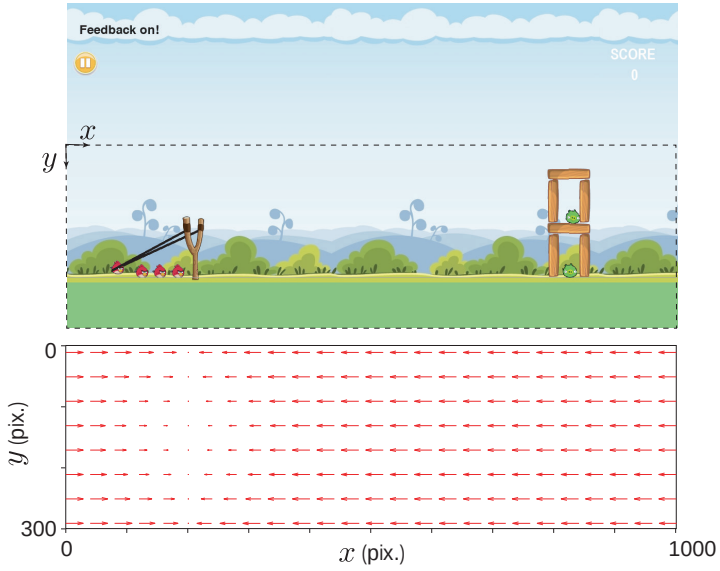

Figure 4.13: Angry Birds Game in which the slingshot creates an attraction field. The lateral force is proportional to the distance to the slingshot.

sensation of a slingshot. Within the maximum stretchable length of the slingshot, the force vector linearly increases with the length. Beyond this limit, the lateral force plateaus. Once the user catches the slingshot, they can perceive both the intensity and direction of the dragging forces, even when stationary.

4.7.2. USER STUDY AND RESULTS

Experimental Procedures. Participants interacted with each of the three applications for three minutes, then completed a comparison questionnaire and answered three open-ended questions. During the interaction, they were encouraged to toggle the haptic feedback on and off to compare the potential fields with the plain aluminum surface. The presentation order of the applications followed a Latin Square design to minimize ordering effects.

The comparison questionnaire, adapted from Levesque et al. [2], assessed the effects of potential fields in seven dimensions: concentration, preference, ease of use, reduced visual load, realism, confidence, and enjoyment. Participants rated each aspect on a 7-point Likert scale (from "strongly disagree" to "strongly agree"). The statements were:

- C1. Concentration: Compared to no feedback, tactile feedback made me more focused and absorbed in the interaction task.
- C2. Preference: I prefer tactile feedback over no feedback.
- C3. Ease: Tactile feedback made the task easier to perform.
- C4. Reduced Visual attention: Tactile feedback reduced my need for visual attention.
- C5. Realism: The interaction felt more realistic with tactile feedback.
- C6. Confidence: With tactile feedback, I felt more confident in my movements and actions.
- C7. Enjoyment: Tactile feedback made the application more enjoyable.

Three open-ended questions of each application were:

- Q1: How would you describe the sensations of the tactile feedback in this application?
- Q2: Is there anything you liked or disliked about the tactile feedback?
- Q3: Do you have any suggestions on how the sensations could be improved?

Participants. We recruited ten participants (five females), aged 22 to 43. One was left-handed, and nine were right-handed. None participated in prior sessions (S1–3).

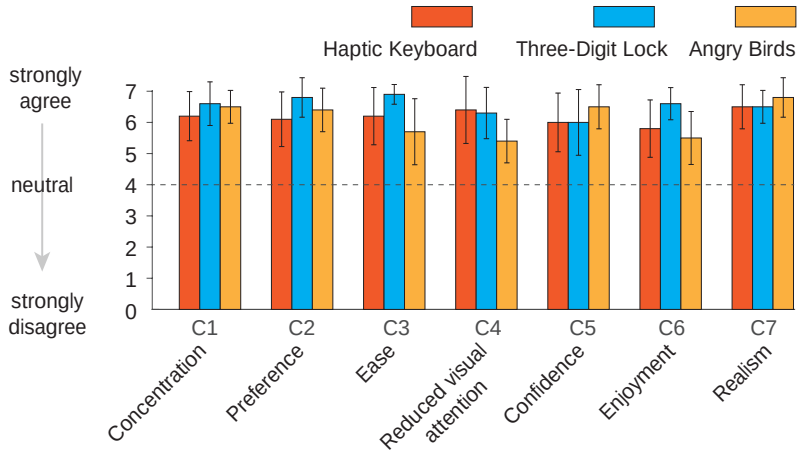

Figure 4.14: Mean and standard deviation of ratings from the comparison questionnaire (C1 to C7) for Haptic Keyboard, Three-Digit Lock, and Angry Birds.

Results. Figure 4.14 presents the average ratings and standard deviations for each question (C1 to C7) across three applications. All averaged ratings across participants of each question and application are positive (above 4, or "Neutral"), indicating favorable feedback from participants.

The **Haptic Keyboard** received the highest score in C4 (reduced visual attention), with an average of 6.4. Participants noted that the tactile feedback helped them locate their fingers on the keys without the need of visual confirmation. For example, P5 remarked, *"It made it easier to feel the location of my fingers on the keyboard without looking at it.*" and "*The distance between keys is similar to my keyboard, so I could move my finger fast*".P1 commented, "*It confirmed I was in the right spot on the keys, not between them.*" Some participants described the sensation as "*like playing with magnets*" (P7) or "*like surfing on the surface, but not like a mechanical keyboard*" (P6).

The **Three-Digit Lock** ranked highest in C1, C2, C3, and C6 (concentration, preference, ease, and confidence). Participants reported that they could find the correct password within seconds after starting searching. They frequently mentioned that the feedback made it easy to locate the correct password, with P2-P9 describing the sensation of reaching to the password as "very clear."

The **Angry Birds Game** scored highest in C5 (realism) and C7 (enjoyment). Participants frequently mentioned a strong sense of realism and fun in Q1 and Q2. Comments included "*I felt like I was dragging a rubber band*" (P6) and "a slingshot" (P10). P10 also stated, "*I could clearly feel that the more I dragged, the more force was pulling my finger.*"

Negative feedback and suggestions for improvement were collected in Q2 and Q3. For the Angry Birds Game, P10 noted, "*Sometimes I couldn't feel the change in force when I pulled the slingshot further.* " For the haptic keyboard, P2 mentioned, "*The force feedback was disappointing when I wasn't in the middle of a key*", while P5 suggested, "*It would be great if the keyboard worked in two dimensions*". P10 proposed integrating *"a key-click sensation"* for enhanced realism."

4.8. DISCUSSION

Advances in active force-based surface haptics have shown the potential to add a new dimension to tactile feedback. However, prior research has primarily focused on hardware development. In this study, we implemented programmable impedance control by real-time modulating traveling wave parameters and designed several user studies to evaluate its effectiveness. For the first time, we demonstrate the positive impact of active force feedback in users during sliding interaction, supported by both measurable performance gains and positive user experience.

Three HCI applications received positive feedback from participants, further confirming the transferability of these benefits observed in S1-3 to practical use cases. These findings could inspire more applications and tactile interface design. Next, we discuss some implications of these results, assess their values, and address the limitations and recommendations for future research.

4.8.1. HAPTIC GUIDANCE WITH POTENTIAL FIELDS

The artificial Potential Field method is widely used in classical haptics and robotic applications, such as haptic rendering for training [37] and teleoperation [38] and path planning for mobile robots [39]. This method generates repulsive fields for obstacle avoidance and attractive fields for path guidance. To display potential fields on a flat surface, the necessity is to have active forces that can build up potential. We successfully implemented programmable surface potential field rendering by controlling traveling waves in real time. Importantly, we have three key observations in users: they have a clear awareness of the scale and polarity of these potentials, they show behavior change by being attracted to lower potential, and experience positive emotional effects.

It is valuable to compare friction modulation and active force feedback in haptic rendering. One can render 3D features by mapping the height of the feature directly to the friction [40], or by mapping the dot product of the sliding velocity and gradient of the feature to the local friction [7]. The resulting frictional field is a pseudo-potential field, due to the non-conservative nature of friction, thus only providing tactile cues on the sliding paths without indicating proximal features. As a result, this approach is often used to augment visually represented features [7], where the finger exploration is consciously guided by visual input. When visual feedback is absent or when the finger stops moving, the haptic guidance severely deteriorates. For example, in the case of guiding along a curved path in Fig. 4.2c, users have to slide back and forth around the path to identify it, and path following becomes inaccurate and time-consuming. In contrast, active forces can create both repulsive and attractive fields that can push the finger to the path effectively and robustly, even without a need for visual input.

Unlike other haptic devices that provide directional guidance through handheld tools, such as tactile compasses [41] or pseudo-forces [42], our approach enables bare-finger interaction by instrumenting a surface with traveling waves. Users can freely use their fingers for other tasks and engage with the guidance only when desired. This feature might be well-suited for integration into haptic touchpads, screen readers for visually impaired users, large touchscreens in vending machines or museum exhibits, and educational displays.These applications can facilitate touch interactions and simulate physics like flowing fluids, or elastic springs.

4.8.2. POINTING FACILITATION USING ACTIVE FORCE VS FRICTION MODULATION

In the pointing task in S2, augmenting the high-friction target with active forces led to a significant permanence gain of 22.9%, compared to the friction modulation approach using the same level of actuation. This improvement does not appear to arise from faster approach but rather from enhanced target awareness, as evidenced by the observations of variation in selection duration, sliding behavior, and participants' descriptions of their target perception.

Indeed, when we look at target rendering from the perspective of a fingertip, it undergoes a temporal evolution of tactile stimuli during reaching. In the active force scheme, the finger experiences a sudden change in impedance, that is from a negative impedance (i.e. pushing forces) to positive impedance (high friction and resisting force). In contrast, friction modulation scheme only involves a sudden increase in friction. This additional reversal of the active lateral force enhances the "braking" effect upon reaching the target, making it easier for the finger to stop near the target.

This advantage is particularly evident for rendering small targets. Due to inertia, the finger may continue sliding upon entering the target area. The friction modulation approach only generates a short duration that users can feel a high friction. This short-lived feeling of high impedance may well be insufficient to trap the finger or even aware users. Consequently, users may miss the target and need to slide back and forth to identify it. This limitation leads to a marked performance degradation. For instance, reaching a small target (width = 1.6 mm) with friction modulation requires 30.94% more time compared to larger targets. In contrast, active forces still possess an abrupt change of lateral force, no matter how small the target is, resulting in reduced degradation due to small target of 18.51%. This feature offers higher rendering resolution, making active force feedback especially suitable for rendering small elements, such as text.

Additionally, the directional cues provided by the active force also contribute to faster target finding. In the active force condition, users receive clear directional guidance, especially when searching near the target at low speeds. Even when the finger is nearly stationary, the active force provides strong directional cues to the finger. These directional cues always drag the finger to the location of the target. In contrast, with variable friction, users must slide back and forth more times to perceive friction changes, making it more difficult and time-consuming to detect and correct for a missed target.

4.8.3. POSSIBILITY TO RESTORE PROCEDURAL MEMORY

While we did not statistically investigate learning effects in this chapter, we did observe variable learning among participants during the training and experimental sessions. In S2, some participants reported noticeable performance improvements in the training, as indicated in their verbal feedback. This improvement is also reflected in their adapted targeting behavior. In some trials, they first performed a fast-reaching movement to quickly estimate the target location and then used more controlled movements to finely locate the target. This strategy resulted in larger overshoots but shorter completion times. These observations indicate the development of procedural memory in users through leveraging tangible potential fields.

We anticipate that further improvements in performance could be achieved with

continued learning. In our experimental design, feedback conditions were randomized across trials, and participants were unaware of the specific conditions they would encounter prior to each trial. Consequently, they were unable to fully exploit the procedural memory that could have been developed. In practical applications where haptic feedback conditions are predetermined, users could build procedural memory more effectively. This would enable them to employ their learned muscle memory with greater confidence, potentially leading to even faster and more efficient target selections. Moreover, when integrating this haptic-assisted pointing with keyclick sensations [8], [13], [15], [43], it is promising to achieve eyes-free control over virtual widgets, benefiting sighted users in visually demanding situations and allowing visually impaired users to access them.

4.8.4. LIMITATIONS AND FUTURE WORK

We acknowledge several limitations in this chapter. First, we did not address the variability in the perceived intensity of stimuli. The apparatus operates in feed-forward. Different pressing forces and fingertip stiffness can cause variable force output between individuals and trials. Second, the force generation model did not consider sliding velocity. We used a data-driven force-phase model, measured with a static finger. Fast and slow-moving fingers may result in different actual force output. These limitations could be addressed by incorporating closed-loop control to monitor and adjust force output.

Furthermore, future work could be extended to the following directions:

Expanding interaction modalities. Future work could explore more interaction modalities using potential fields, such as improving Steering Law tasks or guiding users along curved paths without visual feedback.

Broader application design. More potential fields could be tailored to specific applications, such as rendering racetrack lanes in racing games, creating tactile chessboard grids, or adding periodic potential wells that fit bookmark bars of a computer or fit contents to be scrolled on touchscreens.

Two-dimensional active surface haptic devices. To date, only one-dimensional active surface haptic devices are documented in the literature. This chapter reveals the pressing need for two-dimensional active surface haptic devices that generate lateral forces in any direction on a surface. The demonstrated benefits of the potential field approach in this chapter could be directly extended to two-dimensional applications.

4.9. CONCLUSION

We created artificial potential fields on the fingertip by dynamically adjusting the traveling wave ratio in an active surface haptic device. These potentials significantly enhanced touch interaction in three tasks: (1) perception of bumps and holes, (2) Fitts' pointing tasks, and (3) directional navigation. User studies qualitatively demonstrated that the generated potential fields effectively convey both the height and depth of the fields and guide the finger toward targets.

We designed three applications to showcase the versatility of potential field design. These applications leverage the strengths of the aforementioned qualitative studies. User feedback confirmed that these applications are well-suited for incorporating these hap-

tic renderings. Our findings highlight that rendering potential fields by controling traveling waves is an effective way to guide bare finger interactions with touch alone. This capability is only possible with active force feedback and cannot be replicated with vibrotactile or friction modulation techniques. This research underscores the promise of artificial potential field rendering to enhance touch interactions and provide diverse and immersive tactile experiences.

REFERENCES

[1] E. Koskinen, T. Kaaresoja, and P. Laitinen, "Feel-good touch: Finding the most pleasant tactile feedback for a mobile touch screen button", in *Proceedings of the 10th international conference on Multimodal interfaces*, ser. ICMI '08, New York, NY, USA, Oct. 2008, pp. 297–304, ISBN: 978-1-60558-198-9. DOI: 10.1145/1452392.1452453.

[2] V. Levesque, L. Oram, K. MacLean, *et al.*, "Enhancing physicality in touch interaction with programmable friction", in *Proceedings of the SIGCHI Conference on Human Factors in Computing Systems*, ser. CHI '11, May 2011, pp. 2481–2490, ISBN: 978-1-4503-0228-9. DOI: 10.1145/1978942.1979306.

[3] O. Bau, I. Poupyrev, A. Israr, and C. Harrison, "TeslaTouch: Electrovibration for touch surfaces", in *Proceedings of the 23nd annual ACM symposium on User interface software and technology*, ser. UIST '10, New York, NY, USA, Oct. 2010, pp. 283–292, ISBN: 978-1-4503-0271-5. DOI: 10.1145/1866029.1866074.

[4] G. Casiez, N. Roussel, R. Vanbelleghem, and F. Giraud, "Surfpad: Riding towards targets on a squeeze film effect", in *Proceedings of the SIGCHI Conference on Human Factors in Computing Systems*, ser. CHI '11, New York, NY, USA, 2011, pp. 2491–2500, ISBN: 978-1-4503-0228-9.

[5] Y. Zhang and C. Harrison, "Quantifying the Targeting Performance Benefit of Electrostatic Haptic Feedback on Touchscreens", in *Proceedings of the 2015 International Conference on Interactive Tabletops & Surfaces*, ser. ITS '15, New York, NY, USA, 2015, pp. 43–46, ISBN: 978-1-4503-3899-8.

[6] C. Bernard, J. Monnoyer, S. Ystad, and M. Wiertlewski, "Eyes-Off Your Fingers: Gradual Surface Haptic Feedback Improves Eyes-Free Touchscreen Interaction", in *Proceedings of the 2022 CHI Conference on Human Factors in Computing Systems*, ser. CHI '22, New York, NY, USA, Apr. 2022, pp. 1–10, ISBN: 978-1-4503-9157-3. DOI: 10.1145/3491102.3501872.

[7] S.-C. Kim, A. Israr, and I. Poupyrev, "Tactile rendering of 3D features on touch surfaces", in *Proceedings of the 26th annual ACM symposium on User interface software and technology*, ser. UIST '13, New York, NY, USA, Oct. 2013, pp. 531–538, ISBN: 978-1-4503-2268-3. DOI: 10.1145/2501988.2502020.

[8] Z. Cai and M. Wiertlewski, "Ultraloop: Active Lateral Force Feedback Using Resonant Traveling Waves", *IEEE Trans. Haptics*, vol. 16, no. 4, pp. 652–657, 2023, ISSN: 2329-4051.

[9] H. Xu, M. A. Peshkin, and J. E. Colgate, "UltraShiver: Lateral Force Feedback on a Bare Fingertip via Ultrasonic Oscillation and Electroadhesion", *IEEE Trans. Haptics*, vol. 12, no. 4, pp. 497–507, Oct. 2019, ISSN: 2329-4051. DOI: 10.1109/TOH.2019.2934853.

[10] H. Xu, M. A. Peshkin, and J. E. Colgate, "SwitchPaD: Active Lateral Force Feedback over a Large Area Based on Switching Resonant Modes", en, in *Haptics: Science, Technology, Applications*, 2020, pp. 217–225, ISBN: 978-3-030-58147-3. DOI: 10.1007/978-3-030-58147-3_24.

[11] X. Dai, J. E. Colgate, and M. A. Peshkin, "LateralPaD: A surface-haptic device that produces lateral forces on a bare finger", in *2012 IEEE Haptics Symposium (HAPTICS)*, Mar. 2012, pp. 7–14. DOI: 10.1109/HAPTIC.2012.6183753.

[12] E. C. Chubb, J. E. Colgate, and M. A. Peshkin, "ShiverPaD: A Glass Haptic Surface That Produces Shear Force on a Bare Finger", *IEEE Trans. Haptics*, vol. 3, no. 3, pp. 189–198, Jul. 2010, ISSN: 2329-4051. DOI: 10.1109/TOH.2010.7.

[13] D. Brahimaj, M. Ouari, A. Kaci, F. Giraud, C. Giraud-Audine, and B. Semail, "Temporal Detection Threshold of Audio-Tactile Delays With Virtual Button", *IEEE Transactions on Haptics*, pp. 1–6, 2023, Conference Name: IEEE Transactions on Haptics, ISSN: 2329-4051. DOI: 10.1109/TOH.2023.3268842.

[14] P. Garcia, F. Giraud, B. Lemaire-Semail, M. Rupin, and M. Amberg, "2MoTac: Simulation of Button Click by Superposition of Two Ultrasonic Plate Waves", en, in *Haptics: Science, Technology, Applications*, 2020, pp. 343–352, ISBN: 978-3-030-58147-3. DOI: 10.1007/978-3-030-58147-3_38.

[15] D. Gueorguiev, A. Kaci, M. Amberg, F. Giraud, and B. Lemaire-Semail, "Travelling Ultrasonic Wave Enhances Keyclick Sensation", en, in *Haptics: Science, Technology, and Applications*, D. Prattichizzo, H. Shinoda, H. Z. Tan, E. Ruffaldi, and A. Frisoli, Eds., 2018, pp. 302–312, ISBN: 978-3-319-93399-3. DOI: 10.1007/978-3-319-93399-3_27.

[16] L. Winfield, J. Glassmire, J. E. Colgate, and M. Peshkin, "T-pad: Tactile pattern display through variable friction reduction", in *2007 2nd Joint EuroHaptics Conference and Symposium on Haptic Interfaces for Virtual Environments and Teleoperator Systems*, 2007, pp. 421–426.

[17] L. B. Rosenberg, "Virtual fixtures: Perceptual tools for telerobotic manipulation", in *Proceedings of IEEE virtual reality annual international symposium*, Ieee, 1993, pp. 76–82.

[18] K. Salisbury, D. Brock, T. Massie, N. Swarup, and C. Zilles, "Haptic rendering: Programming touch interaction with virtual objects", in *Proceedings of the 1995 symposium on Interactive 3D graphics*, ser. I3D '95, New York, NY, USA: Association for Computing Machinery, Apr. 1995, pp. 123–130, ISBN: 978-0-89791-736-0. DOI: 10.1145/199404.199426.

[19] J. Ren, K. A. McIsaac, R. V. Patel, and T. M. Peters, "A Potential Field Model Using Generalized Sigmoid Functions", *IEEE Transactions on Systems, Man, and Cybernetics, Part B (Cybernetics)*, vol. 37, no. 2, pp. 477–484, Apr. 2007, Conference Name: IEEE Transactions on Systems, Man, and Cybernetics, Part B (Cybernetics), ISSN: 1941-0492. DOI: 10.1109/TSMCB.2006.883866.

[20] E. Garcia–Canseco, A. Ayemlong–Fokem, A. Serrarens, and M. Steinbuch, "Haptic Simulation of a Gear Selector Lever Using Artificial Potential Fields", *IFAC Proceedings Volumes*, 11th IFAC/IFIP/IFORS/IEA Symposium on Analysis, Design, and Evaluation of Human-Machine Systems, vol. 43, no. 13, pp. 426–429, Jan. 2010, ISSN: 1474-6670. DOI: 10.3182/20100831-4-FR-2021.00075.

[21] T. Watanabe and S. Fukui, "A method for controlling tactile sensation of surface roughness using ultrasonic vibration", in *Proceedings of 1995 IEEE International Conference on Robotics and Automation*, vol. 1, May 1995, pp. 1134–1139. DOI: 10.1109/ROBOT.1995.525433.

[22] M. Wiertlewski, F. R. Fenton, and J. E. Colgate, "Partial squeeze film levitation modulates fingertip friction", *Proc. Nat. Acad. Sci.*, vol. 113, no. 33, pp. 9210–9215, Aug. 2016. DOI: 10.1073/pnas.1603908113.

[23] C. D. Shultz, M. A. Peshkin, and J. E. Colgate, "Surface haptics via electroadhesion: Expanding electrovibration with Johnsen and Rahbek", in *2015 IEEE World Haptics Conference (WHC)*, Jun. 2015, pp. 57–62. DOI: 10.1109/WHC.2015.7177691.

[24] M. Ayyildiz, M. Scaraggi, O. Sirin, C. Basdogan, and B. N. J. Persson, "Contact mechanics between the human finger and a touchscreen under electroadhesion", *Proc. Nat. Acad. Sci.*, vol. 115, no. 50, pp. 12 668–12 673, Dec. 2018. DOI: 10.1073/pnas.1811750115.

[25] R. H. Osgouei, J. R. Kim, and S. Choi, "Improving 3d shape recognition withelectrostatic friction display", *IEEE transactions on haptics*, vol. 10, no. 4, pp. 533–544, 2017.

[26] M. Azechi and S. Okamoto, "Easy-to-recognize bump shapes using only lateral force cues for real and virtual surfaces", in *2023 IEEE World Haptics Conference (WHC)*, IEEE, 2023, pp. 397–402.

[27] C. Choi, Y. Ma, X. Li, *et al.*, "Surface haptic rendering of virtual shapes through change in surface temperature", *Science Robotics*, vol. 7, no. 63, eabl4543, 2022.

[28] S. Saga and K. Deguchi, "Lateral-force-based 2.5-dimensional tactile display for touch screen", in *2012 IEEE Haptics Symposium (HAPTICS)*, ISSN: 2324-7355, Mar. 2012, pp. 15–22. DOI: 10.1109/HAPTIC.2012.6183764.

[29] A. Roudaut, A. Rau, C. Sterz, M. Plauth, P. Lopes, and P. Baudisch, "Gesture output: Eyes-free output using a force feedback touch surface", in *Proceedings of the SIGCHI Conference on Human Factors in Computing Systems*, 2013, pp. 2547–2556.

[30] J. Mullenbach, D. Johnson, J. E. Colgate, and M. A. Peshkin, "ActivePaD surface haptic device", in *2012 IEEE Haptics Symposium (HAPTICS)*, ISSN: 2324-7355, Mar. 2012, pp. 407–414. DOI: 10.1109/HAPTIC.2012.6183823.

[31] J. Mullenbach, M. Peshkin, and J. E. Colgate, "eShiver: Lateral Force Feedback on Fingertips through Oscillatory Motion of an Electroadhesive Surface", *IEEE Trans. Haptics*, vol. 10, no. 3, pp. 358–370, Jul. 2017, ISSN: 2329-4051. DOI: 10.1109/TOH.2016.2630057.

[32] U. A. Alma, G. Ilkhani, and E. Samur, "On Generation of Active Feedback with Electrostatic Attraction", en, in *Haptics: Perception, Devices, Control, and Applications*, F. Bello, H. Kajimoto, and Y. Visell, Eds., ser. Lecture Notes in Computer Science, Cham: Springer International Publishing, 2016, pp. 449–458, ISBN: 978-3-319-42324-1. DOI: 10.1007/978-3-319-42324-1_44.

[33] W. Seemann, "A linear ultrasonic traveling wave motor of the ring type", en, vol. 5, no. 3, pp. 361–368, Jun. 1996, ISSN: 0964-1726. DOI: 10.1088/0964-1726/5/3/015.

[34] M. Biet, F. Giraud, F. Martinot, and B. Semail, "A Piezoelectric Tactile Display Using Travelling Lamb Wave", in *EuroHaptics Conference*, Jul. 2006, pp. 567, 570.

[35] S. Ghenna, E. Vezzoli, C. Giraud-Audine, F. Giraud, M. Amberg, and B. Lemaire-Semail, "Enhancing Variable Friction Tactile Display Using an Ultrasonic Travelling Wave", *IEEE Trans. Haptics*, vol. 10, no. 2, pp. 296–301, Apr. 2017, ISSN: 2329-4051. DOI: 10.1109/TOH.2016.2607200.

[36] J. Ware, E. Cha, M. A. Peshkin, J. E. Colgate, and R. L. Klatzky, "Search efficiency for tactile features rendered by surface haptic displays", *IEEE Transactions on Haptics*, vol. 7, no. 4, pp. 545–550, 2014.

[37] J. Ren, R. V. Patel, K. A. McIsaac, G. Guiraudon, and T. M. Peters, "Dynamic 3-D Virtual Fixtures for Minimally Invasive Beating Heart Procedures", *IEEE Transactions on Medical Imaging*, vol. 27, no. 8, pp. 1061–1070, Aug. 2008, Conference Name: IEEE Transactions on Medical Imaging, ISSN: 1558-254X. DOI: 10.1109/TMI.2008.917246.

[38] T. M. Lam, H. W. Boschloo, M. Mulder, and M. M. van Paassen, "Artificial Force Field for Haptic Feedback in UAV Teleoperation", *IEEE Transactions on Systems, Man, and Cybernetics - Part A: Systems and Humans*, vol. 39, no. 6, pp. 1316–1330, Nov. 2009, Conference Name: IEEE Transactions on Systems, Man, and Cybernetics - Part A: Systems and Humans, ISSN: 1558-2426. DOI: 10.1109/TSMCA.2009.2028239.

[39] P. Vadakkepat, K. C. Tan, and W. Ming-Liang, "Evolutionary artificial potential fields and their application in real time robot path planning", in *Proceedings of the 2000 congress on evolutionary computation. CEC00 (Cat. No. 00TH8512)*, IEEE, vol. 1, 2000, pp. 256–263.

[40] D. Ebert, *Texturing & Modeling, A procedural Approach*. Morgan Kaufman, 2002.

[41] G. Liu, T. Yu, C. Yu, *et al.*, "Tactile Compass: Enabling Visually Impaired People to Follow a Path with Continuous Directional Feedback", in *Proceedings of the 2021 CHI Conference on Human Factors in Computing Systems*, ser. CHI '21, New York, NY, USA, May 2021, pp. 1–13, ISBN: 978-1-4503-8096-6. DOI: 10.1145/3411764.3445644.

[42] J. Rekimoto, "Traxion: A tactile interaction device with virtual force sensation", in *ACM SIGGRAPH 2014 Emerging Technologies*, 2014, pp. 1–1.

[43] H. Xu, R. L. Klatzky, M. A. Peshkin, and J. E. Colgate, "Localizable Button Click Rendering via Active Lateral Force Feedback", *IEEE Trans. Haptics*, vol. 13, no. 3, pp. 552–561, Jul. 2020, ISSN: 2329-4051. DOI: 10.1109/TOH.2020.2990947.

5

VISCOUS DAMPING DISPLAYED BY ACTIVE SURFACE HAPTICS

PREFACE

The previous chapter demonstrated that potential fields on touch surfaces can positively impact users' performance and experience by varying local forces based on finger position. However, this position-based approach requires prior knowledge of target locations. In contrast, this chapter explores the effects of viscous fields, where forces vary as a function of velocity, on user movement in targeting tasks. Using the same experimental setup as the Ultraloop, this study investigates velocity-dependent force feedback, which is independent of predefined targets and instead dynamically responds to users' movement. The results indicate that viscous damping improves targeting performance and enhances user experience, particularly by reducing oscillations around the target and lowering completion times.

This chapter is based on:

Zhaochong Cai, and Michaël Wiertlewski, Viscous damping displayed by surface haptics improves touchscreen interactions, In: Kajimoto, H., et al. Haptics: Understanding Touch; Technology and Systems; Applications and Interaction. **EuroHaptics 2024.**

ABSTRACT

Virtual targets on touchscreens (e.g., icons, slide bars, etc.) are notoriously challenging to reach without vision. The performance of the interaction can fortunately be improved by surface haptics, using friction modulation. However, most methods use position-dependent rendering, which forces users to be aware of the target choice. Instead, we propose using tactile feedback dependent on users' speed, providing a viscous feeling. In this study, we compared three viscous damping conditions: *positive damping*, *negative damping*, and *variable damping* (viscosity was high during slow movements and low during fast movements), against a baseline condition with no tactile feedback. These viscous fields are created by changing net lateral forces based on velocity. Results indicate that, during the initial phase of movement when the finger approaches the target, various viscous feedback has an insignificant impact on targeting trajectories and movement velocity. However, positive damping and variable damping significantly influence behavior during the selection phase by reducing oscillation around the target and completion time. Questionnaire responses suggest user preference for viscous conditions and disapproval of negative viscous forces. This study provides insights into the role of viscous resistance in touchscreen interactions.

5.1. INTRODUCTION

TOUCHSCREENS and capacitive buttons offer designers the flexibility to program human-machine interfaces but deprive users of tactile feedback typically Because of the lack of tactile cues, users interacting with touchscreens and touchpads have to interact using only visual cues. The need for visual attention can be dangerous in situations such as driving or walking. While some manufacturers are reverting back to physical buttons, they are also losing the flexibility that touchscreens provide. Programmable tactile feedback, where feedback is provided to the user's bare finger, circumvents all these limits and reduces the need for visual attention. Moreover, the feedback enhances the performance of the interaction and improves the overall user experience. The standard approach to implement programmable tactile feedback, commonly found in consumer electronics, uses vibrotactile feedback to inform users with vibrations [1]. While effective at signaling the user, vibrotactile feedback only provides transient or periodic stimulation. In contrast, friction modulation offers finer and continuous stimuli providing a natural physical rendering of a target. It has been shown that a simple binary friction profile reduces pointing task completion time by providing more intuitive guidance to users [2]–[4].

However, all existing methods that employ position-based feedback require knowledge of the target location and, consequently, must predict the user's intention in selecting their target. The position-based approach can be effective when the interface has only a few targets but may be impractical when localized targets do not exist. To facilitate interaction across complex interfaces, we need to implement a target-independent rendering strategy, for example, velocity-dependent forces that feel similar to viscous elements to guide the user on the surface.

Pointing tasks, where the finger reaches a target on the screen, are fundamental in human-computer interaction. Fitts demonstrated that the time taken to reach a target

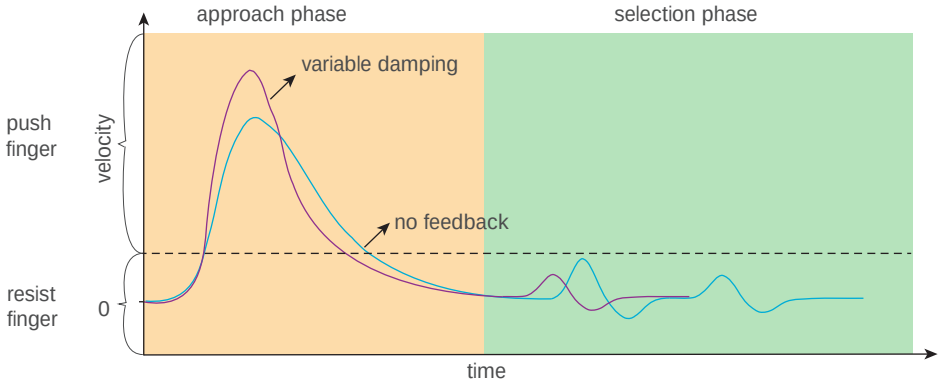

Figure 5.1: Typical velocity profiles observed during a pointing task. The cyan curve represents a typical velocity profile without tactile feedback, where the finger moves back and forth when selecting a target. The purple curve illustrates the proposed approach that varies damping. We hypothesize that, during the approach to the target, low viscosity (or even negative damping) can accelerate finger movement, while during the target selection, high viscous viscosity helps locate the target with fewer back-and-forth movements.

during these pointing tasks depends on its distance and width [5], [6]. The kinematics are governed by the principle of minimum variance control [7]–[9], suggesting that users minimize target variance by slowing down when approaching a target. The velocity profile forms a bell shape, dividing into two phases: an approaching phase, resembling a ballistic movement with minimal sensory feedback [10], [11], and a subsequent slower adjustment phase to pinpoint the exact location using continuous sensory feedback.

Therefore, we postulate that task completion time can be reduced by modulating feedback along these phases. This translates to accelerating the ballistic movement for a quicker approach and slowing down the adjustment phase for finer control, as illustrated in Fig. 5.1. We implemented this strategy by changing the damping coefficients as a function of the user's velocity. For example, we can display negative damping at high speeds to increase speed and positive damping at low speeds to dampen the approach. We expect that this feedback provides better performance with a shorter time to completion compared to scenarios without tactile feedback.

Viscous-based assistance has been implemented in the past using force feedback. In contrast to surface haptics, users interact with force feedback devices through a handle rather than their bare fingers. Despite these differences, the findings offer insights into expected behavior. Notably, it has been observed that adding constant static friction leads to a decrease in reaching times and improves accuracy when moving low-mass objects [12]–[14]. This improvement is attributed to friction forces decelerating and filtering out jittery movements. Keemink et al. demonstrated that both constant damping and position-dependent damping reduce movement time and increase endpoint accuracy [15]. These findings suggest that viscous damping in force feedback operations is beneficial to human operators. Viscous effects have also been studied in the context of texture perception using variable friction [16]. However, the impact of such velocity-based forces on motor performance during direct fingertip interaction remains largely unexplored, in part due to the lack of a surface haptic device capable of providing the

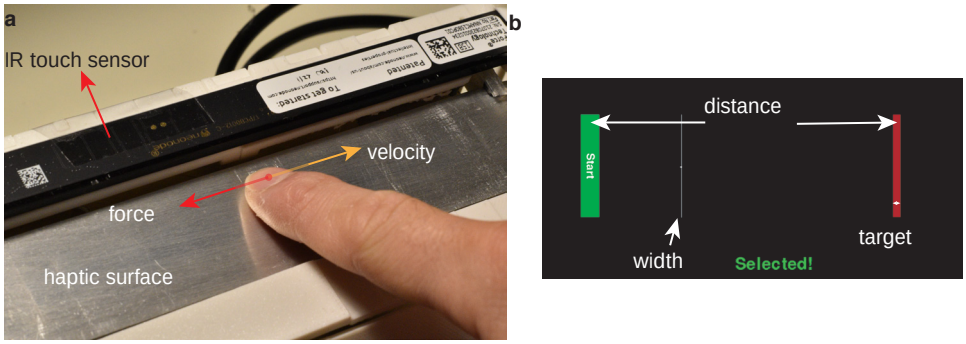

Figure 5.2: **a**, Experimental setup: Participants slide their index finger on the touch surface of the Ultraloop while experiencing lateral forces generated as a function of the measured velocity. **b**, Graphical user interface displaying visuals for a one-dimensional reciprocal targeting task.

desired lateral force.

In this chapter, we investigated the effects of variable viscous damping on users' targeting strategies using a novel surface haptic device called Ultraloop [17]. This device generates lateral forces based on the user's velocity. We compared users' performance when reaching targets when presented with a positive damping, a velocity-dependent damping, a negative damping, and a control condition without any damping. We found that viscous conditions do not significantly affect the movement trajectories during the approach phase but notably decrease the back-and-forth movements during the selection phase.

5.2. METHODS

5.2.1. SETUP

In this chapter, we render viscous environments by changing the net lateral forces, with a consistent reduced friction, as a function of velocity. The lateral forces are produced by active surface haptic devices that use ultrasonic traveling waves, e.g. [17]–[20]. Here, we use a haptic touchpad, called the Ultraloop, which can deliver active lateral forces on a relatively large surface of $140 \times 30\ mm^2$. It has an aluminum ring-shaped cavity in which two degenerate resonant standing wave modes are excited at approximately 40 kHz with a 90° phase shift. These standing waves superimpose into either a counter-clockwise (when the phase is 90°) or a clockwise (when the phase is -90°) traveling wave that propagates around the ring. The traveling wave interacts with the skin and produces a net lateral force that can push or pull fingertips. The direction and magnitude of the force can be modulated by varying the amplitude and phase shift of these standing waves. To create lateral forces as a function of velocity, we used a Teensy 3.6 microcontroller to program the phase of two driving voltages in response to finger velocity, derived from the first-order backward difference of the position tracked by an infrared sensor (Neonode, NNAMC1580PCEV) (Fig. 5.2a).

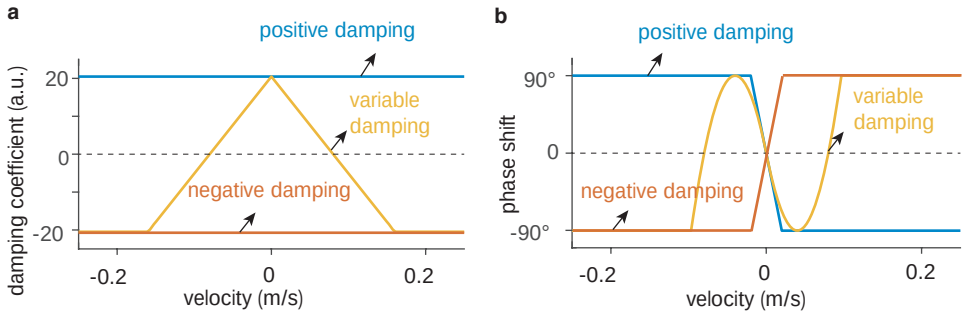

Figure 5.3: **a**, Damping coefficients as a function of finger velocity. **b**, Phase shift between the two channels of driving signals. The maximum lateral forces are generated with a phase shift of ±90°.

5.2.2. EXPERIMENTAL CONDITIONS

In the experiments, participants were asked to reach for a target while being assisted by three different viscous environments or not assisted at all (baseline condition). In the baseline condition, the surface had uniform low friction with no externally applied lateral forces. In the viscous conditions, net lateral forces generated by the Ultraloop were a function of finger movement speed, formulated as $F = -bv$, while the strength of friction reduction remains the same as the baseline condition. We designed three experimental conditions:

1. *Positive damping*: Here, b is a constant positive value, creating a viscous resistance similar to what can be experienced in daily life.
2. *Negative damping*: In this condition, b is a negative value, and the faster the users go the stronger the lateral forces push.
3. *Variable damping*: b varies linearly with velocity, turning negative when the finger moves faster than 0.08 m/s.

Due to the limitations of the Ultraloop, the net forces plateau at approximately 300 mN. Therefore, the damping force cannot increase beyond a certain finger speed. Figure 5.3 illustrates the proposed damping coefficient and phase shift profiles as a function of finger speed for each condition. It is important to note that the amplitude of ultrasonic vibration remains constant across all feedback conditions to minimize variations in the strength of friction reduction. The phase of the driving signals is the only parameter tuned, based on velocity.

5.2.3. PROTOCOL AND DESIGN

The graphical user interface used for the experiment is shown in Fig. 5.2b. Participants conducted one-dimensional reciprocal targeting tasks. Twelve successive tasks with the same target width and viscous condition were grouped together as a block. At the start of each block, they placed their index finger on the active surface of the Ultraloop and slid the cursor to the start area. After holding the cursor in the start area for 0.2 seconds, the first trial of this block started, and the participant slid the cursor to the target and

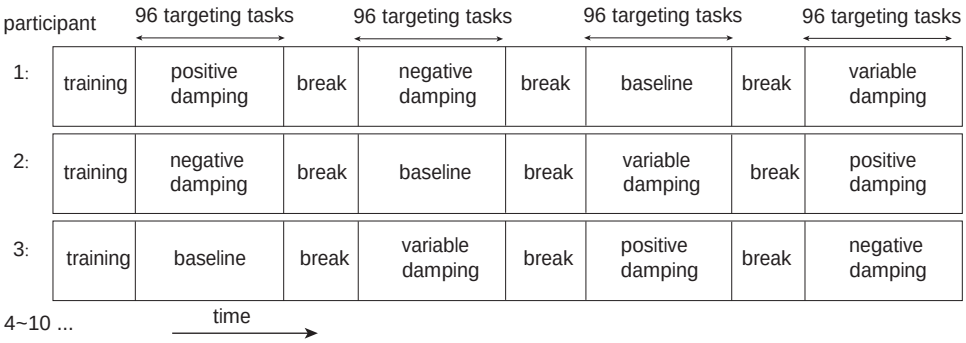

Figure 5.4: Experimental procedure overview. Targeting tasks are organized into sessions based on viscous conditions. The sequence in which these conditions are presented to participants is determined by a Latin Square design.

pressed the "ctrl" key with their non-dominant hand to confirm the acquisition. Next, a new target appeared on the other side of the user interface. Participants were instructed to complete the tasks both quickly and accurately, aiming for a success rate of approximately 96 %. If a participant missed more than one target in a block, a message on the user interface would prompt them to slow down for greater accuracy. Conversely, if they completed one block without any misses, they were encouraged to increase their speed.

We used a repeated within-subject design, with independent variables as viscous environments and target widths. These widths were set at 8, 16, 24, and 32 pixels, equivalent to 0.8, 1.6, 2.4, and 3.2 mm on the touch surface. The target distance is fixed at 7.5 mm. Before experiments, participants spent ten minutes familiarizing themselves with the Ultraloop and the interface.

The experiment consisted of 32 blocks, with each block containing 12 trials with the same target and feedback condition. These 32 blocks were divided into four sessions, each dedicated to one of the viscous conditions. We applied a Latin Square design to counterbalance the presentation order of viscous conditions among participants (Fig. 5.4). Each session had eight successive blocks, with target widths presented in a descending order, and grouped by the same width. Participants were allowed a one-minute break after each block to rest their hands and fingers. In summary, each participant completed 384 trials, calculated as 4 sessions × 4 widths × 2 repeats × 12 targets.

5.2.4. PARTICIPANTS

Nine individuals from TU Delft participated in the experiments (seven males, and two females; aged 22-32, average age 25.4). All participants were right-handed, had no tactile impairments, their fingers were free of cuts and calluses, and were unaware of the aim of the study. Every participant provided informed consent before the experiments. The study received ethical approval from the ethics committee of Delft University of Technology, complying with the Declaration of Helsinki.

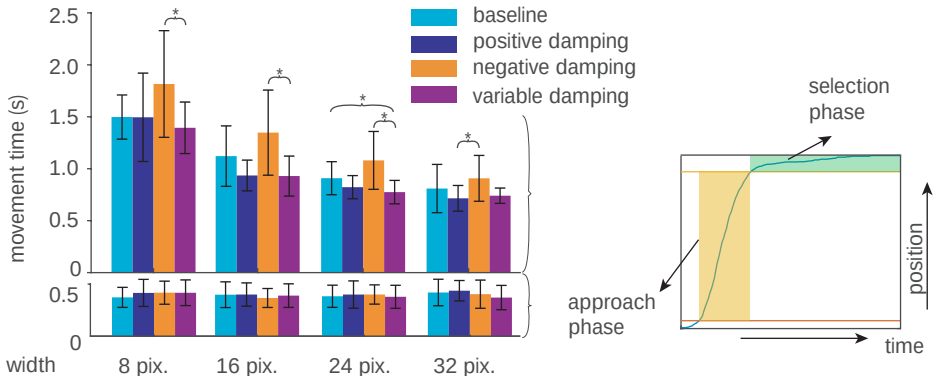

Figure 5.5: Mean movement time during the selection phase and approach phase across all target width conditions. Bar charts for these two phases use the same scaling in the y direction. Stars "*" indicate the significance of $p \leq 0.05$. The inset illustrates a typical movement trajectory, with the two phases indicated by the shaded areas.

5

5.2.5. DATA PROCESSING

The area where participants began the task had a specific width, so we mitigated variations in trajectory timings by aligning the traces to a common reference time point. The velocity profile as a function of position was obtained by interpolating the time-domain position data from each trial. Additionally, we excluded data from the first session of one participant who could not perform movements as fast and accurately as possible, resulting in considerably slower movement compared to the rest of the cohort. In a set of successive trials organized into two blocks of 24 trials, which have the same viscous conditions and target widths, we excluded the first four trials from the first block and the first two trials from the second block to allow for adaptation. The exclusion removed the trial where the learning effect was present, in turn providing focus to the data where the performance was stable.

5.3. RESULTS

Movement time for each trial is defined as the time between the onset of movement to the selection of a target. A repeated measures ANOVA analysis revealed a significant impact of viscous conditions on the average movement time ($F_{3,21} = 13.392$, $p < 0.001$). Notably, both *variable damping* and *viscous damping* conditions exhibited shorter average movement time (mean = 1.41 s and 1.46 s) compared to the baseline condition (mean = 1.54 s). In contrast, *negative damping* increased the completion time of the pointing task (mean = 1.74 s).

To explore the potential source for the variance in movement time across viscous conditions, we divided the movement of a trial into two phases: the approach phase and the selection phase. The approach phase spans from the moment the finger exits the start area to when 90% of the target distance is covered. The selection phase comprises the remaining time until task completion. We chose the divide point at 90 % following preliminary observations indicating that the phase before this point exhibits a rapid,

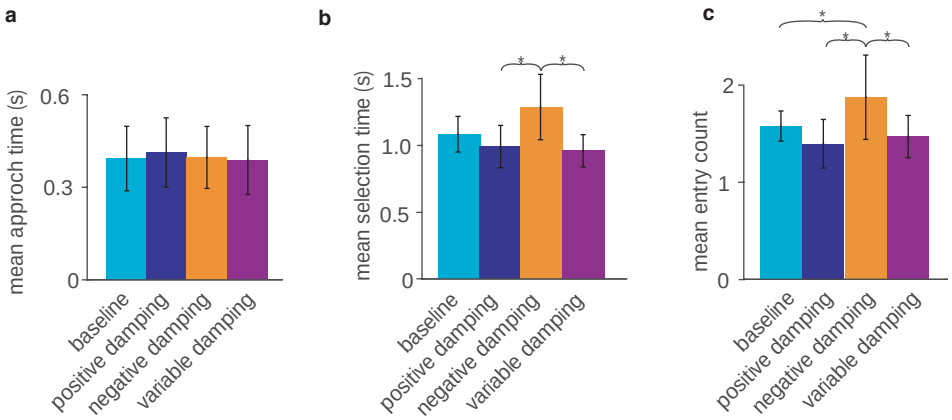

Figure 5.6: **a** and **b**, the mean duration during the approach phase and selection phase. **c**, Mean entry count across different viscous conditions. Standard deviations across participants are indicated by error bars. Stars "*" indicate the significance of $p \leq 0.05$.

5

monotonous movement towards the target, often described by a bell-shaped velocity profile [11]. Beyond this point, user movements become non-monotonous and involve corrective motions, indicating a shift from rapid approach to precise target alignment.

These phases were represented in the inset of Fig. 5.5 and statistically analyzed separately to quantify their distinct contributions to task performance. Notably, significant differences in movement times were predominantly observed during the selection phase. Figures. 5.6 a and b showed that significant differences in movement time were not observed during the approach phase ($F_{3,21} = 1.72$, p = 0.19), but during the selection phase ($F_{3,21} = 12.826$, $p < 0.001$). Specifically, *negative damping* recorded the longest selection time (mean = 1.29 s), while the *variable damping* recorded the shortest (mean = 0.96 s). Further analysis of movement times in different target widths indicated that the primary difference occurred in the selection phase, with minor variations in the ranking of viscous conditions (Fig. 5.6c).

We further analyzed the averaged movement profiles under the same viscous condition and target width, as depicted in Fig. 5.7. Across all width conditions, position and velocity profiles showed small differences between viscous conditions, considering notable standard deviations. Additionally, the averaged peak velocities are similar across different viscous conditions. It further suggests that varying viscous resistance does not effectively speed up or slow down user movement during the approach. Furthermore, averaged velocity versus position profiles during the approach phase also exhibit small deviations from each other for widths of 8, 16, and 24 pixels, yet a relatively larger deviation was observed for a width of 32 pixels. In contrast, the selection phase was notably affected by the viscous conditions. We observed large variations in the number of oscillations around the target and selection duration. The condition *negative damping* significantly increased the average entry count (mean = 1.875), which is the number of times the finger moves into the target area, while both *positive damping* and *variable damping* conditions effectively reduced the number of oscillations around the target (mean =

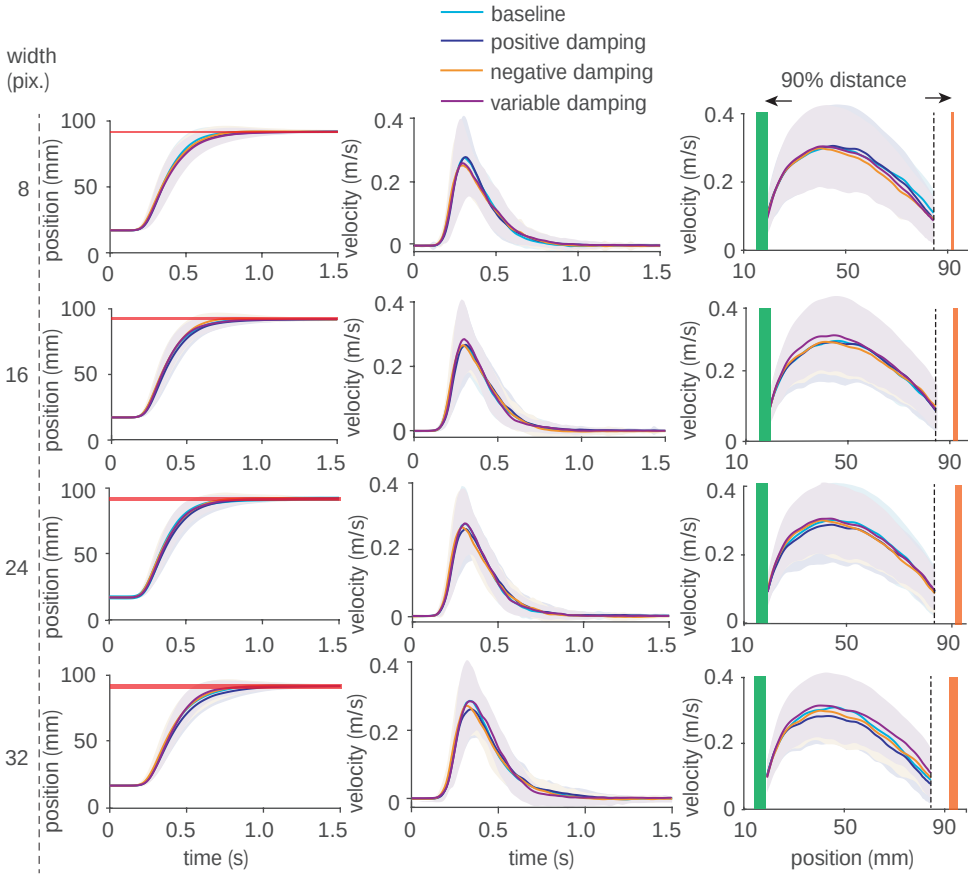

Figure 5.7: Averaged movement profiles. Left and middle panels: Averaged movement and velocity profiles of nine participants. Light red bars indicate the targets. Right panels: Averaged velocity as a function of position during the approach phase. Standard deviations are indicated by the shaded areas.

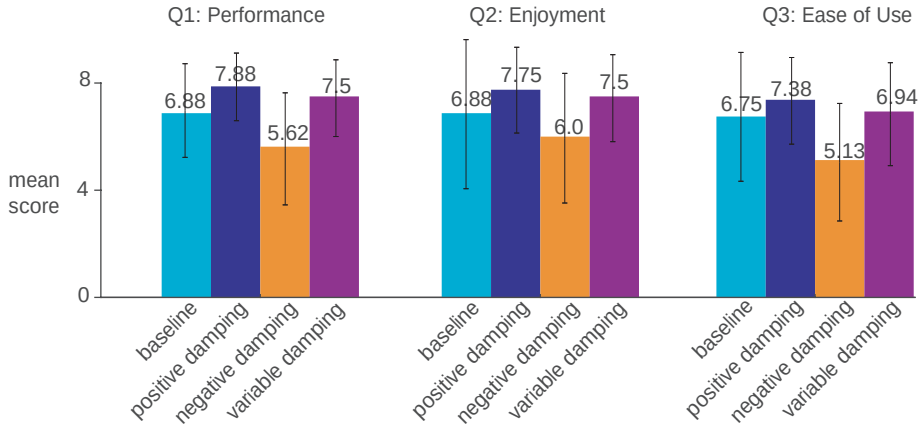

Figure 5.8: Mean questionnaire responses, with 10 = strongly agree and 1 = strongly disagree.

5

1.397 and 1.47), compared to the baseline condition (mean = 1.578). Interestingly, despite the opposite viscosity in the *positive damping* and *variable damping* conditions during the approach phase, participants obtained similar entry counts, as indicated by the pairwise post-hoc analyses. It suggests that the selection behavior is primarily influenced by the viscous conditions in the low-speed regime.

After each viscous condition, participants were asked to respond to three questions, with scores ranging from 1 (strongly disagree) to 10 (strongly agree). The questions were as follows: Q1: "I performed well", Q2: "I enjoyed the tactile feedback when interacting with the touchpad", and Q3: "It is easy to hit the target". Responses were collected from eight participants. One participant did not comply with the requirement to complete tasks both quickly and accurately at the first experimental session and was excluded to ensure the reliability of the data. The average scores for all three questions followed the same order across conditions: *positive damping* > *variable damping* > *baseline* > *negative damping*, as displayed in Fig. 5.8. After completing the experiment, participants were asked to select their most and least preferred conditions. Four out of eight preferred *positive damping*, three *baseline*, and one *variable damping*. In contrast, seven out of eight participants chose *negative damping* as the one to not use, with only one choosing *positive damping*.

5.4. DISCUSSION AND CONCLUSION

We demonstrated a new method to guide users on haptic touchpads and touchscreens. The guidance is created using velocity-dependent forces on the finger, which produce a low damping effect when the finger is moving fast and a high damping effect when it is moving slowly. The user studies indicate that the viscous forces applied to fingertips affect the performance when reaching for a target. The gains in performance are mostly in the later phase of the movement when the user selects the target instead of in the phase when approaching the target. Notably, even when comparing two opposite viscous conditions, i.e., *negative damping* and *variable damping*, their velocity profiles fol-

low similar bell-shaped trajectories, with comparable peak velocities. This observation seems inconsistent with studies using force feedback devices, which reported significant changes in approach trajectories [15]. Two alternative explanations for this inconsistent behavior during the approach phase can be raised.

First, the inconsistency may be attributed to the small variations in the magnitude of the applied force. Hand-operated force feedback devices typically exert forces in an order of 10 N, which are sufficient to impact the limb dynamics. In comparison, the Ultraloop produces much smaller net lateral forces, approximately 0.2 N. The interaction forces at the fingertip —the combination of net lateral force and sliding friction— may differ by a maximum of 0.4 N across different feedback conditions. This variation is notable between *negative damping* and *positive damping*, which produce net tangential forces of opposite signs, with sliding friction consistently opposing movement. These small variations in interaction forces do not significantly accelerate or decelerate finger movement. For instance, in *negative damping*, the forward forces are neutralized by friction forces, possibly leading to resistive interaction forces [19]. The movement during the approach phase likely follows a feedforward behavior, unimpeded by the level of resistance generated by the device.

Second, the short interaction distance in our study was only 7.5 cm, ensuring that participants consistently had a clear visual target throughout the movement. The distance is notably shorter than similar experiments using force feedback devices, such as the 23 cm mentioned in [15]. The salience of the visual cue likely led to a dominance of visual stimuli over haptic stimuli. It is well accepted under the multisensory integration framework that when visual information has a minimal variance, it becomes the primary component of the perceived stimuli. We hypothesize that in this task, participants primarily relied on visual cues, which provided consistent positional feedback. By contrast, the velocity-dependent haptic feedback, which in principle does not infer the target location, played a lesser role. This visual dominance likely explains why variations in viscous damping had minimal impact on the trajectories during the approach phase. This hypothesis is in line with a study by Levesque et al. [2], where the authors report no significant difference in movement speed when using constant low or constant high friction conditions.

Conversely, in the selection phase, where the finger is approaching the target, positive damping gives an advantage to the user for positioning at the right location. We measure the advantage by the reduced oscillations around the target and shorter selection times. The observations align with findings from force feedback device studies [21], where the authors attributed this benefit to haptic damping forces mitigating motor noise during positioning. The positive damping, which creates an energy-dissipative environment, helps dampen unintentional small movements of the user's finger. Our experiments with negative damping show that this effect reverses when the environment is generating energy, creating more oscillations and longer selection times. In addition, participants also described it as the "most challenging," with "unpredictable" movement.

The results regarding active surface haptics can be compared to previous studies that use passive surface haptics with friction modulation. With friction modulation, the target is represented with a low or high friction part, and everything outside is high or low

friction, respectively. In both conditions, the friction pattern provides a distinct sensation upon touching the virtual target, and the additional tactile feedback can effectively reduce the need for visual attention. However, the discontinuity in resistance may not be preferred by users [2], especially if it conflicts with other feedback channels or tasks. In contrast, creating viscous damping environments using ultrasonic traveling waves induced active force does not involve a discontinuity in friction or lateral force, which assists in targeting continuously. We believe it improves the movement by attenuating motor noise during the precision epoch of the movement. This feedback scheme smoothly updates the lateral forces, and as a consequence, feels continuous, free from irregularities, and does not interfere with the visual channel. Therefore, it can be an effective complement to the screen in visual-dominant tasks or shared control tasks.

In conclusion, our investigation focused on the effects of viscous forces using active lateral force feedback in touch interactions. Results reveal that viscous forces do not significantly change targeting strategies during the approach to the target but help in positioning toward the target. However, it should be noted that the insights were conducted with only nine participants, which may potentially affect the generalizability of our findings and an improvement could involve a larger participant pool. Moreover, future work could exploit the potential benefits of viscous damping in tasks where moving targets are tracked. With the right design, viscous damping environments may enhance these dynamic tasks that involve frequent acceleration and deceleration [22], [23]. Another avenue is to explore how humans adapt to viscous environments created through pure friction modulation. This setting may yield different observations, as humans can perceive friction change before sliding occurs [24].

REFERENCES

[1] E. Hoggan, S. A. Brewster, and J. Johnston, "Investigating the effectiveness of tactile feedback for mobile touchscreens", in *Proceedings of the SIGCHI Conference on Human Factors in Computing Systems*, ser. CHI '08, New York, NY, USA, 2008, pp. 1573–1582, ISBN: 978-1-60558-011-1.

[2] V. Levesque, L. Oram, K. MacLean, *et al.*, "Enhancing physicality in touch interaction with programmable friction", in *Proceedings of the SIGCHI Conference on Human Factors in Computing Systems*, ser. CHI '11, May 2011, pp. 2481–2490, ISBN: 978-1-4503-0228-9. DOI: 10.1145/1978942.1979306.

[3] G. Casiez, N. Roussel, R. Vanbelleghem, and F. Giraud, "Surfpad: Riding towards targets on a squeeze film effect", in *Proceedings of the SIGCHI Conference on Human Factors in Computing Systems*, ser. CHI '11, New York, NY, USA, 2011, pp. 2491–2500, ISBN: 978-1-4503-0228-9.

[4] Y. Zhang and C. Harrison, "Quantifying the Targeting Performance Benefit of Electrostatic Haptic Feedback on Touchscreens", in *Proceedings of the 2015 International Conference on Interactive Tabletops & Surfaces*, ser. ITS '15, New York, NY, USA, 2015, pp. 43–46, ISBN: 978-1-4503-3899-8.

[5] P. M. Fitts, "The information capacity of the human motor system in controlling the amplitude of movement", *J. Exp. Psychol.*, vol. 47, no. 6, pp. 381–391, 1954, ISSN: 0022-1015.

[6] P. M. Fitts and J. R. Peterson, "Information capacity of discrete motor responses", *J. Exp. Psychol.*, vol. 67, no. 2, pp. 103–112, 1964, ISSN: 0022-1015.

[7] C. M. Harris and D. M. Wolpert, "Signal-dependent noise determines motor planning", en, *Nature*, vol. 394, no. 6695, pp. 780–784, 1998, ISSN: 1476-4687.

[8] E. Todorov, "Optimality principles in sensorimotor control", en, *Nat. Neurosci.*, vol. 7, no. 9, pp. 907–915, 2004, ISSN: 1546-1726.

[9] E. Todorov, "Stochastic Optimal Control and Estimation Methods Adapted to the Noise Characteristics of the Sensorimotor System", *Neural Comput.*, vol. 17, no. 5, pp. 1084–1108, 2005, ISSN: 0899-7667.

[10] Y. Chen, E. R. Hoffmann, and R. S. Goonetilleke, "Structure of Hand/Mouse Movements", *IEEE Trans. Human-Mach. Syst.*, vol. 45, no. 6, pp. 790–798, 2015, ISSN: 2168-2305.

[11] R. F. Lin and Y.-C. Tsai, "The use of ballistic movement as an additional method to assess performance of computer mice", *Int. J. Ind. Ergon.*, vol. 45, pp. 71–81, 2015, ISSN: 0169-8141.

[12] P. Berkelman and J. Ma, "Effects of Friction Parameters on Completion Times for Sustained Planar Positioning Tasks with a Haptic Interface", in *2006 IEEE/RSJ International Conference on Intelligent Robots and Systems*, 2006, pp. 1115–1120.

[13] C. Richard and M. Cutkosky, "The Effects of Real and Computer Generated Friction on Human Performance in a Targeting Task", en, in *Proceedings of the ASME Dynamic Systems and Control Division*, 2021, pp. 1101–1108.

[14] K. Crommentuijn and D. J. Hermes, "The Effect of Coulomb Friction in a Haptic Interface on Positioning Performance", in *Haptics: Generating and Perceiving Tangible Sensations*, Berlin, Heidelberg: Springer, 2010, pp. 398–405, ISBN: 978-3-642-14075-4.

[15] A. Q. Keemink, R. I. Fierkens, J. Lobo-Prat, *et al.*, "Using position dependent damping forces around reaching targets for transporting heavy objects: A Fitts' law approach", in *2016 6th IEEE International Conference on Biomedical Robotics and Biomechatronics (BioRob)*, 2016, pp. 1323–1329.

[16] D. J. Brewer, D. J. Meyer, M. A. Peshkin, and J. E. Colgate, "Viscous textures: Velocity dependence in fingertip-surface scanning interaction", in *2016 IEEE Haptics Symposium (HAPTICS)*, IEEE, 2016, pp. 265–270.

[17] Z. Cai and M. Wiertlewski, "Ultraloop: Active Lateral Force Feedback Using Resonant Traveling Waves", *IEEE Trans. Haptics*, vol. 16, no. 4, pp. 652–657, 2023, ISSN: 2329-4051.

[18] D. Gueorguiev, A. Kaci, M. Amberg, F. Giraud, and B. Lemaire-Semail, "Travelling Ultrasonic Wave Enhances Keyclick Sensation", en, in *Haptics: Science, Technology, and Applications*, D. Prattichizzo, H. Shinoda, H. Z. Tan, E. Ruffaldi, and A. Frisoli, Eds., 2018, pp. 302–312, ISBN: 978-3-319-93399-3. DOI: 10.1007/978-3-319-93399-3_27.

[19] S. Ghenna, E. Vezzoli, C. Giraud-Audine, F. Giraud, M. Amberg, and B. Lemaire-Semail, "Enhancing Variable Friction Tactile Display Using an Ultrasonic Travelling Wave", *IEEE Trans. Haptics*, vol. 10, no. 2, pp. 296–301, Apr. 2017, ISSN: 2329-4051. DOI: 10.1109/TOH.2016.2607200.

[20] M. Biet, F. Giraud, F. Martinot, and B. Semail, "A Piezoelectric Tactile Display Using Travelling Lamb Wave", in *EuroHaptics Conference*, Jul. 2006, pp. 567, 570.

[21] A. Q. Keemink, N. Beckers, and H. van der Kooij, "Resistance is Not Futile: Haptic Damping Forces Mitigate Effects of Motor Noise During Reaching", in *2018 7th IEEE International Conference on Biomedical Robotics and Biomechatronics (Biorob)*, 2018, pp. 357–363.

[22] D. McRuer and H. Jex, "A Review of Quasi-Linear Pilot Models", *IEEE Transactions on Human Factors in Electronics*, no. 3, pp. 231–249, 1967, ISSN: 2168-2852.

[23] J. De Winter, D. Dodou, S. De Groot, D. Abbink, and P. Wieringa, "Hands-on experience of manual control in a human-machine systems engineering course", in *Proceedings of the 37th Annual Conference of the European Society for Engineering Education SEFI,(MCM)*, 2009.

[24] L. Willemet, K. Kanzari, J. Monnoyer, I. Birznieks, and M. Wiertlewski, "Initial contact shapes the perception of friction", *Proc. Natl. Acad. Sci. U.S.A.*, vol. 118, no. 49, e2109109118, 2021.

6

FLATLOOP: LOW-PROFILE ACTIVE FORCE FEEDBACK DEVICE USING TRAVELING WAVES

PREFACE

Chapter 3 introduced the Ultraloop, an oblong ring-shaped cavity capable of generating resonant traveling waves. However, the Ultraloop has a significant height of 2R, making it unsuitable for integration into thin consumer electronics. This chapter presents the flatLoop, a low-profile version of the traveling wave-based surface haptic device designed to enhance usability in modern consumer devices. The chapter begins by detailing the design of the thickness profile using an analytical model, followed by geometric refinements using FEM simulations. Next, force measurements were conducted under varying normal forces and phase shifts, demonstrating that the flatLoop achieves force production performance comparable to the Ultraloop. Finally, a proof-of-concept application "haptic keyboard" is introduced, showcasing how the flatLoop can render two-dimensional force fields for interactive haptic feedback.

This chapter is based on:

Zhaochong Cai, Koen Renkema, and Michaël Wiertlewski, "flatLoop: Low-profile active force feedback device using traveling waves," published in IEEE World Haptics Conference 2025, Suwan, Korea.

ABSTRACT

Active surface haptic devices can push and pull users' fingers as they move to guide them to targets. These devices generate active forces directly on the fingertip using resonant traveling waves. Modulating the amplitude of the wave and its phase allows fine control over the force applied to the fingertip, which in turn can be used to create compelling tactile sensations such as elastic potential fields, which attract or repel the finger, emulating the feel of curved surfaces. However, the existing designs are bulky, with ring-shaped cavities unsuitable for thin consumer electronics. This chapter introduces flatLoop, a compact surface haptic device with a height of just 5 mm. It uses a planar aluminum structure with two straight and two curved beams along which flexural waves travel. The thickness of the curved beams varies, steering the wave propagation around corners. Experimental results demonstrate that flatLoop generates uniform traveling waves and produces lateral forces of up to 0.3 N on an 80 × 30 mm² flat surface. This innovative design can deliver rich tactile effects in a compact form, ideal for applications like rendering a flat keyboard where users can feel the shape of keys. This design can facilitate the integration of the technology in consumer electronics.

6.1. INTRODUCTION

SINCE the adoption of touchpads and touchscreens in consumer-electronics, there has been a drive to provide realistic haptic feedback on flat surfaces. While vibrotactile devices are the leading approach, surface haptics has been gaining popularity because these devices let users feel rich tactile feedback during bare finger interactions by modulating the interaction force. The force modulation is typically achieved by varying the friction force via ultrasonic bending waves [1], [2] or electroadhesive attraction [3], [4], enabling the creation of shape illusions [5] or frictional textures for guiding users to specific targets [6], [7]. However, while changing friction produces a salient sensation, it is only effective when the finger is sliding on the surface and little tactile sensation can be created on static fingers. Moreover, because the feedback is passive, the modulated force is always collinear with the direction of movement, and thus not able to effectively guide the user to an arbitrary target. These limitations have been overcome by a new class of surface haptic devices generating *active lateral forces* on sliding or stationary fingers. With active forces, users can be attracted or repelled from specific points. By modulating the force according to finger position or velocity, active force feedback provides tactile guidance or rendering, including navigation through directional cues [8], contour following [9], simulation of button clicks [10], [11], or creating "potential fields" on a surface [12], [13].

Several techniques can generate active forces. The oldest uses asymmetric friction, where the friction of a laterally oscillating surface is changed synchronously to induce a high friction state when the plate moves forward and a low friction state when it moves back [9], [13]–[15]. While effective, these systems are often noisy and complex to control. A more recent approach uses ultrasonic flexural traveling waves. When the beam is excited by flexural waves, the surface of the beam follows an elliptical trajectory. This elliptical motion is non-linearly interacting with any object in contact, including skin, creating a net force. The active force is however noticeable only if the wave has a large enough

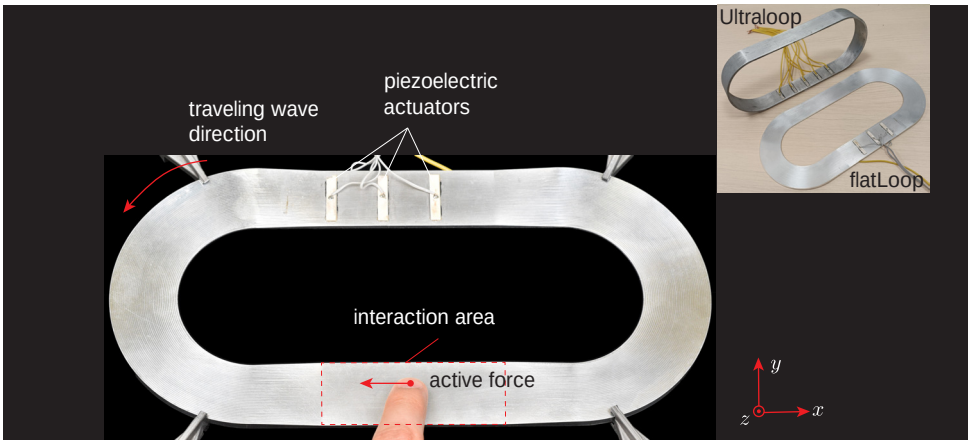

Figure 6.1: The flatLoop is a low-profile haptic display that uses flexural traveling waves to provide active force feedback on a bare finger. The inset illustrates a comparison of the dimensions between the Ultraloop and the flatLoop.

amplitude, on the micrometer scale. To create traveling waves with sufficient amplitude, one can use powerful actuators to vibrate the beam, but the method achieves a small amplitude-to-input power ratio. Instead, it is possible to use resonance to produce traveling waves. To achieve resonance, we can remember that every traveling wave can be decomposed into two standing waves with a quarter wavelength shift. If these standing waves can be made resonant at the same frequency, they form degenerate modes and produce a resonating traveling wave with a large amplitude compared to the input. A circular ring used in traveling-wave ultrasonic motors [16], has been used to produce strong active forces on human fingertips [17] and deliver haptic effects such as button clicks [18]. However, their hollow and non-flat shapes are not suitable for touch applications. Another type of structure involves an oblong ring-shaped cavity, as used in a haptic device, the Ultraloop [10]. This structure consists of two straight beams and two semicircular beams, allowing bending waves to propagate along its centerline. The Ultraloop can generate uniform lateral forces on a flat surface and produce tactile effects such as button clicks [10] and viscous damping [19].

Despite its advantages, the Ultraloop has an inherent height of twice the radius ($2R$), which is 100 mm in its current configuration. While reducing the radius R could lower the height, the intrinsic $2R$ dimension remains significant, making the design ill-suited for integration into most touch-enabled devices, such as touchpads, car dashboards, and display screens in educational or museum settings, which are flat and thin.

In this chapter, we propose a low-profile design, the flatLoop (Fig. 6.1), which can support degenerate modes on a flat configuration, reducing the height of the device to that of the thickness of the beam. The design uses the same modes along the centerline as the Ultraloop. However, the planar arrangement includes two curved parts, similar to a running track. These curved parts introduce distortions in the bending wave propagation since the inside of the curve is shorter than its outside. Consequently, to have the same number of wavelengths, the speed of the wave should be higher in the out-

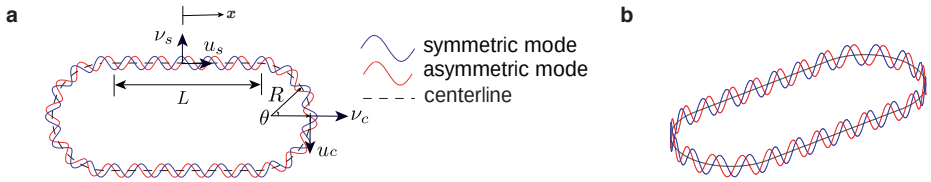

Figure 6.2: (a) The oblong centerline of the Ultraloop has two orthogonal degenerate modes. (b) The flatLoop uses the same centerline as the Ultraloop but features transverse vibrations orthogonal to the centerline's plane.

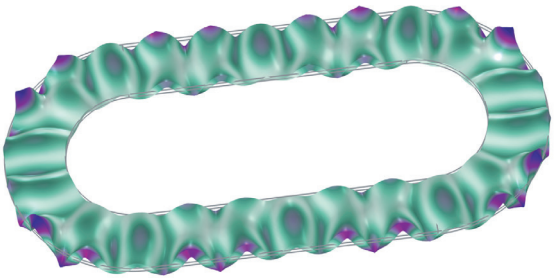

Figure 6.3: FEM simulation of the 24th bending mode shape of the flatLoop with a uniform thickness of 2.75 mm. The difference in the curve length results in 26 wavelengths along the outer circumference and 22 wavelengths along the inner circumference.

side. Failing to take the difference in length into account causes the nodal lines in the straight part to be tilted and force generation becomes non-uniform. To address this issue, we employ a variable thickness profile at the curved parts where the thickness follows a power-law function of the radius. This design leads to colinear propagation of the traveling waves in the straight part and uniform force generation. We show how this device can be used by demonstrating a proof-of-concept haptic keyboard, showcasing the potential of the flatLoop for practical applications in touch-based interfaces.

6.2. LOW-PROFILE DESIGN OF A TRAVELING WAVE STRUCTURE

6.2.1. ORTHOGONAL DEGENERATE MODES

Previous devices used an oblong ring-type structure excited by two orthogonal modes at the same frequency to create a flexural traveling wave. This type of structure, formed by two straight beams of length L connected by two semicircular segments with a radius R, can be used as a surface haptic device, such as the Ultraloop [10] , or as an acoustic levitation transportation system [20]. To achieve a sufficient amplitude with regular piezoelectric elements, this structure leverages resonance of both modes having an identical resonant frequency. This so-called degenerate mode exists only for specific length-to-radius (L/R) ratios. Determining the geometrical conditions for frequency degeneracy has been discussed in [21], [22]. The flatLoop design revolves around the same oblong centerline loop as the original Ultraloop. Below, we briefly review the analytical model

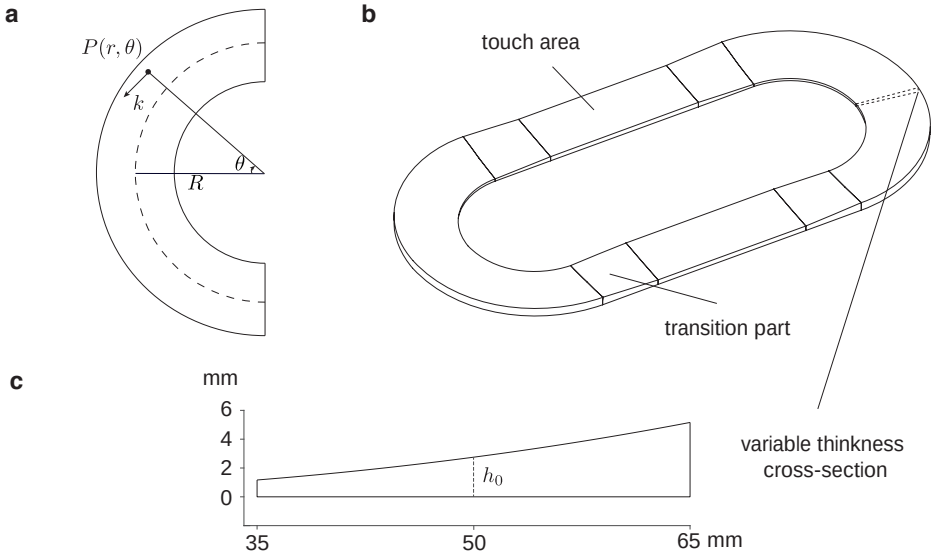

Figure 6.4: (a) Top view of the curved segment. (b) The flatLoop design includes two straight beams as the touch surface, two curved bends with variable thicknesses, and four transition sections connecting the curved bends to the straight beams. (c) Cross-section of the curved bend.

for finding resonances and mode shapes with a given oblong structure.

We define a Cartesian coordinate system and a polar coordinate system for the straight and curved sections respectively (Fig. 6.2a). The transverse displacements of the straight and curved parts are denoted as v_s and v_c . We assume that the form of displacements can be separated into a spatial component (i.e. the mode shape), which depends on coordinate x and θ, and a harmonic component with a variable t. Thus displacements are expressed as $v_s(x,t) = V_s(x)\sin(\omega t)$ and $v_c(\theta,t) = V_c(\theta)\sin(\omega t)$.

We now consider the 24^{th} bending modes along the centerline. The mode shapes take trigonometric forms, i.e. $\pm\sin$ and $\pm\cos$, and are expressed as:

- Symmetric mode: $\{V_s, V_c\} = \{A_s \cos k_s x, A_c \cos k_c\theta\}$
- Asymmetric mode: $\{V_s, V_c\} = \{A_s \sin k_s x, A_c \sin k_c\theta\}$

where k_s is the wave number (with unit in meters) for the straight parts and k_c is the wave number (with units in radians) for the curved parts, and A_s and A_c are the amplitudes of the transverse displacements in the straight and curved parts respectively.

Using the Euler-Bernoulli beam assumption and Hamilton's principle, the dispersion relations coupling k_s, k_c , and ω (angular frequency) are previously derived as Eq. 6.1 and Eq. 6.2. For the reader's convenience, they are restated below as:

$$k_s^4 - \alpha_s k_s^2 \omega^2 - \gamma_s \omega^2 = 0 \tag{6.1}$$

$$\omega^2(\gamma_c k_c^4 - 2\gamma_c k_c^2 + \alpha_c k_c^2 + \alpha_c + \gamma_c) - k_c^6 + 2k_c^4 - k_c^2 = 0 \tag{6.2}$$

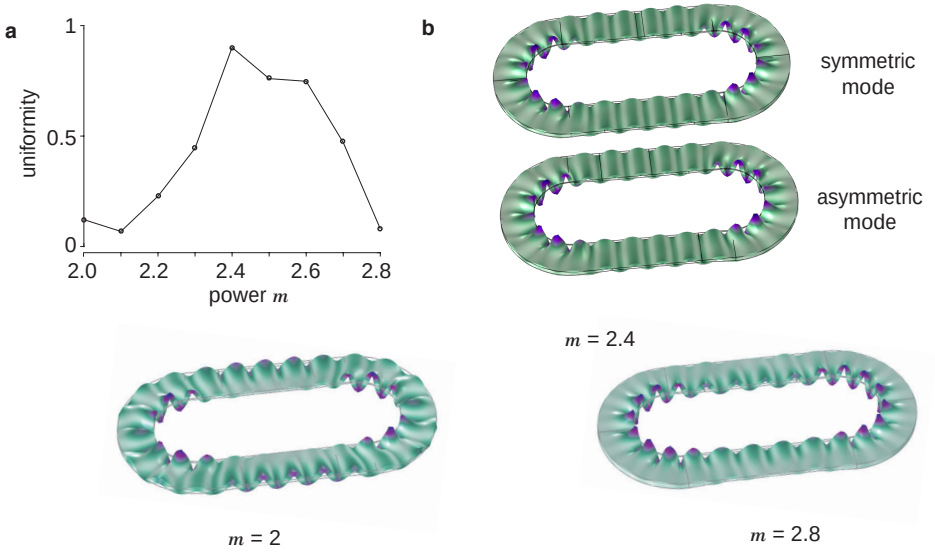

Figure 6.5: (a) Uniformity of wave distribution in the straight parts as a function of the power m. (b) FEM simulation of the 24$^{\text{th}}$ bending mode shape of the flatLoop with a power-law thickness profile in the bends, $h_0(\frac{r}{R})^m$, where m = 2, 2.4, and 2.8. For m = 2, the outer circumference exhibits more wavelengths than the inner circumference (symmetric mode and asymmetric mode are both presented here). Conversely, for m = 2.8, the outer circumference has fewer wavelengths. For m = 2.4, waves are distributed evenly in the straight parts.

where $\alpha_s = \rho/E$, $\gamma_s = \rho A/EI$, $\alpha_c = \rho AR^4/EI$ and $\gamma_c = \rho R^2/E$. Here, ρ is the material density, E is the Young's modulus, A is the cross-sectional area, and I is the second moment of area.

For the symmetric mode, the boundary conditions ensuring continuity of displacement and rotation between the straight and curved segments are:

$$A_s \cos\left(k_s \frac{L}{2}\right) = A_c \cos\left(-k_c \frac{\pi}{2}\right) \tag{6.3}$$

$$-A_s k_s \sin\left(k_s \frac{L}{2}\right) = -\frac{A_c k_c}{R} \sin\left(-k_c \frac{\pi}{2}\right) \tag{6.4}$$

Now Eq. 6.1, 6.2, 6.3, and 6.4 form a set of coupled equations with four unknowns k_s, k_c, ω and the amplitude ratio $\Gamma = A_s/A_c$. These unknowns, which fully define the symmetric mode shape, can be solved numerically for any given geometry (defined by L, R and h). Similarly, the asymmetric mode shape can be solved using its boundary conditions.

Only at specific discrete L/R ratios, the natural frequencies of symmetric and asymmetric modes coincide. By plotting the $\omega_{sym.}$ and $\omega_{asym.}$ as functions of L/R, configurations with degenerate modes can be identified at their intersection points.

6.2.2. VARIABLE THICKNESS DESIGN

The flatLoop adopts the same oblong centerline as the Ultraloop, with the length L being 140 mm and the radius R being 50 mm. This configuration ensures that all the degener-

ate modes found valid for the Ultraloop are also present in the flatLoop. However, unlike the Ultraloop (Fig. 6.2a), the flexural waves in flatLoop are orthogonal to the plane of the centerline (Fig. 6.2b), creating a planar structure excited by flexural waves. A crude solution to the design of the flatLoop is expanding the oblong centerline in the x-y plane by 30 mm and then extruding the planar shape by 2.75 mm, which matches the width and thickness of the Ultraloop, respectively. However, this uniform-thickness design introduces disparities in the lengths of the wave paths along the inner and outer bends of the curved segments. As shown by finite element method (FEM) simulations using COMSOL Multiphysics (Fig. 6.3), the outer bend accommodates more waves than the inner bend. This discrepancy results in tilted nodal lines in straight sections, which challenges the placement of piezoelectric actuators and the uniformity of force generation.

To address this issue, we explored how a variable thickness profile for the curved segments can modulate the wave speed and ultimately achieve aligned nodal lines in the straight part. The idea of the design is to make the flexural waves along the inner and outer bends arrive simultaneously at the end of the curved segment. As illustrated in Fig.6.4a, for a point $P(r,\theta)$ in polar coordinates on the curved segment, the wave equality condition means the number of waves along different paths in the curved bend should be constant, expressed as

$$\pi r / k = C_1$$

where k is the local wavenumber at the point P with a local thickness h, and C_1 is a constant. The local wavenumber k is determined by the geometry and material properties, and can be approximated using the dispersion equation from Euler-Bernoulli beam theory:

$$k^4 = \omega^2 \frac{\rho A}{EI} \tag{6.5}$$

Considering a rectangular cross-section, $I = bh^3/12$ and $A = bh$, and substituting these expressions into the equation gives:

$$k^4 = \omega^2 \frac{12\rho}{Eh^2} \tag{6.6}$$

Assuming ω, E, and ρ are invariant, the condition for wave equality simplifies to:

$$\frac{h}{r^2} = C_2 \tag{6.7}$$

Assuming the thickness in the centerline of the curved segments is h_0, we have $C_2 = h_0/R^2$. This yields a quadratic thickness profile for the curved segment:

$$h(r) = h_0 (\frac{r}{R})^2 \tag{6.8}$$

To connect the variable thickness curved bend to the uniform thickness straight part, we use a 30-mm long transition part to linearly transfer the cross-sections (Fig. 6.4b). FEM simulations were performed to evaluate this design. We observed that the outer bend still had more waves than the inner bend (Fig. 6.5b), indicating that the quadratic profile was insufficient to fully equalize the wave numbers. This discrepancy is likely due to approximations in the dispersion equation Eq. 6.5.

To address this, the quadratic thickness equation was modified to include a variable power m:

$$h(r) = h_0 \left(\frac{r}{R}\right)^m \tag{6.9}$$

We explored the effect of the power m using FEM to conduct an eigenfrequency study in which the power m was varied from $2.0 \leq m \leq 2.8$ with steps of 0.1. The uniformity in the mode shape, defined as the ratio between the minimum amplitude and the maximum amplitude along the antinodal lines in the straight parts, was evaluated as a function of m, as shown in Fig. 6.5a. The value of $m = 2.4$ was found to equalize the number of waves across the curved segments and produce parallel nodal lines on the straight segments (Fig. 6.5b). This optimized thickness profile resulted in an outer thickness of 5.16 mm and an inner thickness of 1.16 mm, and was used in the final physical prototype design.

6.2.3. MANUFACTURING AND VALIDATION OF THE MODE SHAPES

The flatLoop was fabricated from aluminum 5052 ($E = 69$ GPa and $\rho = 2680$ kg/m^3) using CNC machining. Six piezoceramic plates (SMPL25W5T30311, Steiner & Martins Inc), measuring 25×5×0.3 mm, were glued to one of the straight section of the flatLoop using epoxy adhesive (DP490, 3M). They were arranged in two sets of three: one set on the top surface and the other on the bottom. The piezoceramic elements were spaced one wavelength apart within each set, with the two sets offset by one-quarter wavelength. Each set was connected to an ultrasonic signal source, amplified by a 20× amplifier (PD200, PiezoDrive Inc.). The opposite side of the loop is used as the touch surface, providing a flat interaction area of 80×30 mm^2.

To validate our design, we measured the vibration using a laser Doppler vibrometer (OFV-503 and OFV-5000, Polytec) with a custom scanning attachment. The frequency response of the symmetric and asymmetric modes were obtained by scanning the frequency around the resonance and measuring vibrations at the antinodes of each mode. The frequency sweep signal was generated by a data acquisition board (USB-6351, National Instruments). The resonant frequencies of the two degenerate modes were closely spaced at 38,601 Hz and 38,596 Hz, as shown in Fig. 6.6a. Because both modes are close, we set the working frequency as the average which was sufficient to excite traveling waves with a high vibration amplitude.

The symmetric and asymmetric mode shapes were further characterized by scanning the 80×30 mm^2 touch surface with a 1×1 mm^2 grid. These mode shapes were orthogonal (Fig. 6.6b and c), although some modal lines appeared distorted. These distortions may be attributed to manufacturing imperfections or the influence of transition parts, which requires further investigation.

A traveling wave pattern can be observed by superimposing these two degenerate modes with a 90-degree temporal phase shift, see Fig. 6.6d, although several nodal regions are still visible.

6.3. CHARACTERIZATION OF FORCE GENERATION

The main performance metric of these devices is how salient the sensation is. To quantify the saliency, which is linked to the strength of the stimulus, we measured the net

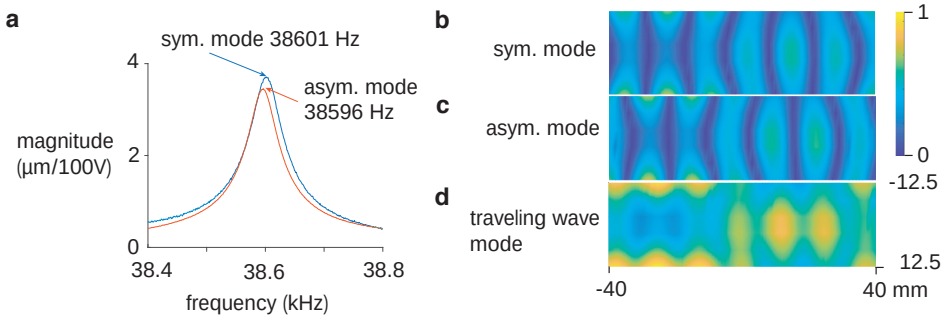

Figure 6.6: (a) Experimental frequency response of the two frequency-degenerate modes. (b) Normalized colormaps of the mode shapes of symmetric mode, asymmetric mode, and the resulting traveling wave mode.

lateral force on a stationary human finger under varying normal forces and phase shifts. Additional measurements were conducted on a sliding finger to evaluate force behavior during dynamic interaction.

6.3.1. FORCE MEASUREMENT SETUP AND FORCE GENERATION

The flatLoop was supported by four 3D printed PLA fixtures attached to its curved segments. These fixtures were mounted on a 250 mm×70 mm PMMA plate, which was fastened to a 6-axis force/torque sensor (HEX32, ReSense). A 3D-printed finger holder fixed to a grounded structure constrained the finger movement in the lateral direction. This setup enabled the force sensor to measure the net lateral force exerted on the stationary finger.

During the measurements, the experimenter placed his index finger in the holder and maintained a normal force of approximately 1 N. The phase shift of the driving signal was then abruptly switched from 0° to 90 °, while the voltage sent to the piezoelectric actuators remained constant at ±3 V × 20. The net lateral force was calculated as the change in force when the phase shift was switched to 90 °. The averaged lateral force across 18 trials was measured as 0.31 N (Fig. 6.7a).

6.3.2. LATERAL FORCE VERSUS NORMAL FORCE

To study the effect of normal force on the lateral force generation, we measured the lateral force under varying normal forces of 0.2, 0.5, 0.8, 1.0, 1.5, and 2 N at $x = 30$ mm on the touch surface. Each normal force condition was tested in three trials, with each trial comprising eight times of phase switches from 0° to 90°. As shown in Fig. 6.7b, the lateral force increased approximately linearly with normal force for $F_N \leq 1$ N. However, at higher normal forces ($F_N = 1.5$ N and 2 N), the lateral force decreased, which is likely due to damped vibrations. These results suggest that for optimal tactile feedback on traveling wave devices, the applied normal force should remain within an appropriate range, ideally not exceeding 1 N.

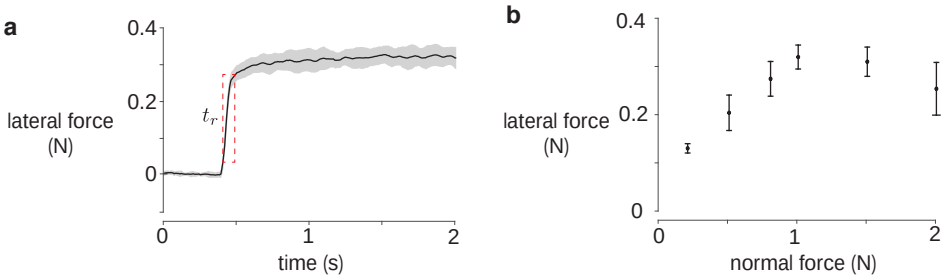

Figure 6.7: (a) Net lateral force measured at $x = 30$ mm on a stationary finger when the phase shift was abruptly switched from 0° to 90 °. The curves are aligned to the moment of phase switching. The rise time $t_r = 0.12$ s. The shaded area represents the standard deviation. (b) Net lateral force as a function of the normal force.

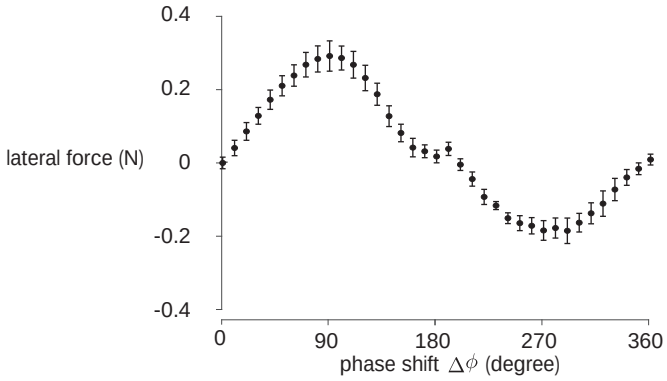

Figure 6.8: Lateral force as a function of phase shift $\Delta\phi$ with each condition repeated nine times. Error bars represent the standard deviation.

6.3.3. LATERAL FORCE VERSUS PHASE SHIFT

The lateral force at $x = 30$ mm was measured under varying phase shifts between two standing waves, with the normal force maintained at 1 N. Each phase shift in the range of 0° to 360° with an increment of 10° was measured nine times. As shown in Fig. 6.8, the lateral force exhibits a sinusoidal relationship with phase shift, reaching a maximum rightward force of 0.3 N at 90° and a maximum leftward force of 0.2 N at 270°. The lateral force was near zero at 0° and 180°. This sinusoidal force-phase trend is consistent with previous observations on the Ultraloop. The observed asymmetry between force magnitudes at 90° and 270° may result from the non-uniform mode shape at these phase shifts, as seen in Fig. 6.6b.

6.3.4. LATERAL FORCE VERSUS SLIDING DIRECTION

Lateral force generation is typically evaluated on a stationary fingertip. However, sliding gestures are common in touchpad or touchscreen interactions. In this experiment, we measured the lateral force when a finger is sliding in and against the traveling wave direction. The experimenter slid the index finger back and forth eight times while main-

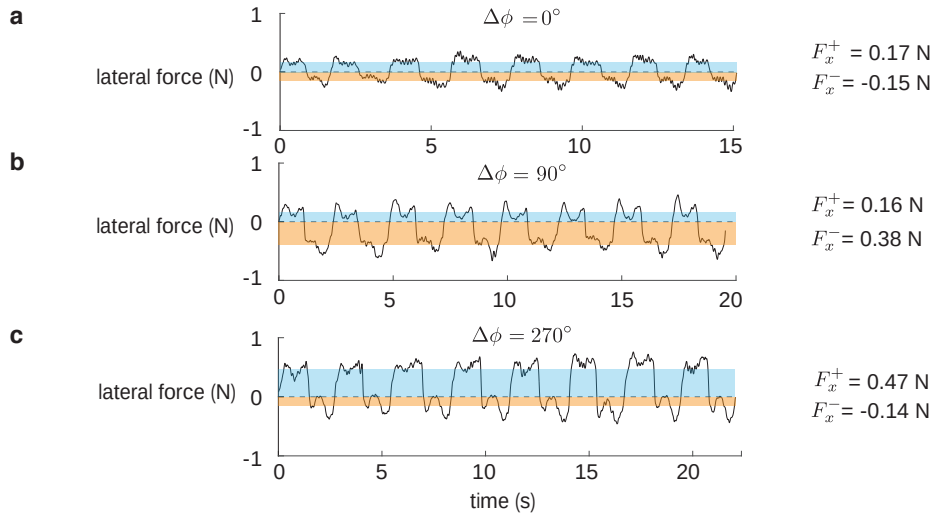

Figure 6.9: Symmetric resistance was observed in (a) under a standing wave condition. In contrast, in (b) and (c), higher resistance is observed when the finger slides against the particle motion, compared to when the finger slides in the direction of particle motions. The shaded areas represent the average positive (blue) and negative (orange) forces.

taining a normal force of approximately 1 N. The phase conditions in these trials were 0°, 90° or 270°.

At a 0° phase shift, the flatLoop generates standing waves. The lateral force was roughly symmetric between both sliding directions, with the average positive force being 0.17 N, and the average negative force being 0.15 N, see Fig. 6.8a. This symmetry indicates that no net lateral force was produced under these conditions. Instead, the fingertip experienced only sliding friction opposing the motion.

At a 90° phase shift, where the traveling waves propagate clockwise, the surface generates rightward lateral forces on a stationary finger. However, when the finger is sliding, it encounters resistance in both sliding directions, as shown in Fig. 6.8b. Notably, when sliding against the net force direction, a higher resistance force is observed, with an average force of 0.38 N compared to 0.165 N when sliding back. Similarly, at a 270° phase shift, the observed asymmetry reversed (Fig. 6.8c). These observations suggest that the active lateral forces might only generate a "pushing" effect on a static or a slow-moving finger. When a finger slides in the direction of the surface particle motion but at a speed exceeding the particle velocity, the global force is still resistive and not propulsive, contrary to the behavior observed with a static finger.

6.4. DEMONSTRATION: A HAPTIC KEYBOARD

Active haptic devices can effectively provide force feedback on users and can be used to construct artificial potential fields or guide users' limb in virtual or remote environments [23], [24]. However, the application of potential field rendering for fingertip guidance remains limited in human-computer interaction (HCI) applications [9]. Here, we

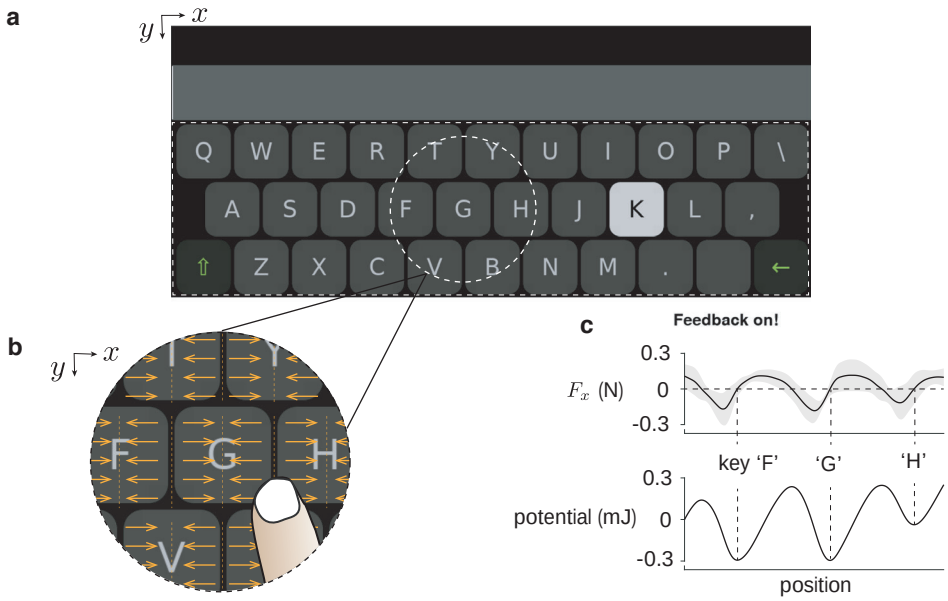

Figure 6.10: Demonstration of a haptic keyboard. (a) The user interface displayed on an external screen. Users can interact with the interface by sliding on the flatLoop. (b) Visualization of the desired force fields within the dashed circle. (c) The lateral force measured on a slowly sliding finger across the centerline in the dashed circle area. The graph below shows the calculated potential values derived as the integral of the lateral force. The shaded area represents the standard deviation.

designed a haptic keyboard application using the flatLoop to demonstrate the practicality of our device in real-world scenarios. The haptic keyboard aims to restore the tangibility of physical keys by generating attractive potential wells aligned with the keyboard layout. Fig. 6.10a illustrates the interactive user interface displayed on a screen, which consists of three rows of keys arranged in the standard "QWERTY" configuration. Each key is represented by an individual Gaussian potential well, and the corresponding local force field is derived as the negative gradient of the potential field (Fig. 6.10b). As a user's finger slides over the touch surface, a position sensor (Neonode, NNAMC1580PCEV) located above the surface tracks the finger's x and y coordinates. The position data is transmitted to a microcontroller (Teensy 3.6), which generates haptic signals to produce the desired lateral forces. These potential fields could help users to navigate over the keys, enabling faster and easier typing.

To evaluate the system, we recorded the lateral forces generated as a finger slid across the center row of the keyboard 6 times. Fig. 6.10c shows the measured force as a function of position. The integration of the averaged force curve reveals distinct potential wells aligned with keys "F," "G," and "H" (Fig. 6.10c), aligning with the proposed tactile experience.

6.5. DISCUSSIONS AND CONCLUSIONS

We designed a low-profile active surface haptic device that uses resonant traveling waves. The cross-section follows a power-law with a power of 2.4, which was determined by analytical model and FEM simulations, leading to even wave distribution. Our design achieves comparable performance to the original device, the Ultraloop, while significantly reducing its height. The flatLoop generated 3.58 μm/100 V versus 3.73 μm/100 V in the Ultraloop, and a maximum force of 0.31 N vs. 0.3 N when the normal force is 1 N. The current design reduces the height from 100 mm to 5 mm by using a planar configuration, as seen by a side-by-side comparison of dimensions in the inset in Fig. 6.1.

One limitation of the prototype is that the observed nodal lines in the straight parts are not fully parallel compared to FEM simulations, resulting in less uniform wave distribution and uneven force production. This discrepancy may arise from imprecision in the CNC machining process or the potential suboptimal selection of $m = 2.4$ based on FEM results. Refining the mode shape through further investigation of the power parameter of m may improve uniformity. Additionally, the effect of uneven force production can be mitigated in real applications by tuning the actuation level to normalize local vibration amplitudes.

Another limitation is the absence of an explicit force production model that accounts for sliding velocity and the geometry of the elliptical trajectory. Our experiments measured the forces during sliding against and along the wave propagation direction. The variation in force of these two cases supports the model proposed by Ghenna et al., who measured the lateral force in a surface haptic device with elliptical surface motions [8]. Future studies should investigate force production as a function of sliding velocity and the potential field rendering can consider the velocity as an input, which currently depends solely on position.

In conclusion, we introduced the flatLoop, a low-profile active force feedback device with a height of 5 mm, designed for potential field rendering. The flatLoop features a touch surface of 80×30 mm^2 and generates a maximum lateral force of 0.31 N, comparable to the Ultraloop while offering improved usability due to its compact size. This innovation makes it suitable for integration into devices such as information terminals and car dashboards. Future work should focus on modeling and optimizing the transition region to further increase the area of the touch surface and conducting user studies to evaluate 2D potential field rendering.

REFERENCES

[1] L. Winfield, J. Glassmire, J. E. Colgate, and M. Peshkin, "T-pad: Tactile pattern display through variable friction reduction", in *Second Joint EuroHaptics Conference and Symposium on Haptic Interfaces for Virtual Environment and Teleoperator Systems (WHC'07)*, IEEE, 2007, pp. 421–426.

[2] M. Wiertlewski, R. Fenton Friesen, and J. E. Colgate, "Partial squeeze film levitation modulates fingertip friction", *Proceedings of the national academy of sciences*, vol. 113, no. 33, pp. 9210–9215, 2016.

[3] O. Bau, I. Poupyrev, A. Israr, and C. Harrison, "Teslatouch: Electrovibration for touch surfaces", in *Proceedings of the 23nd annual ACM symposium on User interface software and technology*, 2010, pp. 283–292.

[4] M. Ayyildiz, M. Scaraggi, O. Sirin, C. Basdogan, and B. N. Persson, "Contact mechanics between the human finger and a touchscreen under electroadhesion", *Proceedings of the National Academy of Sciences*, vol. 115, no. 50, pp. 12 668–12 673, 2018.

[5] S.-C. Kim, A. Israr, and I. Poupyrev, "Tactile rendering of 3d features on touch surfaces", in *Proceedings of the 26th annual ACM symposium on User interface software and technology*, 2013, pp. 531–538.

[6] V. Levesque, L. Oram, K. MacLean, *et al.*, "Enhancing physicality in touch interaction with programmable friction", in *Proceedings of the SIGCHI conference on human factors in computing systems*, 2011, pp. 2481–2490.

[7] C. Bernard, J. Monnoyer, S. Ystad, and M. Wiertlewski, "Eyes-off your fingers: Gradual surface haptic feedback improves eyes-free touchscreen interaction", in *Proceedings of the 2022 CHI Conference on Human Factors in Computing Systems*, 2022, pp. 1–10.

[8] S. Ghenna, E. Vezzoli, C. Giraud-Audine, F. Giraud, M. Amberg, and B. Lemaire-Semail, "Enhancing variable friction tactile display using an ultrasonic travelling wave", *IEEE transactions on haptics*, vol. 10, no. 2, pp. 296–301, 2016.

[9] E. C. Chubb, J. E. Colgate, and M. A. Peshkin, "Shiverpad: A glass haptic surface that produces shear force on a bare finger", *IEEE Transactions on Haptics*, vol. 3, no. 3, pp. 189–198, 2010.

[10] Z. Cai and M. Wiertlewski, "Ultraloop: Active lateral force feedback using resonant traveling waves", *IEEE Transactions on Haptics*, vol. 16, no. 4, pp. 652–657, 2023.

[11] H. Xu, R. L. Klatzky, M. A. Peshkin, and J. E. Colgate, "Localizable button click rendering via active lateral force feedback", *IEEE Transactions on Haptics*, vol. 13, no. 3, pp. 552–561, 2020.

[12] X. Dai, J. E. Colgate, and M. A. Peshkin, "Lateralpad: A surface-haptic device that produces lateral forces on a bare finger", in *2012 IEEE Haptics Symposium (HAPTICS)*, IEEE, 2012, pp. 7–14.

[13] H. Xu, M. A. Peshkin, and J. E. Colgate, "Ultrashiver: Lateral force feedback on a bare fingertip via ultrasonic oscillation and electroadhesion", *IEEE transactions on haptics*, vol. 12, no. 4, pp. 497–507, 2019.

[14] J. Mullenbach, M. Peshkin, and J. E. Colgate, "Eshiver: Lateral force feedback on fingertips through oscillatory motion of an electroadhesive surface", *IEEE transactions on haptics*, vol. 10, no. 3, pp. 358–370, 2016.

[15] H. Xu, M. A. Peshkin, and J. E. Colgate, "Switchpad: Active lateral force feedback over a large area based on switching resonant modes", in *Haptics: Science, Technology, Applications: 12th International Conference, EuroHaptics 2020, Leiden, The Netherlands, September 6–9, 2020, Proceedings 12*, Springer, 2020, pp. 217–225.

[16] C. Zhao, *Ultrasonic motors: technologies and applications*. Springer Science & Business Media, 2011.

[17] M. Biet, F. Giraud, F. Martinot, and B. Semail, "A piezoelectric tactile display using travelling lamb wave", 2006.

[18] D. Gueorguiev, A. Kaci, M. Amberg, F. Giraud, and B. Lemaire-Semail, "Travelling ultrasonic wave enhances keyclick sensation", in *Haptics: Science, Technology, and Applications: 11th International Conference, EuroHaptics 2018, Pisa, Italy, June 13-16, 2018, Proceedings, Part II 11*, Springer, 2018, pp. 302–312.

[19] Z. Cai and M. Wiertlewski, "Viscous damping displayed by surface haptics improves touchscreen interactions", in *International Conference on Human Haptic Sensing and Touch Enabled Computer Applications*, Springer, 2024, pp. 352–364.

[20] G. P. Thomas, M. A. Andrade, J. C. Adamowski, and E. C. N. Silva, "Development of an acoustic levitation linear transportation system based on a ring-type structure", *IEEE transactions on ultrasonics, ferroelectrics, and frequency control*, vol. 64, no. 5, pp. 839–846, 2017.

[21] G. Thomas, C. Kiyono, A. Gay Neto, and E. Silva, "Conceptual design of oblong ring vibrators", *Journal of Vibration and Acoustics*, vol. 142, no. 2, p. 021 001, 2020.

[22] X. Liu, D. Shi, Y. Civet, and Y. Perriard, "Modelling and optimal design of a ring-type structure for the generation of a traveling wave", in *2013 International Conference on Electrical Machines and Systems (ICEMS)*, IEEE, 2013, pp. 1286–1291.

[23] J. Ren, K. A. McIsaac, R. V. Patel, and T. M. Peters, "A potential field model using generalized sigmoid functions", *IEEE Transactions on Systems, Man, and Cybernetics, Part B (Cybernetics)*, vol. 37, no. 2, pp. 477–484, 2007.

[24] P. Marayong and A. M. Okamura, "Speed-accuracy characteristics of human-machine cooperative manipulation using virtual fixtures with variable admittance", *Human Factors*, vol. 46, no. 3, pp. 518–532, 2004.

7

CONCLUSION

This thesis explored the design of traveling wave surface haptics and their applications in human-computer interaction. This concluding chapter summarizes the main contributions, limitations and implications of this work and discusses potential future directions.

7.1. CONTRIBUTIONS AND LIMITATIONS

Modulating the friction of a touch surface can provide users with rich tactile feedback. However, friction modulation essentially modulates the resistance of a sliding finger, making it ineffective for guiding users when the finger is stationary or not moving toward a target. To overcome this limitation, this thesis introduces novel prototypes that generate net lateral forces and investigates how touch interactions can be enhanced using elastic potential fields. The primary contributions of this doctoral work are threefold:

1. **Development of traveling wave surface haptic devices.** Generating net tangential forces on a touch surface has been challenging. With ultrasonic traveling bending waves, it is possible to move fingers that is in contact with the surface by leveraging the elliptical motions of the surface participles [1]. A key challenge in developing traveling wave device is designing an acoustic cavity that supports high-Q resonant traveling waves while providing a relatively large and flat surface for touch interactions. This thesis introduced two novel device designs:

    - Oblong ring-shaped design (Ultraloop)

      Chapter 3 presented the Ultraloop, an oblong ring-shaped structure composed of two straight beams of length L, where the user can interact with, and two curved beams of radius R that redirect the ultrasonic wave and create a connection. This structure possesses a pair of orthogonal bending modes of the same order. Traveling waves are generated by exciting both modes with ultrasonic driving signals that are shifted by $\pi/2$. These two orthogonal modes only have the same resonance frequency (i.e. mode degeneracy)

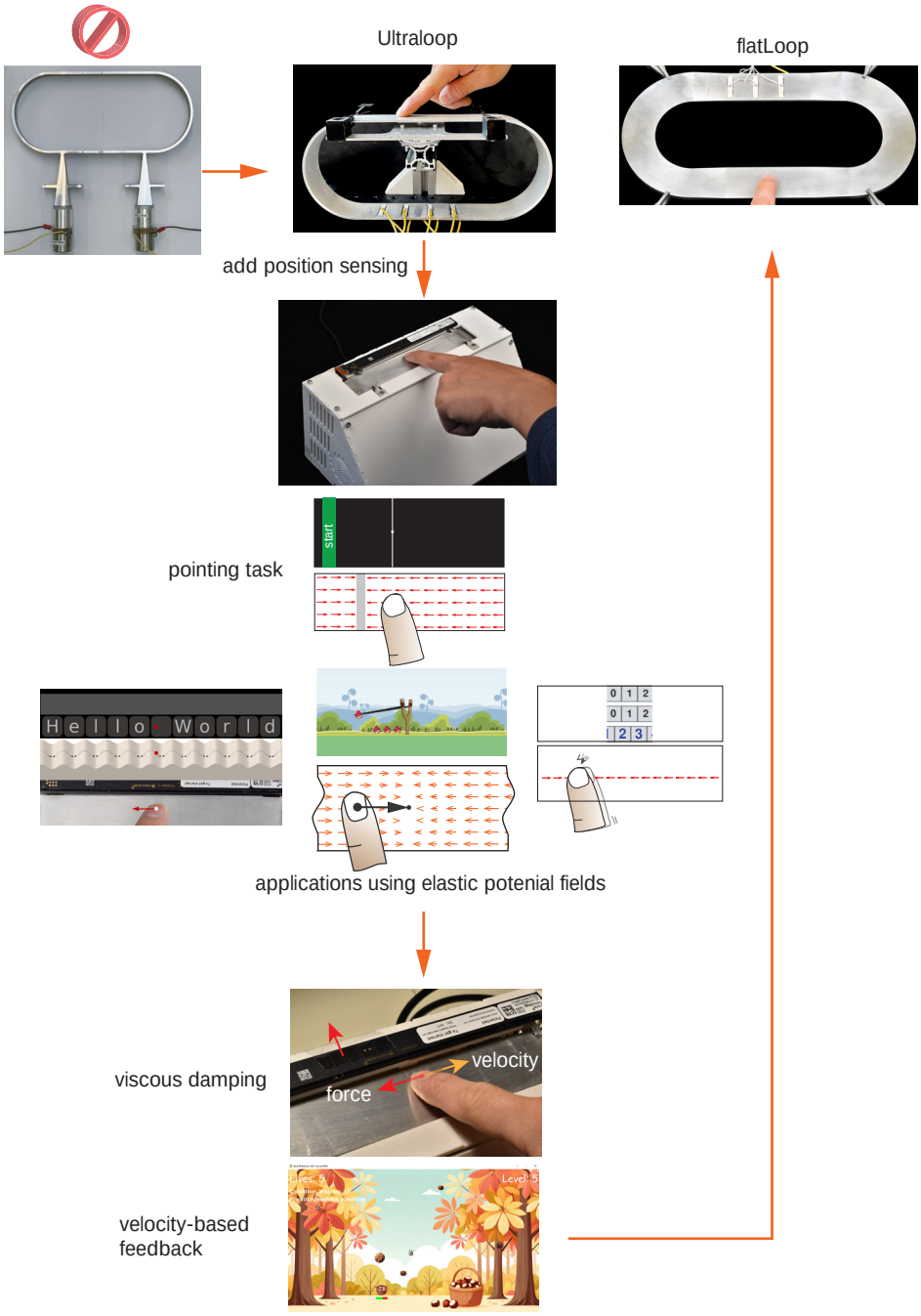

Figure 7.1: A visual representation of the evolution of the doctoral work.

under specific geometric constraints. Analytical and numerical studies revealed that mode degeneracy occurs at several discrete length-to-radius ratios, independent of beam width and thickness. Experimental results confirmed that the Ultraloop could produce traveling waves with amplitudes of up to ± 3 μm, resulting in lateral forces of ± 0.3 N. The design can be adapted to various applications by modifying its length-to-radius ratio or scaling its dimensions.

- Low-profile design (flatLoop)

  Despite its ability to generate uniform and substantial forces, the Ultraloop has a height of $2R$, making it unsuitable for integration into most modern touch devices. Chapter 6 introduced the flatLoop, a low-profile device, with a planar design. This structure maintains the same oblong centerline as the Ultraloop but positions the touch surface on the same plane as the centerline, reducing the device's height to its thickness. However, the planar design introduces a mismatch between the outer and inner circumferences, leading to an unequal number of waves and tilted nodal lines in the straight parts. To address this issue, a power-law thickness profile was implemented, where the outer bend is thicker than the inner bend to "speed up" the bending waves. This adjustment ensures an equal number of waves and straight nodal lines. By superimposing the two degenerate modes, the flatLoop achieves uniform traveling waves for fingertip guidance.

Both designs exhibit high Q-factors due to the use of resonance, relatively large touch areas, and relatively compact dimensions, making them suitable as haptic displays for delivering diverse tactile effects.

2. **Exploration of elastic potential fields to enhance touch interactions.** While several studies on active force feedback devices have demonstrated potential field rendering on surfaces, none have explored the design of potential fields for touch interactions and their effects on users. Chapter 4 examined how touch interactions can be enhanced by using several types of potential fields. These force fields were created as the negative gradient of desired potentials with the Ultraloop. Several positive impacts were observed:

   - Differentiation of 3D shapes using attractive and repulsive force fields

     Users were able to perceive attractive or repulsive force fields as bumps and holes with varying heights or depths. However, detecting holes was found to be more challenging, with a high JND reported. When these tactile features were integrated into a virtual keyboard, participants expressed a preference for the haptic feedback and commented that it helped navigation over the keyboards and reduced the cognitive load.

   - Improved pointing task performance

     Rendering stepwise force fields around a target improved pointing task performance by 15.5%, compared to no tactile feedback. Additionally, participants could accurately locate invisible targets through guidance from the

stepwise force field, enabling eye-free interaction. This method also outperformed friction modulation techniques in targeting invisible targets, leading to a 22.9% performance gain. These findings highlight the potential of stepwise force fields for sliding-based tasks in human-computer interaction.

- Communicating directional cues
  Active force fields could also effectively convey directional cues to users, with participants initiating movement in the intended direction 88% of the time. User's perception of direction was also used to simulate elastic physics, such as the pulling sensation in an interactive game like Angry Birds.

These examples underscore the benefits of potential fields in touch interactions, including improved task performance and enhanced user experience. These applications hold promise for broader implementation in sliding-based interactions and beyond.

3. **Exploration of effects of viscous rendering on users.** Chapter 5 investigated how surfaces with viscous damping influence users' sliding interactions. Three viscous environments were evaluated in a pointing task: positive damping, negative damping, and variable damping (where the damping coefficient switches to negative during fast finger movements). Analysis of movement trajectories and performance data revealed that damping conditions have insignificant effects during the initial phase of reaching tasks, likely because visual cues dominate in these tasks, allowing users to plan their trajectories primarily based on their initial target estimation. During the selection phase, positive damping assisted users' movement with reduced completion times. This effect may be attributed to reduced motor noise during the precision phase.

   These findings suggest that the viscous damping environments can enhance interaction tasks that involve dynamic targeting and may also be useful for simulating viscous physics in virtual and augmented reality.

In conclusion, for the first time, we developed haptic interfaces capable of generating uniform net lateral forces on flat and rectangular surfaces using resonant traveling waves. Additionally, it is the first to investigate the effects of active force feedback on users by designing both position-based tactile feedback (i.e., potential field rendering) and velocity-based feedback (i.e., viscous damping). These contributions advance the field of surface haptics, expanding the design space for interactive touch surfaces.

Despite these advancements, several limitations have been identified. First, the resonance of the Ultraloop and flatLoop shifts over time due to thermal effects, leading to a reduction in actuation efficiency. The current solution involves sweeping the frequency to track the resonance, but this introduces delays in real-time applications. Second, the aspect ratio of the elliptical structures, which directly influences force production, remains fixed and has not yet been optimized for performance. Finally, the current designs focus on generating one-dimensional force feedback; extending this capability to two-dimensional force generation and two-dimensional applications remains an open challenge. Addressing these limitations will be an important direction for future research, as discussed in the next section.

Additionally, several critical experimental insights were uncovered during this work, which are not documented in my publicized work but proved essential to achieving successful results. Initially, the Ultraloop design included two horns (Figure 7.1), but this resulted in weak vibrations. It is likely that the horns introduced significant wave reflections at the interfaces between the ultrasonic transducers, the horns, and the oblong ring, preventing efficient energy propagation to the main structure. By eliminating the horns and instead using direct piezoceramic plate actuators, wave reflections were minimized, leading to significantly improved vibration amplitudes. Furthermore, the choice of adhesive for bonding piezoceramic elements to the aluminum body played a crucial role in ensuring effective stress transmission. Early experiments using DP 120 (3M) epoxy did not provide sufficient bonding strength. Switching to DP 490 (3M) significantly improved adhesion and resulted in better overall performance of the devices.

7.2. FUTURE DIRECTIONS

These promising results also facilitate several avenues for further investigation, including haptic interface design, the study of the physics of force generation, and improving usability across various touch-based devices, detailed below:

How can we improve the traveling-wave surface haptic devices regarding robustness, usability, and power efficiency? Several opportunities exist for refining and expanding the capabilities of traveling-wave surface haptic devices. First, optimizing the frequency selection process of the device remains a promising direction. We observed that the resonance of the device would shift due to the heating of the aluminum beam in the Ultraloop and flatLoop. When operating for 5 minutes, the temperature can rise by 8°C, leading to a 50 Hz shift in the resonant frequency. Considering the high Q factor of the resonator, this 50-Hz deviation from the resonance significantly reduces vibration amplitude. The frequency selection procedure implemented in Chapters 4 and 5 mitigates this issue by performing a frequency sweep and amplitude measurement via a pick-up piezo. However, this process currently requires 10-20 seconds, which could be further refined to enable faster and more seamless real-time adaptation. Future work could explore more efficient real-time tuning methods to enhance the device's responsiveness.

Second, refining the sensing approach for position- and velocity-based tactile feedback is also an avenue for improvement. This thesis used a commercial infrared touch sensor for tracking finger positions. However, optical sensing does not provide a high resolution and may produce incorrect positions. While errors are rare, incorrect position estimations can result in unintended force feedback and an unpleasant user experience. In addition, this sensor increases the size and cost of the device. Incorporating projected capacitive sensing could offer greater sensitivity, reliability, and compactness in future versions.

Third, adapting the length-to-radius ratio of the Ultraloop to align with modern touch-based interfaces would expand its applicability. The current design, with a 30 mm-wide touch area and a 100 mm height, may not be optimal for commercial integration. Exploring alternative geometric configurations, such as wider and lower-profile designs, could make these devices more suitable for applications in museum exhibits, automo-

tive interfaces, and interactive displays.

Lastly, optimizing power efficiency is also valuable for the future direction. While power consumption has not yet been evaluated, understanding and improving energy efficiency will be crucial, particularly for portable and wearable applications. Future efforts could focus on quantifying energy consumption and developing strategies to minimize power requirements without compromising performance.

Can we scale down the Ultraloop for wearable devices? With the growing demand for haptic feedback in wearable technology, an exciting direction for future research is the miniaturization of Ultraloop devices. Potential applications include integration into wearable electronics such as smartwatches, where compact haptic feedback mechanisms could enhance user interaction. A key question is whether the current design can be effectively scaled down, and more specifically, whether it can be reduced to the size of a watch. Let's consider the governing equation for a beam with a rectangular cross-section, $\omega^2 = k^4 \frac{Eh^2}{12\rho}$, using the Euler-Bernoulli assumption. We can find that a smaller device requires a higher frequency, a smaller thickness, and a lower order of bending mode for wave propagation. However, these adjustments face trade-offs or constrains: higher frequencies may reduce the amplitude and force generation, thinner devices complicate the manufacturing, and the order of modes has to be at least 2 to allow for degenerate mode generation. One has to balance these constraints when designing for practical applications.

Can two-dimensional potential fields using one-dimensional lateral force effectively guide users? The prototypes developed in this work generate one-dimensional forces but could also render two-dimensional potentials or force fields, i.e. $F = F(x, y)$. For instance, Chapter 6 demonstrated a haptic keyboard with periodic potential fields along both x and y directions, their effectiveness in guiding users along the y-axis remains an open question. Future studies should investigate whether these force fields can provide directional guidance in both dimensions, particularly in applications like virtual keyboards or navigation interfaces.

Additionally, psychophysical experiments could offer valuable insights into users' ability to follow more complex force patterns. For example, early work by Chubb et al. on the ShiverPad device demonstrated that participants could successfully perceive and follow curved contours generated by lateral force feedback [2]. Extending this line of research, future studies could quantitatively assess users' ability to follow tilted lines of the form $y = xtan\theta$ or curved contours. These experiments would help determine the extent to which one-dimensional force cues can be leveraged to create effective two-dimensional haptic guidance.

Is there an optimal aspect ratio of the ellipses that maximizes the lateral force generation? This thesis uses a fixed elliptical motion geometry in the experiments. An intriguing avenue for future research is to explore the effect of elliptical motion geometry on lateral force generation. There is evidence that the aspect ratio between the longitudinal displacement and the transverse displacement of the surface particles can affect the lateral force generation. Indeed, when the ratio is extreme, for example, the longitudinal displacement is much larger than the traverse displacement, the ellipses shrink to a vertical line and cannot propel objects laterally. Conversely, if the ellipses shrink

to a line in the longitudinal direction, the leftward and the rightward lateral forces cancel each other, resulting in zero net lateral force. Preliminary findings also suggest the existence of an optimal ratio. Garcia et al. reported that participants had the lowest detection threshold when the aspect ratios were between 0.5 and 2/3 [3]. However, the optimal value for the aspect ratio has not been identified and the setup they conducted human study was not based on traveling waves.

In the traveling surface haptic devices, the aspect ratio of ellipses can be expressed as $kh/2$, where k is the flexural bending wave number and h is the thickness of the beam[4]. To investigate the effects of aspect ratios, one needs to design an experimental setup that allows for continuous adjustment of aspect ratios. Alternatively, fabricating multiple devices with discrete aspect ratios could provide practical insights into force generation efficiency. These findings could help optimize device designs for maximizing lateral force output.

How can we develop two-dimensional active force feedback devices? Current prototypes, including those in this work and existing literature, primarily generate lateral forces along a single axis. Extending this capability to two-dimensional force feedback would enable richer interactions by guiding fingers in arbitrary directions through the superposition of force vectors in both x and y dimensions. However, achieving two-dimensional force generation presents significant design challenges.

A straightforward method might be to introduce a second ring-shaped cavity perpendicular to the original, but this configuration would cause wave interference at their intersections. Moreover, fabricating such a structure would be complex and difficult to manufacture. Designing a structure that allows resonant traveling waves along both x and y directions requires substantial innovation in hardware design.

Another possible direction is to use non-resonant traveling waves, where waves are absorbed or dampened to prevent reflections. For example, by attaching high-damping material to the sharpened edge of a plate, it is possible to absorb vibration and allow for traveling waves. By placing multiple vibration sources at different locations, it may be feasible to generate force vectors in arbitrary directions within the x-y plane. Further, leveraging acoustic metamaterials is also a possible way to confine and direct wave propagation. Metamaterials engineered with phononic bandgaps have been shown to enable highly controlled wave transmission [5] and could be explored for active force generation.

Achieving two-dimensional force feedback could significantly enhance touch-based interactions, including precise icon selection, gesture-based navigation [6], and path-following along curved contours [7].

Can we render 2D shapes with edges using active forces? Rendering graphical elements (e.g., squares, triangles, or maps) on touch surfaces requires users to clearly perceive edges. While friction modulation has been used to render 3D shapes such as bumps and holes [8], it fails to create a distinct tactile sensation akin to brushing over edges, likely due to its passive nature. For instance, Xu et al. attempted to render raised dots and geometric shapes (e.g., circles, squares, triangles) using an electrotactile display but reported low detection rates among participants [9].

In contrast, subjective responses from Chapter 4 suggest that stepwise force fields can produce distinct edge sensations. Similarly, Chubb et al. demonstrated that users

could track notch contours rendered with active forces applied orthogonally to movement direction [10]. Future advancements in 2D active force feedback displays could enable the rendering of a variety of 2D-edged shapes, making them valuable tools for studying edge perception and designing more effective tactile elements.

This work represents a significant advancement in active surface haptics, introducing a novel approach to generating lateral forces using resonant traveling waves. Through rigorous experimentation and analysis, this thesis has demonstrated the benefits of active force feedback in enhancing touch interactions, both quantitatively and subjectively. These promising results have the potential to drive further innovations in haptic research and inspire new solutions that address the challenges outlined in the future work section.

Looking ahead, this technology has the potential to extend beyond one-dimensional force feedback, enabling guidance across two-dimensional surfaces. Such advancements could allow users to reach arbitrary locations or follow complex trajectories. Additionally, this approach could be applied to a wide range of real-world touch-enabled devices, including consumer electronics such as tablets, smartphones, and smartwatches, as well as interactive exhibits in museums, car dashboards, educational panels, and public kiosks.

Ultimately, active surface haptics holds great promise in restoring the tactile dimension to touch interfaces, revolutionizing human-computer interaction by enabling effortless control of digital systems through the fingertips. By reducing visual and cognitive loads, these advancements could make touch interactions more intuitive, accessible, and engaging across diverse domains.

7

REFERENCES

[1] W. Seemann, “A linear ultrasonic traveling wave motor of the ring type”, en, vol. 5, no. 3, pp. 361–368, Jun. 1996, ISSN: 0964-1726. DOI: 10.1088/0964-1726/5/3/015.

[2] E. C. Chubb, J. E. Colgate, and M. A. Peshkin, “ShiverPaD: A Glass Haptic Surface That Produces Shear Force on a Bare Finger”, *IEEE Trans. Haptics*, vol. 3, no. 3, pp. 189–198, Jul. 2010, ISSN: 2329-4051. DOI: 10.1109/TOH.2010.7.

[3] P. Garcia, F. Giraud, B. Lemaire-Semail, M. Rupin, and M. Amberg, “2motac: Simulation of button click by superposition of two ultrasonic plate waves”, in *Haptics: Science, Technology, Applications: 12th International Conference, EuroHaptics 2020, Leiden, The Netherlands, September 6–9, 2020, Proceedings 12*, Springer, 2020, pp. 343–352.

[4] M. Kuribayashi, S. Ueha, and E. Mori, “Excitation conditions of flexural traveling waves for a reversible ultrasonic linear motor”, *J. Acoust. Soc. Am.*, vol. 77, no. 4, pp. 1431–1435, Apr. 1985, ISSN: 0001-4966. DOI: 10.1121/1.392037.

[5] T. Daunizeau, D. Gueorguiev, S. Haliyo, and V. Hayward, “Phononic crystals applied to localised surface haptics”, *IEEE Transactions on Haptics*, vol. 14, no. 3, pp. 668–674, 2021.

[6] D. S. Dunnam and H. Stallings, *Gesture-based navigation*, US Patent 8,443,303, May 2013.

[7] J. Accot and S. Zhai, "Beyond Fitts' law: Models for trajectory-based HCI tasks", en, in *Proceedings of the ACM SIGCHI Conference on Human factors in computing systems*, Atlanta Georgia USA: ACM, Mar. 1997, pp. 295–302, ISBN: 978-0-89791-802-2. DOI: 10.1145/258549.258760.

[8] S.-C. Kim, A. Israr, and I. Poupyrev, "Tactile rendering of 3d features on touch surfaces", in *Proceedings of the 26th annual ACM symposium on User interface software and technology*, 2013, pp. 531–538.

[9] C. Xu, A. Israr, I. Poupyrev, O. Bau, and C. Harrison, "Tactile display for the visually impaired using teslatouch", in *CHI'11 Extended Abstracts on Human Factors in Computing Systems*, 2011, pp. 317–322.

[10] E. C. Chubb, J. E. Colgate, and M. A. Peshkin, "Shiverpad: A glass haptic surface that produces shear force on a bare finger", *IEEE Transactions on Haptics*, vol. 3, no. 3, pp. 189–198, 2010.

ACKNOWLEDGEMENTS

First of all, I would like to express my gratitude to my promoter, **Michaël**, for your guidance and support throughout my PhD journey, for your warm words that encouraged and motivated me, and for serving as a true role model through your dedication and passion for research. I remember when I just started my PhD, you were always patient and willing to explain even the most basic concepts and equations. Over the years, you have taught me many essential skills in programming, experimental tips, writing guidelines, figure preparation, and scientific presentation. Beyond technical skills, you also guided me on how to formulate research questions and make meaningful contributions to science. These lessons became the building blocks of my research approach, and through them, I could clearly see my own growth. This progress gave me confidence and encouraged me to become increasingly independent in my research. I am also deeply grateful for your words of encouragement and positive feedback whenever I made progress or achieved something. I still remember your positive feedback you gave me after my oral presentations at the World Haptics and EuroHaptics conferences, when I sent you my revised manuscripts, and when I first got promising experimental results. Your timely feedback in those moments always lifted my spirits, strengthened my confidence, and made me feel that all the hard work was worthwhile. Beyond direct supervision, your way of doing research and your life philosophy also inspired me and set an example. I have seen how dedicated and passionate you have been about research projects, and how efficiently you could accomplish tasks. Your advice that "time is most important" and "don't wait" has left a lasting impact on me. Your broad knowledge, great sense of humor, curiosity, and optimism have also made a deep impression, and they will continue to serve as an example for me in both research and life.

Then, I would like to thank my other promoter, **David**. I enjoyed these meetings we had, where you always gave insightful comments on my work and thesis. Your feedback was critical and constructive while keeping me very motivated. I was often impressed by how clearly and patiently you could explain concepts, sometimes with really good analogies and examples. I also appreciate that you were not only a senior professor but someone who genuinely cared about the well-being of your PhD students. You are also a wonderful leader, with enthusiasm, expertise, caring, and a great sense of humor. Working with you is both inspiring and enjoyable.

It was also a pleasure to meet other staff members of the CoR department. **Yasemin**, I appreciated our casual conversations, your suggestions on my career, and the time we spent together at EuroHaptics and World Haptics. I would also like to thank **Luka** for the good lectures in cHRI course you gave and for the enjoyable experience of working with you while I was a teaching assistant.

A lot of the fun during my PhD came from my colleagues in the Tactile Machines group. I cannot forget these fun moments that we spent together in the lab, in the office, and during outings for drinks or other activities. You are all incredibly talented in

research and creativity. **Mostafa**, we joined the lab at almost the same time. I greatly appreciated the period we spent together and admired your good level of independence as a PhD researcher, your ability to find the resources you needed for your research, and the useful advice you generously shared with me. I also learned a great deal from your dedication to your PhD work on ultrasonic lubrication catheters, your insights into multiple research projects during group meetings, and the effective ways you supervised MSc students. **Kate**, thank you for organizing so many group events and meetings. You are always reliable, creative, and full of energy. We also shared many moments in the haptics community, attending WHC and EuroHaptics, and the research school in Malta together. Whenever you were around, the pressure seemed to ease and the atmosphere felt lighter. **Giuseppe**, you always brought fun and warmth. I admire your achievements in building successful tactile sensors and appreciate how willing you were to offer me help. **Lukas**, you are incredibly talented at designing and building elegant experimental setups. It was always a joy to see your creations. You are always open and curious about new technologies and science. You are such a great science buddy whom I always feel no barrier to starting a discussion with at any time. I also appreciate the many evenings we worked side by side until the ME building closed. I would also like to thank **Laurence** for the insightful discussions and for the fun we shared during running events, social gatherings, and conference trips to Hamburg and Lille. My gratitude also goes to **Alberico** for your guidance when I was developing the Ultraloop, and to **Agnes, Domas, Basile, Jaimy, Corentin, and Nicolas** for your support and the enjoyable conversations we had during group events and meetings.

I would also like to thank the two MSc students I had the pleasure of supervising: **Koen Renkema**, who developed the prototype of the flatLoop, and **Kenny**, for your dedicated work on user studies with Ultraloop. I was impressed by how much both of you achieved in such a short time. I am also grateful to other MSc students in the group, including **CoCo, DiDi, Felix, Valerie, Finn, Janne, Jelte, Jeroen, Jingwen, Nihar, Pepijn, Sherif, Tammo, and Thijs**.

I would also like to thank my other CoR colleagues outside the lab. **Jagan**, your all-around expertise, especially in electronics, and your hard work were an inspiration for me, especially during difficult times. I also enjoyed the trips and conferences together in Lille and Suwon. Thanks as well to **Umut, Koen Wösten, Salvo, Italo, Alex** and **Ashwin**, and to the technicians, **Maurits** and **Kseniia**, as well as the secretarial team. I appreciated all your support.

Another important group of people who made my PhD journey warm and enjoyable were my Chinese colleagues in the CoR department, with whom I shared many gatherings and conversations. I would like to thank **Hongpeng, Jihong, Sihao, Jiatao, Guopeng, Gang Chen, Xiaolin, Yancong, Cong Wang, Li Zou, Desong, Xiangyu, Heye, Zimin, Yujie, Renchi, Chuhan, Jinyue, Zhaoting,** and **Yuxuan**. I am truly grateful for the time we spent together, from the delicious food you invited me to enjoy, to our coffee-break conversations, hotpot dinners, the many fun activities we experienced, and the valuable suggestions and support you gave me for my career. A special thanks goes to **Yujie** for your efforts in representing the CSC community in the PhD Council.

Beyond the lab and daily work, one of the most important ways I relaxed during my PhD was hiking with friends in the mountains across Europe. I will never forget the spec-

tacular views and the engaging conversations during our hikes and mountaineering trips to Mount Etna, Mont Blanc, the Matterhorn, the Eifel National Park, and more. I am deeply grateful to **Pan Fang**. We have several common hobbies and are even from the same hometown. We have enjoyed countless enriching conversations on research, life, and our shared passions. Your dedication and determination have had a positive impact on me, especially when I was struggling with my research and felt uncertain about my future. Thank you, **Binbin**. We faced harsh weather and challenging conditions together while climing the Matterhorn and Dufourspitze, and we always encouraged each other. I will never forget the delicious dishes you prepared during our camping and mountaineering trips, as well as the many lively conversations about life we shared. I am also very thankful to **Renchi**, from the same HRI section. We had many lunches, bouldering sessions, hiking trips and camping experiences together. We have also spent our busy PhD days working in nearby labs and sharing light-hearted complaints over coffee breaks. I always found our conversations both fun and insightful. Also thanks to **Yangyang Guan** for a great trip we had in Mont Blanc.

Besides hiking, bouldering in DelftsBleau became another activity that brought me joy during my PhD. Many thanks to my friends with whom I shared these sessions: **Zichao**, a fellow alumnus from my undergraduate university, who also inspired me in cycling, even though I have not yet had the chance to fully explore it in the Netherlands; **Qi Shen**, whose dedication to each climbing session and impressive progress in such a short time were truly encouraging, and whose WeChat articles are inspiring to read; and of course **Pan, Binbin, Renchi**, **Yujuan, Nianlei, Weichen, John, and Luobo**, who made our sessions even more enjoyable.

I am also grateful for the fun and friendship from playing beach volleybal and running. **Xiaoyu**, you were the first person I got to know when I arrived in Delft, and I have always enjoyed our countless conversations, both in person and online, that never seemed to end. We also share many similar feelings and opinions. Thanks as well to **Yifei**, from the AE faculty, for those summer evenings when we played volleyball until very late. And thank you, **Jinbao**. We always encouraged each other to run more, though I often skipped my sessions. I appreciate the tips and running routes you shared, as well as the events we joined together. Thanks also to my other running friends, **Wei Yuan**, **Binbin**, and **Hanqing**.

Beyond sports, I would also like to thank my PhD colleagues whom I often met and caught up with in the ME faculty buildings: **Minkai, Sifeng, Kai Wu, Zhilin, Xiliang, Yang Yang**, and **Yuheng** from PME; **Kai Liu** from MSE; **Yun Li** from DCSC; and **Xiaohuan** from MTT. Thank you for the meals, gatherings, and fun chats. Spending time with you was always relaxing. Thanks to **Xinxin** for all the fun and inspiring conversations we had about PhD topics and PhD life, and for your interest in my WeChat articles; Thanks to **Qi An**, for always bring very delicious Jiangxi cuisine during gatherings. I also deeply appreciate friends from other faculties around TU Delft. **Tianlong**, from CEG, I appreaicie your energy and optimism and enjoyed the outings we had together. I would also like to thank **Yiru, Siyuan** and **Yaoxue** from CEG; **Jingyi, Wenchan** and **Ziqing** from the AE faculty; **Qiang Liu** and **Xueqing** from IDE, **Shengren** and **Sen Yuan**, from EWI; and **Shuaiqi** from TPM, **Min Li** and **Ziying** from AS. I am also grateful to many other colleagues whose names I may not be able to list here, but with whom I shared memorable moments dur-

ing my PhD journey.

Another special part of my PhD life was the "TUD Library Group". We spent a lot of our spare time together in the TU Delft library, working on our research, relaxing over coffee breaks, having lunch, and even making trips to Zeeland to collect oysters. We shared countless conversations, exchanged useful ideas, and most importantly, supported each other through the challenges of our PhD journeys. Over time, most members of the group graduated one by one and moved on to new chapters in their careers. Yet I know that whenever and wherever we meet again, we will always cherish the memories of those days. The members of this group are: **Yunzhong, Pan Fang, Yitao, Xiuli, Xin Ren, Yuexin, Xue Yao, Di Yan, Weijun**, and **Alex Wang**. I would especially like to thank **Yunzhong** for sharing practical advice on sales and for the entertaining videos about the Chinese rural dog, which we both love. Thanks also to **Xin Ren** for the thoughtful gift you gave to my young daughter.

In the later part of my PhD, I was also fortunate to have met my "library coffee partners", **Yubao** and **Jinbao**, both from CEG. We enjoyed many coffee breaks together, which helped me stay relaxed during the final months of my PhD.

I am also grateful to the China Scholarship Council for the financial support.

Finally, I would like to express my deepest gratitude to my family. I thank **my father** and **my mother** for their continuous and unconditional love and support throughout my life. Thank you, my dad, for always encouraging me to pursue whatever I wished for. I am certain that you are the one who always believes in me, whenever I felt frustrated or lacked confidence. I am also deeply grateful to my younger **brother**, who has taken on great responsibilities for our family and become a true pillar of strength.

Most of all, I would like to thank my beloved wife, **Ziqi**, for your unwavering support. You have accompanied me through all the ups and downs of this journey, cared for our daughter, Xun, with such dedication, and given me endless warmth, comfort, and the determination to keep moving forward. I am also sincerely thankful to my parents-in-law, **Mr. Zhou** and **Mrs. Zheng**, for your constant support and care. I wish all my family members good health and lasting happiness.

Zhaochong Cai
Delft, August 2025

CURRICULUM VITÆ

Zhaochong Cai was born in December 1994 in Jiangxi, China. He enrolled at Beihang University in 2013, majoring in Optoelectronic Information Engineering. In 2017, he received a Bachelor's degree with the honor of Outstanding Graduate of Beijing.

Exempted from the admission examinations, he pursued a master's degree in Optical Engineering at Zhejiang University under the supervision of Prof. Jun Qian. His research focused on high-resolution in vivo fluorescence bioimaging in the second near-infrared region (NIR-II). He completed his Master's degree in June 2020.

In December 2020, he began his Ph.D. at Delft University of Technology in the Netherlands under the supervision of Assoc. Prof. Dr. Michaël Wiertlewski, who leads the Tactile Machines Lab, and Prof. Dr. David Abbink. His research focuses on haptic human-robot interaction, particularly utilizing resonant traveling waves to generate tactile feedback on touch interfaces. His Ph.D. dissertation is titled *"Traveling-wave surface haptics to guide bare finger movement over touchscreens"*.

LIST OF PUBLICATIONS

Publications related to the PhD study (*: equal contributors)

4. **Zhaochong Cai***, Koen Renkema*, and Michaël Wiertlewski, flatLoop: Low-profile active force feedback device using traveling waves, published in **IEEE World Haptics Conference 2025**, Suwan, Korea.

3. **Zhaochong Cai**, David Abbink, and Michaël Wiertlewski, Attracting Fingers with Waves: Potential Fields Using Active Lateral Forces Enhance Touch Interactions, in **CHI Conference on Human Factors in Computing Systems (CHI '25)**, April 26–May 01, 2025, Yokohama, Japan. ACM, New York, NY, USA.

2. **Zhaochong Cai**, and Michaël Wiertlewski, Viscous damping displayed by surface haptics improves touchscreen interactions, In: Kajimoto, H., et al. Haptics: Understanding Touch; Technology and Systems; Applications and Interaction **(EuroHaptics 2024)**.

1. **Zhaochong Cai**, and Michaël Wiertlewski, Ultraloop: Active lateral force feedback using resonant traveling waves, **IEEE Transactions on Haptics**, 16(4), 2023.

Touch is essential to how we perceive and interact with our surroundings, yet today's touch-enabled interfaces offer little tactile feedback. This thesis introduces the Ultraloop and the flatLoop, new surface-haptic devices that use resonant traveling waves to generate active lateral forces on flat surfaces. These devices enable the rendering of virtual 3D shapes, enhance target-search performance, and improve the user experience during touch interactions.

TU Delft Delft University of Technology

ISBN: 978-94-6518-120-2